Interreg
Italy - Croatia
METRO

EUROPEAN UNION

WP4 / Act. 4.1

CHARGING STATIONS AND PEER INFRASTRUCTURE

Prepared by:

University of Trieste, Dept of Engineering and Architecture

Faculty of Maritime Studies, University of Rijeka

Port Network Authority of the Eastern Adriatic Sea

Summary

1 Introduction

This report is aimed at providing information about "Charging stations and peer infrastructure" in the context of METRO project. Specifically, the goal is to provide a general insight about the technologies available for introducing charging stations in existing port infrastructure, and then define a methodology to design the overall system by correctly integrating all the available elements. In fact, the correct exploitation of a more environmentally friendly transport system involves the analysis of the infrastructure in which it has to be integrated. Indeed, it is worth nothing to have a ship capable of sailing using the energy stored in its onboard energy storage system, if it is recharged from the shore by using nonrenewable energy. Similarly, if the port infrastructure is unable to supply the required energy to allow the ship operation throughout its daily routine, at a certain point the onboard energy storage system will be depleted, thus making it necessary to rely on the onboard Diesel generators. This means that the achievement of a lower environmental impact for the ship involves not only the design of a new ship, but also modifications to the port electrical infrastructure. Being these elements strictly interrelated, it is necessary to develop a methodology able to take into account all the significant variables and data. This activity is focused on the port side; thus, the ship design is taken as a given. This means excluding any modifications to the ship, besides for operative conditions (like starting or stopping onboard generators, connecting to the port infrastructure, or defining when the onboard energy storage system has to be recharged). Since the ship design activities are still ongoing, this study is based on one of the preliminary designs defined in the document "*Preliminary Considerations on Machinery Configurations*".

As the METRO project is based on a collaboration between Italy and Croatia, the routes connecting these two countries are the ones on which focusing the analysis and evaluation process. As an example, three routes are important considering the Ro-Pax ships:

- Ancona – Zadar (distance ~103 nm)
- Ancona – Split (distance ~130 nm)
- Bari – Dubrovnik (distance ~106 nm)

Albeit the routes connecting the two countries represents notable examples on which to develop the study, the research group has preferred to consider the short referent line Brestova – Porozina (refer to the document "*Identification of research area, referent lines and referent ships*"), thus between the peninsula of Istria and the island of Cres in Croatia. In such a way the study case is specifically located only in Croatia, and the transfers between countries are not considered. While such decision could appear limiting, the considered route is characterized by all the characteristics of interest. In detail, the Brestova-Porozina is a “short” route (only 2.7 nm), but the double ended ferry operates in a heavy traffic condition throughout the whole year. Moreover, in both ports there is a weak electrical infrastructure, thus making it possible to highlight several different options for the correct integration of new elements and different solutions to specific issues. For such a reason, such a route has been selected as the most convenient in the proposed study.

Although the Brestova-Porozina is a short distance path, it deserves importance in the matter of METRO project. As the partners have a good knowledge on this particular route, it constitutes the best starting point on which developing the methodology used to define the best integration among the ship, the port electrical infrastructure, the charging stations, and other relevant apparatuses (such as energy storage systems). It will be then possible to use the developed methodology and concepts to other routes, taking the provided example as a guide.

Despite the focus is given to the Brestova-Porozina route, additional specific information is given in regards to the infrastructure on the Port of Trieste. This because the Port Network Authority of the Eastern Adriatic Sea, which is the authority that manages such port, is one of the project partners and it is actively working towards increasing the quota of its piers endowed with shore connection technologies. In this regard, the project will also include the electrification of such port. However, due to time constraints connected to the public procurement actions of the partner, the final contribution regarding the port of Trieste will be included in the final deliverables (as decided by the partners during the bi-annual meeting held in the RITEH premises (Rijeka) on 3 December 2019.

2 Analysis of port infrastructure

The ports to be analyzed directly depend on the route selected for the study. In this regard, the Brestova-Porozina route is one of the routes selected for focusing the study in the document "*Identification of research area, referent lines and referent ships*". Thus, data about these two ports will be given, considering also possible future port updates in the renewable trail. All the studies and analyses will define the methodology, thus a strategy for a future adoption on different routes. However, additional specific knowledge about the infrastructure on the Port of Trieste is given, since it is one of the project partners and it is actively working towards increasing the quota of its piers endowed with shore connection technology. Secondly, the port of Trieste constitutes another important example on which analyze possible recharging infrastructure. Such a port is experiencing a notable grow in terms of goods movements and business; therefore, it is a valuable target on which discussing about port issues. As the Port Network Authority of the Eastern Adriatic Sea (formerly known as Trieste Port Authority) is partner in the METRO project, this study case gets a particular importance. Indeed, such an authority is developing several projects in the regards of port recharging infrastructure, thus the METRO project is a profitable framework where integrating different knowledge/experiences. For extending the recharging topic opened in the Brestova-Porozina route, the data of the port of Trieste will be taken into account for exploring the systems already installed in the Trieste Port. In such a way, the topic is proficiently addressed and debated.

2.1 Brestova-Porozina

As already expressed, the considered route is the round trip between Brestova and Porozina. These two small ports are both located in Croatia, respectively in the Istra region and on the island of Cres (Primorsko-goranska region). Although the route is less than 3 nautical miles (Figure 1), it is actually very important for the local economy. Indeed, the majority of tourists to Cres (notable touristic location) arrives at the island by following two possible sea paths. The route Brestova-Porizina and a second one from Krk island, which is linked to the land by a bridge. Focusing on the first possibility, the Cres island is reached thanks to a car transportation towards Brestova in Istra and then the ferry boat to the island. As the life on Cres is essentially based on tourism, it is evident the importance of one solution for improving the environmental impact of transportation. In this regard, the METRO project acquires a great impact, not only for research institution involved in but also for the Croatian tourism.

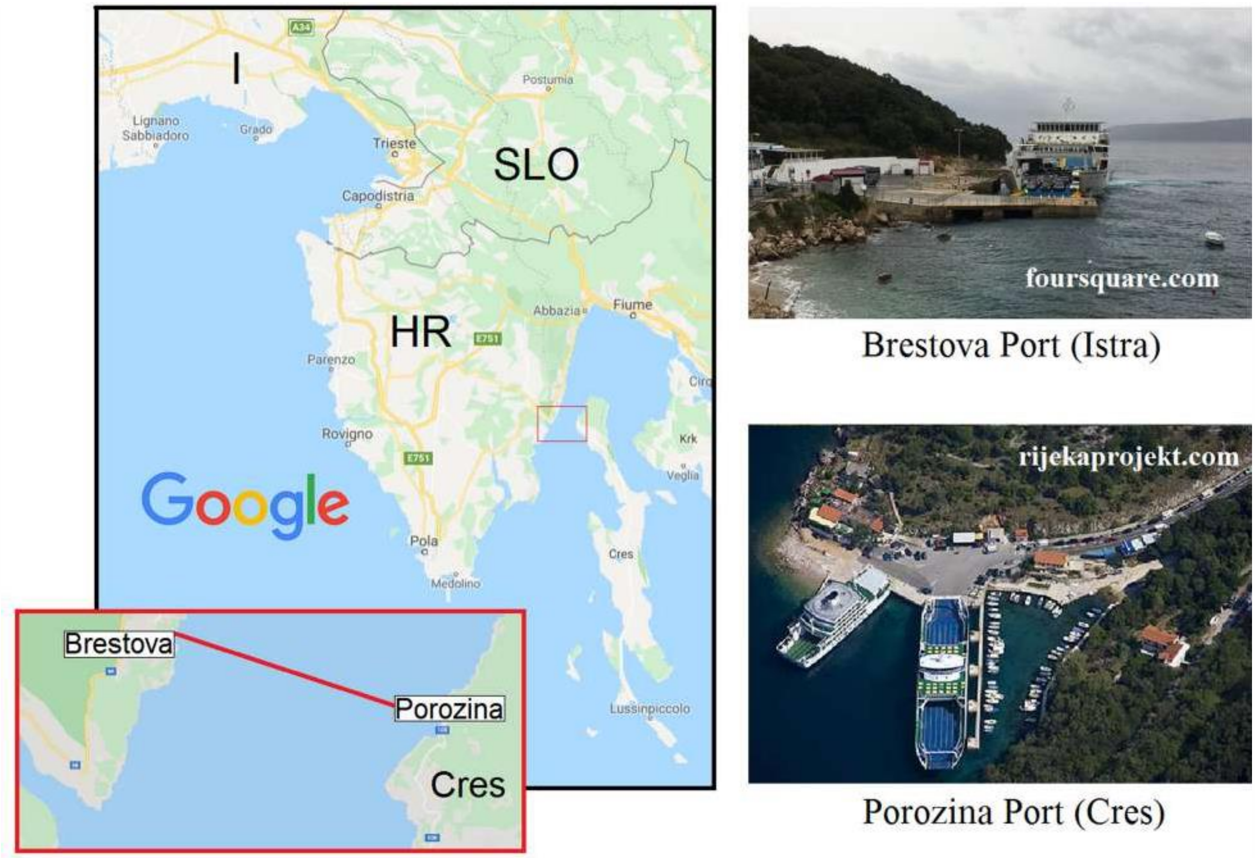

Figure 1 - Brestova-Porozina round trip (Istra-Cres, Croatia) [1].

As the METRO project's goal is an integrated strategy between ships and ports to reduce pollutant emissions, a paramount role is the one spent by the port electrical power infrastructure. If the onboard energy storage systems can strongly decrease the vessel's environmental impact during sailing, specular approach must be applied when mooring at the port. In such a case, only a well-designed recharging infrastructure can provide the green energy for refilling the batteries. In this context, two are the aspects to be considered. On one hand, the source for recharging the onboard storage, possibly carbon-free. On the other one, the time for recovering the full battery capacity, thus at the final stage the power of the electrical infrastructure. Larger the power, smaller the time, then forcing the interest towards Medium-

High Voltage infrastructures for lowering the current in the power cables. As well understood, the port electrical infrastructure deserves a great attention when designing solutions for increasing the environment friendliness in maritime transport. For such a reason the two ports are treated in the following, together with some interesting considerations about future-desirable developments.

2.1.1 Brestova port

The first information regards the distribution system operator (DSO), which is HEP in Croatia in both cases. Then, some data about the present port grid can be provided. At present, a single step-down AC transformer is installed in the port premises, for providing the low voltage (400 V) at the existing loads, starting from an existing medium voltage (20 kV) supply. The rated power of the transformer is 50 kVA, which is nowadays oversized considering the installed loads. Indeed, all the transformer power is practically available as the loads are limited to a lighthouse, a restaurant, and a ticket shop. It is well evident how the requested power from these loads is smaller compared to the transformer rated power. For giving the present consumption at a glance, it is possible to hypothesize 5% of total installed power. This number constitutes an estimation, as the power request from these loads during summer time is not known at present. In the existing housing, the largest transformer that can be installed can reach up to 250 kVA. Conversely, the existing distribution power line can hold up to 2 MVA. However, such a high power requires also the building of a new substation for the transformer and its apparatuses.

2.1.2 Porozina port

The Porozina port existing power system allows to provide a maximum active power of about 50 kW, by taking into account the existing LV supply by means of the DSO cable. The latter starts from the Porozina transformer substation (the black one in Figure 2), whose maximum power is approximately 100 kW. Therefore, the final cable is the limiting factor.

However, the DSO (HEP) is planning for an overhaul to the electrical infrastructure in the Porozina area. In particular, it is planned to build two new transformer substations (the orange ones in Figure 2), one connected to the same MV cable supplying the existing one and one supplied by a new cable. The port will be then supplied by Porozina2 substation (type KTS, 20/0.4 kV), which will provide up to 400 kW.

In the case that even such solution demonstrates to be capable of providing an insufficient power level, an additional possibility is available. Indeed, the port can build his own substation connected to the existing 20 kV cable line (supplied by a 35/20 kV transformer substation in Cres). Such line is characterized by an Al cable (150 mm2), plus a final section of Al/Fe (35 mm2). The latter part is intended for future replacement, since it is the limiting factor fur such a line. The power deliverable by means of the Al/Fe 3x35 mm2 cable at 20 kV is approximately 4.5 MW, while the actual load is less than 1 MW, thus allowing for a significant power availability in case of a dedicated power supply to the port.

Figure 2 - Electrical power system in the Porozina port area

2.2 Port of Trieste

Albeit the target is well configured on the Brestova-Porozina route, a different scenario based on Port of Trieste electrical grid is here shown to provide scientific references on the shore connection matter. Therefore, the final application is certainly different, but the motivations/methods/outcomes are still valid.

The new Port of Trieste has a 6 kV Medium Voltage AC (MVAC) distribution system designed between the 70's and the 80's. As discussed in [2], such an electrical network has been installed to feed all the electrical utilities installed in the Trieste new harbor area depicted in Figure 3a, while Figure 3b shows all the Trieste terminals. The Trieste port area is located in Italy along the north-east end of the Adriatic Sea, thus in the heart of Europe near Slovenia and Croatia. The new port behaves as a hub between the commercial flows coming from the TEN-T Mediterranean Sea routes and the Mediterranean/Adriatic-Baltic terrestrial corridors. As the exchanges between European Union and deep East are increasing day-by-day, the port of Trieste is coming back to a key role in the international commercial traffic, thus largely increasing the development opportunities for the city.

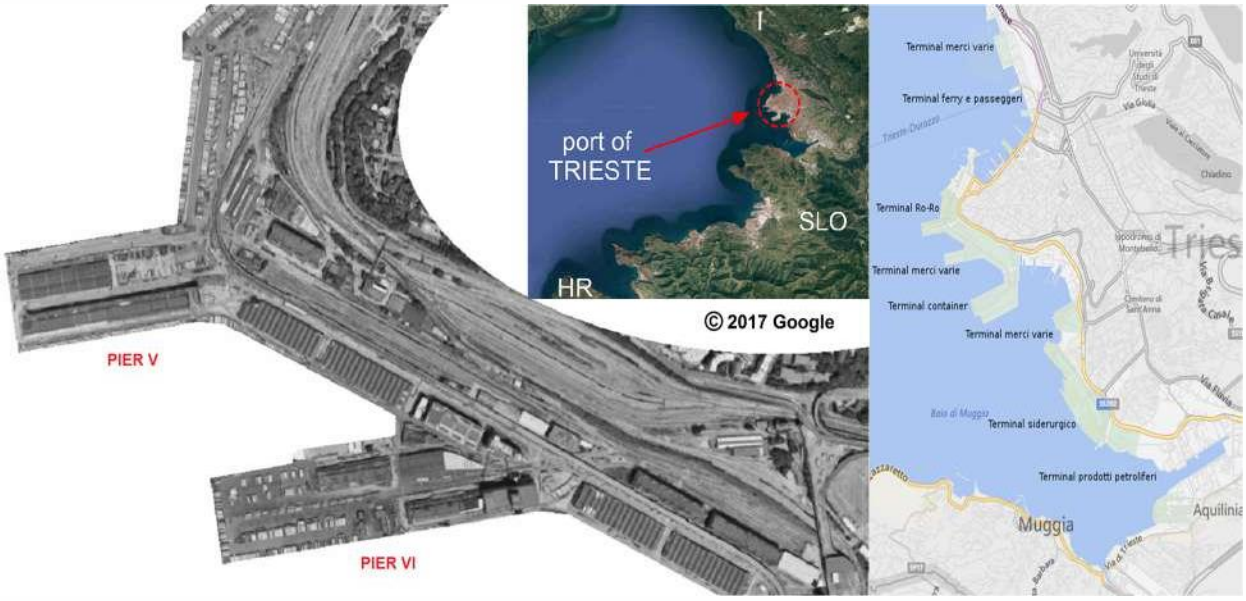

a) b)

Figure 3 – a) Part of the Trieste New Port Area [2]; b) Trieste Terminals

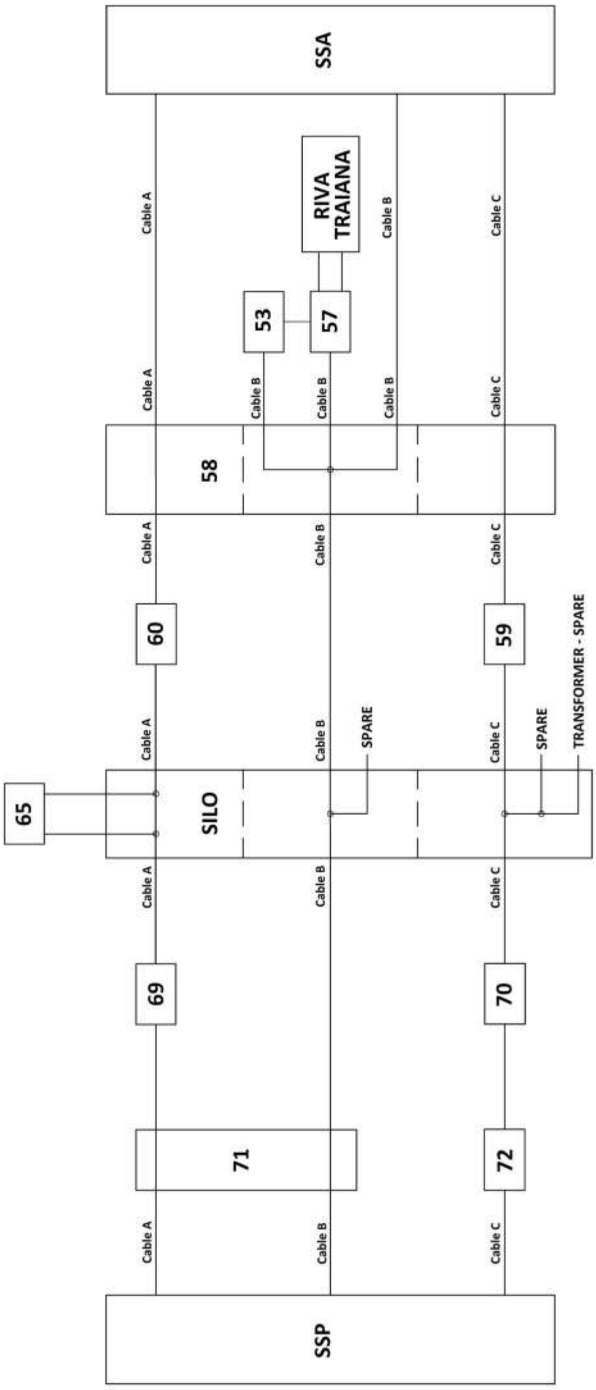

Figure 4 - Port of Trieste Electrical Distribution System (Pier V, Pier VI and common areas) [2].

The port is located in the western seaside of the city, seamless respect to the historical center and touristic areas. By considering the proximity to the city center area, the reduction in port emissions becomes of primarily importance. There are 12 km of docks and piers organized in 58 operating moorings, which can effectively accommodate a large variety of ships (e.g. multi-purpose vessels, ro-ro, ferries, etc.). As highlighted in Figure 4, the 6 kV MVAC electrical port grid is a complex system, build using three main MV power lines, which start from two primary transformer stations connected to the 27.5 kV public grid. These two stations are the SSP (main port transformer station) and the SSA (backup transformer station, used in case of maintenance on SSP or in case of faults), which have both 6.5 MVA transformers and are connected to two different feeders from the DSO (to assure redundancy). In the port there are 12 MV/LV substations (Figure 4), identified by the name of the pier were they are installed (most of the piers have a numerical name, while two of them have a proper noun). The total apparent power used by the port is approximately 800 kVA, but it can reach up to 1 MVA in some operative conditions. Thus, the main stations have a utilization factor that is approximately equal to 16% of the rated value (since only one of them is used at a time, normally the SSP). As the available power capability is relevant, interesting can be the scenarios of port development (e.g. cold ironing, recharging infrastructure, electrical hub). As an example, the shore connection can be useful in decarbonizing the port site for the Italy-Turkey maritime route [3]. In such a case, a possible power requirement level for these ships can be 540 kW, thus leading to shore connection hubs of 750 kVA (considering a 0.8 power factor and a 0.9 oversizing coefficient). By using such values, in [2] and [3] it has been demonstrated the possibility of installing these two cold ironing platforms endowed with AC-AC power converters, by means of power flow analysis. As both nodes voltages and load currents are in accordance to the specification during the grid operation, the two shore connections are proved to be effective and manageable, thus enhancing the port decarbonization [3]. Moreover, to increase the Return On Investment the two platforms can additionally be used separately, when feeding refrigerated containers or recharging possible Electric Vehicles. Since the port must be sized not only for actual routes, but also for the possible future ones, a higher shore power level in respect to the above presented one may be useful to cope with new ships' needs. Thus, to include all the possible RO-RO ferries that can be berthed in the port, it is possible to consider a 1 MVA ship power as a suitable design value. Therefore, shore connection apparatuses sized for 1.5 MVA should be sufficient to cover all the possible future needs for such ships.

Not only the cold ironing can improve the environmental impact in the industrial port, but also this technology can be adopted in the city moorings for large cruise vessels. In this context, these large vessels are nowadays moored and bunkered on Molo Bersaglieri, in the city center near the main square "Piazza dell'Unità di Italia". As a matter of fact, during the cruise vessel stop in the city port, the pollutant emissions are today consequent as the main diesel engines run to feed the base onboard loads. It is evident how a shore connection in Molo Bersaglieri could be able to solve this city pollution. During the last years, several are the proposals in this regard. One of the most feasible foresees the installation of two multi-MW shore connections on the Molo Bersaglieri (Figure 3 b). By taking into account the large requested power during cold ironing (i.e. 10-20 MW for each platform), the High Voltage supply is consequent thus opening interesting scenario of grid development.

3 Shore connection systems

When talking about shore connection systems, it is useful to start from the high-power application to proficiently present the basic idea. Indeed, the same base concept is used (resized and adapted) in the ferry context. In the following, at first consideration is given to the cruise liners' cold ironing, as the one expected in the Trieste port. After that, small power infrastructures are analyzed.

3.1 High power shore connection

The high-voltage shore connection (HVSC) system is used to locally eliminate pollutant emissions for berthed ships [4] [5] [6]. Such a technology had a fast development in the past ten years, being at present a standard application for many shipbuilders. However, while being a well-proven technology nowadays, its diffusion is still lacking. This is due to several different causes, among which it has to be highlighted the need of having such technology integrated in both the ship and most of the ports where the ship will be berthed.

The base idea is to connect the ship power system to the land one, to allow shutting off the onboard generators at berth. The need of multi-MW scale power (to supply large ships, such as cruise ones) calls for the adoption of high-voltage (HV) systems (1–11 kV). It has to be noticed that in ship sector all voltages above 1 kV are high voltage, while in land application there is the further distinction among medium voltage (MV, 1-35 kV) and high voltage (above 35 kV). Due to that, the term HVSC is commonly used to address this technology in marine sector, while from the land side point of view this is a MVSC.

The electrical power for ship services is provided from the land, by using a dedicated cable line as in Figure 5. However, since the land power system and the ship's one most of the time have different voltage levels, at least one transformer is required for performing voltage adaptation. Moreover, the ship can have either a 50 or 60 Hz power system, thus making it necessary to install a dedicated power converter if the land and onboard frequencies are different. All these components are shown in Figure 5, which depicts the most general case of high power HVSC.

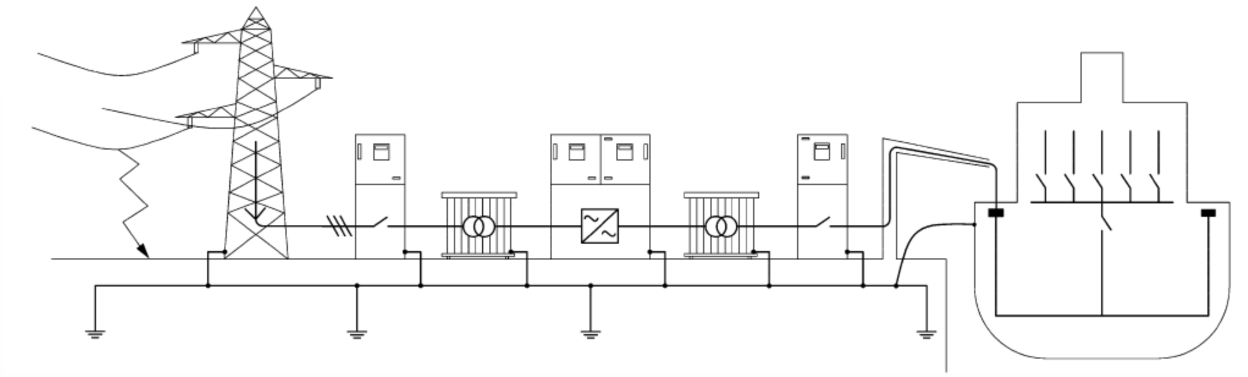

Figure 5 - HVSC system supply by a HV primary line [4].

Figure 6 – Examples of LV shore connection pedestals: single phase 16A, three phase 125/250A, three phase 600A [7].

3.2 Low power shore connection

The low power shore connection system basic aim is the same of the high-power ones: to supply the power system of a berthed vessel. However, the power is much lower due to the lower needs of the vessels that are connected to them. In fact, these can span from basic boats where the connection is used to keep the onboard batteries charged, to big yachts that are similar to modern cruise ships, although at lower power levels. The low power shore connection technology does not require any particular apparatus (besides the ones needed to assure the compliancy with the safety rules) and in fact it is well-proven, being based on low voltage AC components. In particular, in the marinas where the leisure crafts are generally berthed the installation of pedestals able to provide the electrical connection, as well as fresh water supply, is common. In this regard, at present there are several suppliers that have commercial off the shelf solutions for such applications (like the ones depicted in Figure 6) [7] [8]. These low power shore connections are either single-phase 230 VAC, with current rating from 16 to 125 A, or three phase 400 VAC, with current ratings from 16 to 630 A (it can reach up to 1000 A for some specific applications).

It is relevant to notice that in the automotive sector there is a fast development of charging stations, due to the interest in enabling electric mobility in cities. The fast charge stations are reaching peak power values that are starting to be into the range of interest also for shipboard applications. As an example, the Tesla supercharger V3 has a peak power of 250 kW [9]. Obviously, the marine application follows different standards and regulations in respect to automotive ones, and presents additional stress factors (saline atmosphere, mechanical strength, presence of salt water as a high conductive element, etc.). However, in the future it may be possible to use similar power conversion, control, and management technologies for both applications.

3.3 Innovative applications for shore connections

By starting from the standard recharging stations already installed in several ports, the technology is nowadays ready for more advanced green solutions. In this regard, the advantages to be attained are well explained in [10]: 1) fast recharge of embarked storage system (e.g. batteries); 2) optimal management of renewable source installed in the port area (e.g. photovoltaic energy); 3) supply of ancillary services to the external distribution network (e.g. storage functionality for the DSO). If the first two items are important for offering a premium service to the clients (the owners of the berthed boats), the last one is a profit for the port authority. Clearly, the achievable advantages depend on three essential requirements: a) presence of a considerable amount of berthed ships endowed with onboard storage systems; b) port power system re-design; c) availability of renewable energy sources. Evidently, basic shore connection apparatuses can allow the evolution of the port into a smart carbon-free one only in presence of a wide utilization of power electronics converters.

As discussed in [11], the shore connection platform for supplying either small hybrid ferries or large cruise liners can be based on two different configurations, i.e. internal DC link distribution (Figure 7 left), or internal AC link distribution (Figure 7 right). In both solutions several types of power electronics converters are required to ensure the ship supply (DC or AC) from the land AC line, as well as the integration of all the available power sources (renewables ones included). The most important characteristics of such an innovative shore connection and smart port infrastructure are: redundancy (i.e. duplication/interchangeability of essential components), operability (i.e. ability to maintain safety and reliability during system operation); and easy to operate HMI (human machine interface) (i.e. simple operation/maintenance). The output voltage depends on the ship to be supplied, as well as its power. Since the power supplied by the shore connection can vary up to tens of MW, the power input is to be designed accordingly (with consequent impact on the port-grid interface).

When the shore connection power is limited, the preferred solution is the one using an internal DC link (Figure 7 left). Indeed, DC power equipment able to manage up to some hundreds of kW is commercially available, thus making it possible to correctly manage the internal DC distribution system (mostly in regards to faults, which directly affect the reliability of the entire system). Conversely, the AC distribution solution (Figure 7 right) is useful in presence of high power, to make the management of the high-power distribution easier by means of conventional AC components. Obviously, since the most used converters in both cases are the Voltage Source PWM (Pulse Width Modulation) ones (Figure 8), it is evident how the DC-link solution leads to lower space occupation.

The integration of the shore connection system with the port power system, including the possibly present renewables power sources and energy storage system, is shown in Figure 9 in its basic configuration, and in Figure 10 as a general multi user application. The resulting smart power system allows to exploit both renewables and energy storage systems, making the shore-to-ship platforms not only smart as the storage is optimized, but also eco-friendly as the recharging energy is totally green and renewable.

The application of such concepts to the specific aims of this research project is shown in Section 6.4.2 (page 74) of this document.

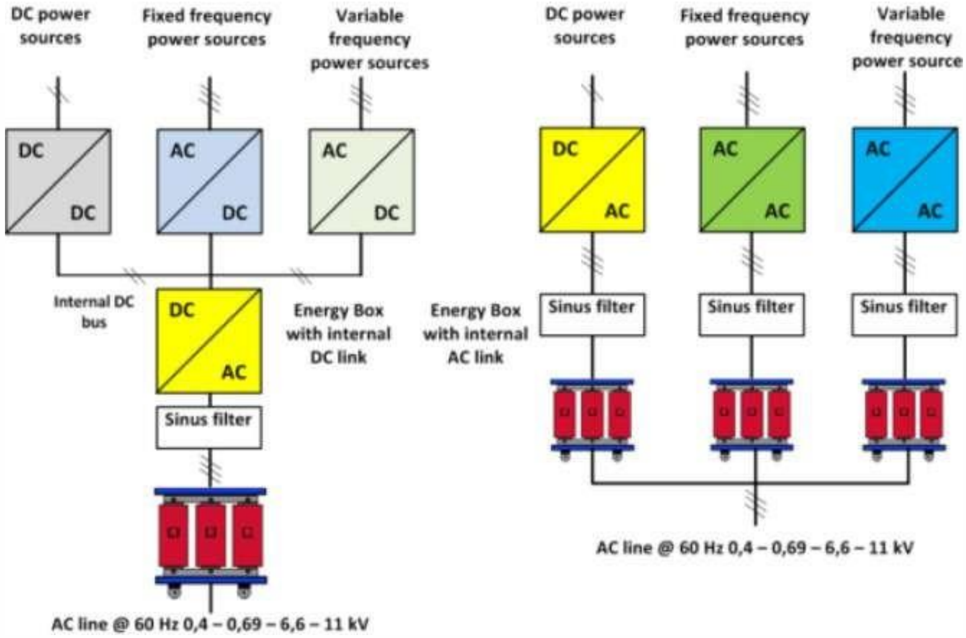

Figure 7 - Port supply line with y-Δ-y transformer with neutral resistance grounded [11].

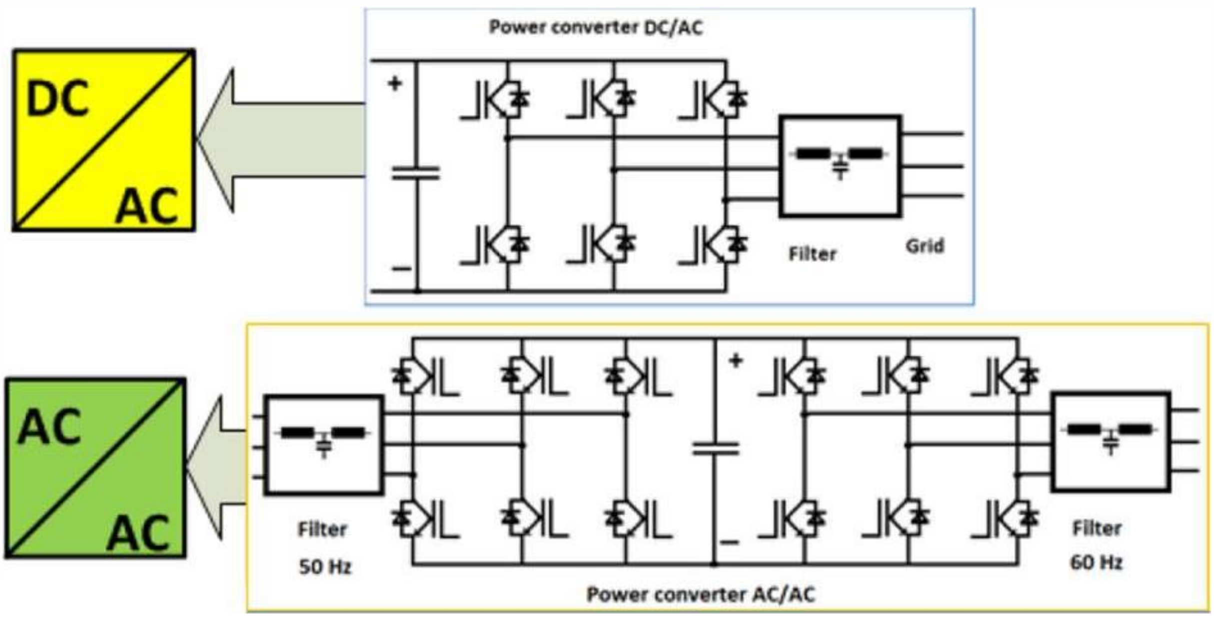

Figure 8 - Electrical schemes of DC/AC and AC/AC power converters [11].

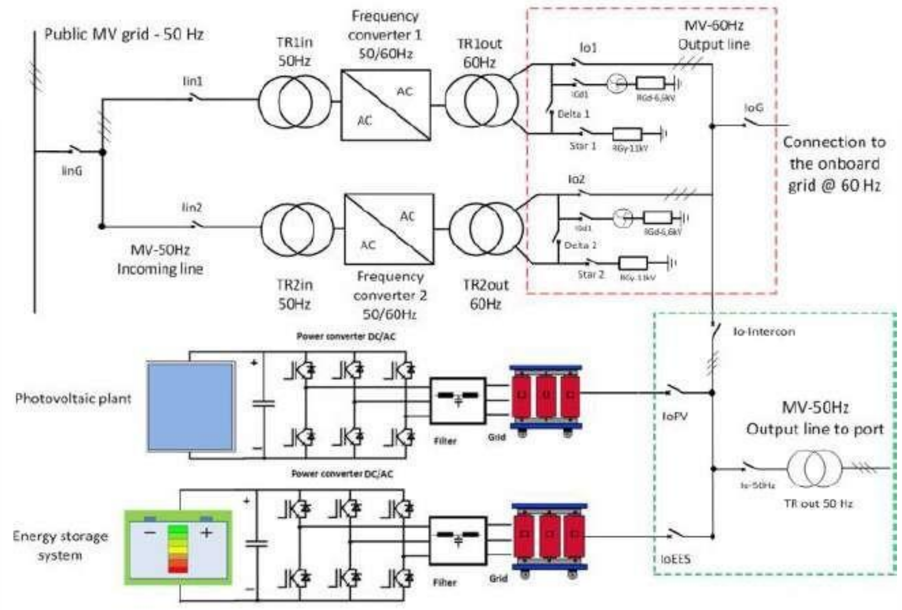

Figure 9 - Basic arrangement: shore-to-ship connection for small and large ports [11]

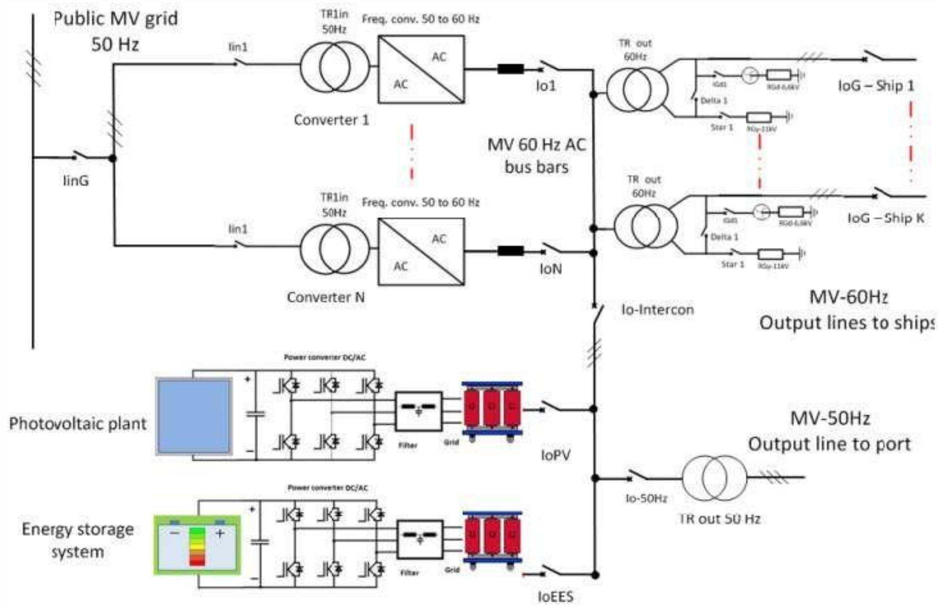

Figure 10 - General arrangement: shore-to-ship connection for small and large ports [11].

4 Energy storage systems

4.1 Introduction

The market of battery storage systems can be roughly subdivided into three classes, which differ in voltage level connection, rated power, storage capacity, as well as in their applications [12]. In Figure 11 an overview of this classification is given.

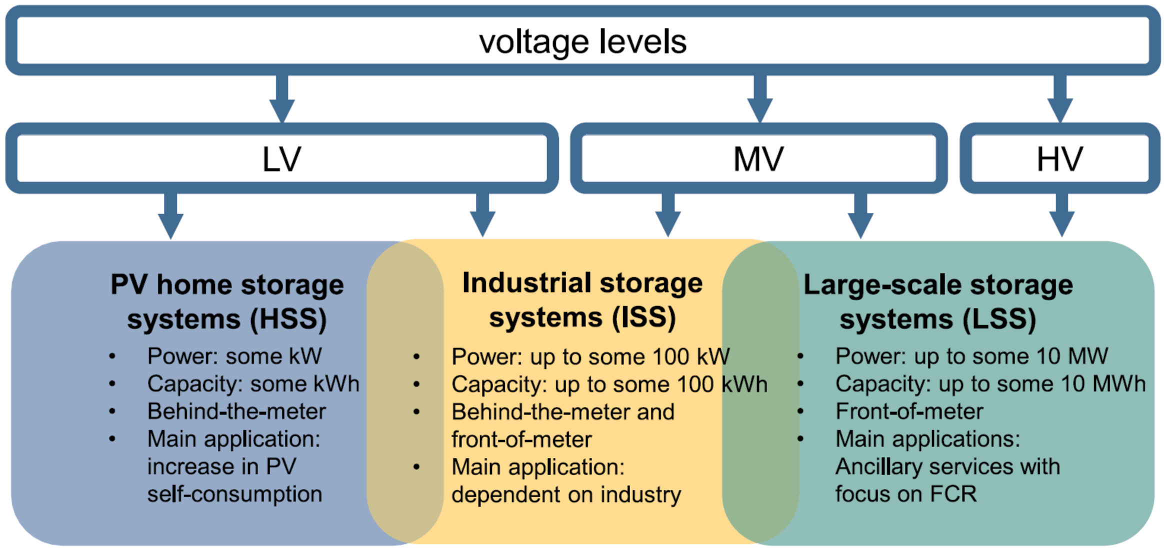

Figure 11 - Overview of BSS market and grid connection characteristics [12]

The smallest battery storage systems (BSS) are home storage systems (HSS) integrated with PV systems. These are connected at the low voltage level and have typical power level in the kilowatts order of magnitude. The storage capacities are also limited to some kilowatt-hours [12]. Their main application is the increase in PV self-consumption for the user, to reduce the electricity costs as a behind-the-meter (BTM) market. Moreover, decentralized HSS are a promising technology to deal with grid problems that can arise due to high local penetration of PV power generation [13].

The industrial storage systems (ISS) greatly span in size. The smallest one can have power similar to the large HSS, and thus being connected to the low voltage level. Conversely, the largest one can be connected to the medium voltage level, with up to some 100 kilowatts power and some 100 kilowatt-hours capacity, depending on the application. Their main applications are BTM products like peak shaving, UPS, increase in PV self-consumption, or the support of charging stations for electric vehicles (EV), as well as front-of-meter products like frequency containment reserve (FCR) [12].

The front-of-meter large-scale storage systems (LSS) are either connected to the MV level or to the high voltage level. These start in the range of large ISS (some 100 kW) and end in the range of 50 megawatts and 50 megawatt-hours. Their main applications are ancillary services (AS), with a strong focus on frequency containment reserve (FCR), which is a fast frequency control reserve for the land power grid [12].

4.2 Most significant energy storage technologies (related to the application)

In this section are briefly presented the energy storage technologies that are considered suitable for the specific application. In particular, the focus is given to the ESS that can be installed in port for fast charging ships' onboard ESS, while being slowly charged by the land power grid and/or by means of local renewable energy sources (refer to Section 6.4.2, page 74). It is noteworthy to highlight that the ESS can perform other services for the both port and the land electrical infrastructure, once it is installed in the port for supplying the ship. A brief list of these additional services has been presented in the introduction, but these will not be addressed here since this is the objective of the Activity 5.4 of the present Research Project.

The technologies here are the ones most suited for a land based ESS, considering the amount of power and capacity that may be needed by an industrial application (like a port). Conversely, in Section 6.4 (page 72) the solution conceived for the case study will be discussed, considering also the most suitable ESS technologies (Section 6.5, page 78).

4.2.1 Electrochemical Battery Technologies

The main electrochemical technologies that are being used in grid applications are lithium-ion, sodium-sulfur, lead-acid, and redox flow batteries [14]. Other technologies that are in different stages of development, but have not reached a commercial availability will be not addressed here. Grid-connected electrochemical storage is characterized in terms of energy density, efficiency, lifetime, and costs, as illustrated in Figure 12 and discussed in the following.

Lead-Acid batteries were the first rechargeable battery technology invented in 1889 by the French physicist Gaston Planté. Nowadays lead-acid batteries are considered a mature technology, which is characterized by a low cell cost (50-600 $/kWh) and good efficiency (80-90 %) [15], [16], [17]. They also present small daily self-discharge (< 0.3 %) and fast response times. They are natural choice for several applications because of their ruggedness, safe operation, temperature tolerance, very good cycle efficiencies, low maintenance and low capital costs [18]. Their main drawback is the low cycling life (up to 2500 cycles), compared to other technologies, [15], [19] and low energy density (20–30 Wh/kg). Their weight (specific power of about 180 W/Kg) is not an issue for land applications, but may become one for transportation systems. Besides, lead-acid batteries lifetime is negatively affected by a high depth of discharge [20], [21], while they also require periodic maintenance.

Sodium-sulfur (NaS) batteries were developed by NGK Insulators Ltd in collaboration with TEPCO. Molten-salt batteries are characterized by high operating temperature (around 300 °C), reasonable efficiency (*75-90*%), high energy density (in the range of 150-240 Wh/kg) and long cycling life (up to 4500 cycles) [22], [23]. These batteries also present almost zero self-discharge rate (*0.05-1%*), and long life (typically up to 5000 full cycles) This technology has been already adopted as grid-connected energy storage to mitigate the impact of renewable energy-based generators [23], [24], [25]. The main issues are related with the high operating temperatures and the corrosive nature of their molten cathodes, which requires a particular care in their construction and thermal management system, with additional related costs (any failure may lead to fire and explosion hazards). A lower temperature variant of these molten-salt batteries has been developed, using a different chemical (Sodium-nickel chloride). These are commercially known as ZEBRA batteries, which present both lower issues and lower performance in respect to the original NaS ones.

Redox Flow (RF) batteries were first developed by NASA in 1974 [26]. They consist of two separate tanks, where the two chemical reactants are contained, and two electrodes separated by a membrane, where the two components are combined and the reaction of oxidation-reduction (redox) occurs. The energy capacity of flow batteries is defined by the quantity of reactants stored in the tanks, whereas the power is defined by the electrodes and membrane system. Power and energy ratings are then separated, and this adds flexibility in the design and operation. Redox flow batteries have a low energy density (15–30 Wh/kg), very low losses, and a number of lifecycles usually above 10000. The efficiency is nearly 75% [27], but can reach up to 90% in light load conditions [28]. Moreover, RF batteries can be instantly recharged by swapping their electrolyte with a pre-charged one. Thus, flow batteries are not subject to limitations in terms of reactants' life cycle and by the depth of discharge [29]. Besides the technical peculiarities, redox flow batteries have been recognized as a potential candidate for grid-scale storage also due to their economic performance [30]. Several chemical compositions for the reactants have been studied and proposed. However, Vanadium based and Zn-Br are the most prominent ones, with the former being the most mature technology. [31] Besides their low energy density and the danger involved in handling chemical solutions in large volumes, the main issue at present is the electrolyte cost [28].

Lithium-ion batteries were firstly commercialized by Sony in 1991. The electrochemical properties of Li-ion batteries are defined by the chemical composition of the cathode, typically a lithium metal oxide, and of the anode, typically graphite [32]. This technology shows high efficiency, that can reach over 90%, although some commercial products offer a rated round trip efficiency over 95%, high energy density (90–200 Wh/kg) [28] [33], and a long lifetime, that can reach up to 10000 cycles depending on the Li-ion chemistry, as shown in Figure 13 [19], [32]. The lifetime is nonetheless affected by the cell temperature, which is a critical factor in the degradation process [34]. Moreover, Li-ion batteries have low self-discharge rate (<8% per month), fast charge/discharge, and rapid response times [28]. Li-ion batteries have been widely used in electronics devices, and in recent years, it has become the main technology for EVs. Despite being still relatively expensive, this technology is well suited for grid-connected applications [35]. Today many Li-ion technologies exist, e.g., Lithium cobalt oxide-based ($LiCoO_2$), Lithium manganese oxide-based ($LiMn_2O_4$), Lithium nickel oxide-based ($LiNiO_2$), Lithium nickel cobalt aluminum oxide-based ($LiNiCoAlO_2$), Lithium nickel manganese oxide-based cobalt ($LiNiMnCoO_2$), Lithium titanate oxide-based ($Li_{24}Ti_5O_{12}$), and Lithium iron phosphate-based ($LiFePO_4$) [36]. Figure 13 presents the performances of (a) Lithium iron phosphate, (b) Lithium nickel manganese cobalt and (c) Lithium nickel aluminum cobalt [19], [32]. Between the considered electrochemical compositions, Lithium-nickel-manganese-cobalt based technology, NMC, offers the best performance. Its good performance, among other factors, have contributed to bringing about NMC as the primary Li-ion technology for stationary storage and EVs [37]. Figure 14 shows the cost of lithium-ion battery cells and pack over the past years [38]. What stands out is the substantial cost reduction, roughly −75% in 6 years, from 650 $/kWh in 2013 to 156 $/kWh in 2019. Following this trend, further cost reduction is expected. Consequently, with a lower total cost of ownership (TCO), energy storage systems could further establish themselves in the electricity sector.

Figure 12 and Figure 13 illustrate the main performance indicators of the electrochemical battery technologies just discussed. As can be easily seen from the figures, Lithium-ion batteries outperform the other technologies, offering higher power and energy density, efficiency, and low daily self-discharge [14].

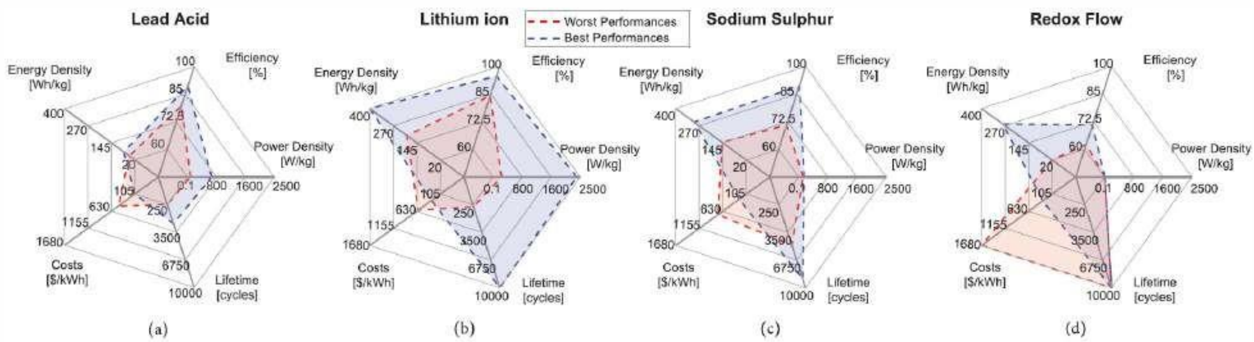

Figure 12 - Performance of different electrochemical battery technologies: (a) Lead Acid, (b) Lithium ion, (c) Sodium Sulfur, and (d) Flow Battery. [14]

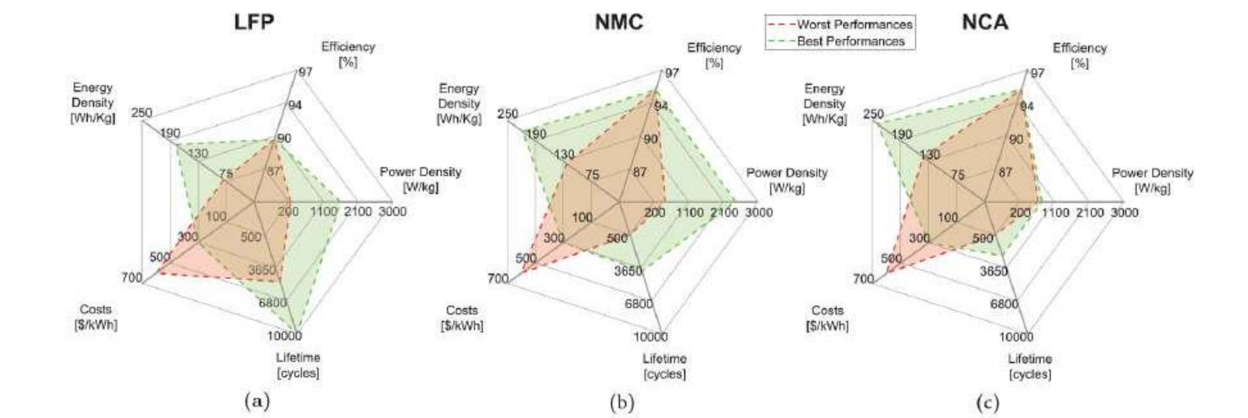

Figure 13 - Performance of different Li-ion battery technologies: (a) Lithium iron phosphate, (b) Lithium nickel manganese cobalt, and (c) Lithium nickel aluminum cobalt. [14]

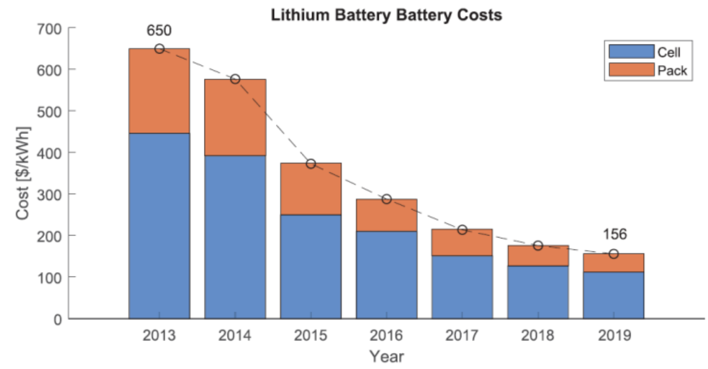

Figure 14 - Costs of Lithium-ion battery cell and pack over the last years [14]

4.2.2 Mechanical Energy Storage Systems

Considering the amount of power and energy required by the application, as well as the maturity of the technologies, at present only flywheels can be considered in the family of mechanical ESS.

In a flywheel energy storage system (FES) the angular momentum of the flywheel mass is used to store the power in the form of kinetic energy. They are typically employed in short duration with short discharge time applications such as the requirement of power over 80 kW within a period of 1-100s [28], [39]. They have high power and energy density with a nearly infinite number of charge-discharge cycles (which is also independent from the depth of discharge) and used for stabilizing voltage and frequency [40]. The efficiency of FES system is in between 85% to 90% due to decreased mechanical friction by using magnetic bearing and very low aerodynamic resistance achieved through vacuum enclosure [41].

The amount of energy that can be stored in the flywheel is a function of moment of inertia of rotor and the speed at which it can be rotated along with its tensile strength and stress restrictions. Based on these properties they are classified into two groups: low speed steel FES systems with speeds up to 10 thousand rotations per minute and high-speed FES systems with speeds up to 100 thousand rotations per minute. As shown in Table 1 [42], high speed FES systems are manufactured from advanced high-speed composite materials such as carbon fiber [39]. Although low speed FES systems have very high-power density about 2000 W/kg, nevertheless, they have an average energy density of about 5 Wh/kg. They suffer from high self-discharge due to the idling losses when flywheel is on standby (up to 20% per hour). Therefore, low speed FES are mainly employed in power quality applications which needing high power for short durations with high number of charge-discharge cycles. Whereas high speed FES system has very high-power density along with higher energy density in the range of 200 Wh/kg. But they are not economical due to the high cost of high-speed composite materials, so, their use is limited to specific longer storage systems. In general, FES are relatively behind in terms of commercial maturity in respect to Li-ion batteries. However, they are rapidly becoming an alternative to batteries for high-power/high-energy/short-response-times applications.

Table 1 - Comparison of low speed and high speed flywheels [42]

Specification	**Low speed FES**	**High speed FES**
Material	Steel	Composite
Electrical machine	Induction, permanent magnet synchronous and reluctance machines	Permanent magnet synchronous and reluctance machines
Quarantine atmosphere	Partial vacuum	Absolute vacuum
Required enclosure weight	Double the flywheel weight	Half the flywheel weight
Typical applications	Power quality improvement	Aerospace and traction
Costs and availability	Low cost and commercially available	High cost and build for purpose

4.3 Energy storage systems producers

Energy storage systems are usually designed and commercialized by an Energy Storage System Integrator (ESSI). ESSIs buy or internally manufacture the battery packs, the power conditioning system, the auxiliary system, and the controlling software. These are then assembled inside standardized containers, to ease the field deployment. Obviously, specific applications may require dedicated approaches to the installations, which can be engineered in collaboration among the ESSI and the overall system designer. The modular BESS solutions offered by the ESSI range from hundreds of kW to few MW in terms of both power and energy ratings.

ESSIs play a crucial role in the proliferation of energy storage systems, striving for an optimized product and seeking for new applications and use cases. Main players in the utility scale ESSI market are Fluence, Nidec ASI, Tesla, RES, Powin Energy, Greensmith, LG CNS, NEC Energy Solutions, NextEra Energy Resources, and Doosan GridTech. Other Energy Storage Systems Integrators are also ABB, Alfen, General Electric, and Schneider Electric. Concerning the battery cell manufacturing, some of the main players in the market today are, for lithium-ion based technologies: A123Systems, CATL, Electrovaya, Fiamm, Johnson Control, LG, Panasonic, Saft, Samsung, and Toshiba; for Flow Batteries: Cell-Cube, Primus Power, Rongke Power, UniEnery Technologies, and Vionx Energy; and for Sodium Sulfur batteries NGK Insulators. Regarding the only mechanical ESS presented in this document (i.e. the flywheels), some of the above-mentioned producers also offer flywheel solutions, while several small companies are being created for promoting specific products with innovative technologies.

A brief collection of commercially available ESS datasheets is attached to this Document, excluding the UPS and Residential applications (not relevant for the Project). The collected documents are not representative of the entire market, but have been included to provide some insights on the present state of the market regarding fully integrated ESS solutions.

4.4 Power converters for Energy Storage Systems

Energy Storage Systems require a proper interface device to be connected to a power system. Such an interface is a static power electronics converter, which allows to: 1) adapt the electric power characteristics between the ESS and the power system (e.g. in most of the ESS the storage side is in DC, while the power system is AC); 2) manage the storage system side, to allow the recharge and discharge of the energy storage elements within their operative limits; 3) properly regulate the electrical variables on the power system side, to allow the correct connection to the power system and the required power exchange. Additional elements can be also integrated in the control systems of such converters, if needed and not provided by other control systems, to autonomously provide functions like frequency regulation capabilities, peak shaving, and so on.

In the following the main converters technologies used to interface ESS to the power system are presented [43], considering topologies able to provide Low Voltage (LV – voltage < 1 kV) and Medium Voltage (MV – 1 kV < voltage < 35 kV) output. The difference among them lies in the complexity of the power conversion stages. Indeed, ESS are mostly LV systems. As an example, Lithium-ion battery cells range from 3 to 4 V per cell, which are the connected in series in order to reach higher voltages (which is usually in the range of 600 V). While a connection of more elements allows to reach MV voltages for the storage section, it also makes it more likely a failure of the entire ESS due to the failure of a single element. Thus, the storage section can be always considered in LV. Consequently, the connection to a LV system will require less components in respect to the connection to a MV one, because a voltage adaptation stage from LV to MV is not necessary.

The connection of an ESS to a LV power system can be either a single (for low power applications) or a three phase (for higher power applications) one. Given the levels of power required by the Case Study application, single phase converters are not considered here. Conversely, the connection to a MV power system is always a three-phase one. Moreover, since the ESS are characterized by a LV output, it is required to have an additional apparatus (either standalone or properly integrated into the converter) to assure the voltage adaptation up to the MV level. Regarding MV converters, in the following only the converters that have integrated LV/MV transformation stages will be presented. Indeed, the other solution is the coupling of an LV converter with a conventional LV/MV transformer at industrial frequency. In such a solution the LV converters are the ones already covered in the LV section, while the transformer is a standard three-phase one. Multi-pulse solutions using multi-three-phase transformers are also possible However, being these well-known solutions, it has been deemed not required to provide additional explanations.

The power electronics converters can be divided into three different categories: standard topologies, multilevel topologies and multiport topologies [43]. Standard topologies are usually known as two-port converters due to the input port that connects to the energy source and the output port that connects to the load. The structure of the power converter can be divided into single stage or double stage. In the single stage, only a unique power converter is used to control the charge and discharge of the storage system and at the same time to connect to the AC grid. In the double stage, two power converters are used: a DC/DC converter to control the charge and discharge of the storage systems and a DC/AC converter to interface with the AC grid. The multilevel topologies are normally used for high voltage applications. These topologies allow synthesis of a desired AC voltage from several levels of DC voltages and reduce the voltage blocking of the power switches. Finally, the multiport topologies allow the processing of the energy from multiple energy sources or to a multiple load. For what it concerns multiport topologies, their goal is to integrate in a single design multiple sources and/or loads, interconnecting and controlling them as a whole. While a similar situation may be present in a real application, multiport converters have yet to reach a commercial maturity. Thus, they have not been considered in this report.

4.4.1 Standard topologies

Single stage

The non-isolated single stage topologies are the simplest and most efficient for the interfacing of energy storages with AC systems. For the three-phase systems, the three-phase bidirectional AC/DC converter is the most convenient choice (Figure 15) [44], [45], [46]. In several applications the neutral wire is required, in that case the single capacitor in the DC side of the converter must be replaced with split capacitors. Under unbalanced AC load conditions these capacitors will absorb the current from the neutral wire to balance the AC output. The split capacitors will face an excessive current stress at a highly unbalanced AC load or supply grid, which is the major drawback of this topology. The problem could be solved by adding one transistor leg (neutral leg) instead of split capacitors [47], [48]. By proper control of the neutral leg, the three-phase outputs could be more easily equalized, which will finally result in size and weight reduction of the passive components. During the energy transfer from storage to the AC grid, the converter behaves like a voltage source inverter (VSI), which can normally perform only the voltage buck function. Thus, the voltage on the DC side has to be higher than the AC output voltage. This means that such a converter can be used as it is only for LV applications, since increasing the voltage of the energy storage component (by connecting more elements in series, if considering an electrochemical ESS, or by dimensioning the electrical machine for higher voltages, if considering FES) it is not convenient for several reasons.

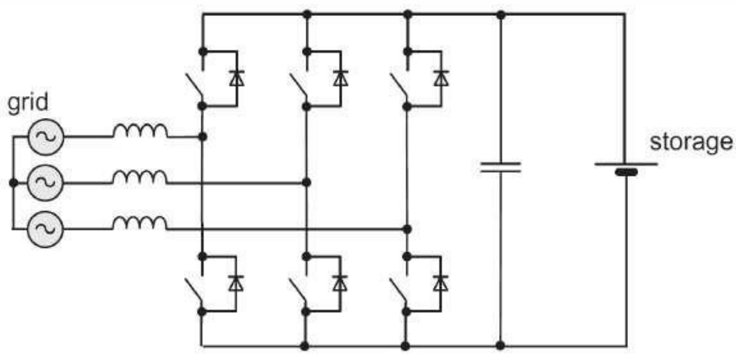

Figure 15 - Three-phase bidirectional single stage AC/DC converter [43]

To overcome some of the limitations and problems of the VSI configuration, the Z-source inverter (ZSI, Figure 16 a) has been proposed [49]. In particular, such topology provides a boost function, which means that it can provide a voltage on AC side that is higher than the DC side one, when injecting power into the system. Further improvements can be achieved by the quasi-Z-source inverters (qZSI, Figure 16 b) [50], [51], like reduced passive component ratings, continuous input current, and a common DC rail between the DC source and the inverter. Both the ZSI and qZSI have wider regulation freedom in respect to the Figure 15 converter, thus providing better utilization of the energy storage. While being originally unidirectional converters, due to the presence of a diode in the impedance networks, the ZSI and qZSI can be made bidirectional by adding a switch across the diode. In such a way the converter can operate in rectifier mode, and recharge the battery [52].

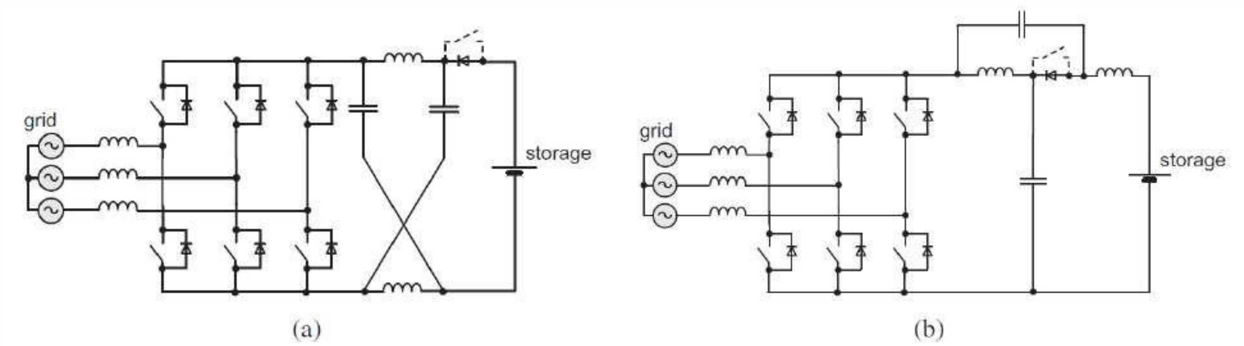

Figure 16 - Three-phase impedance source bidirectional AC/DC converters: ZSI (a) and qZSI (b) [43]

The bidirectional matrix converter (Figure 17) is another alternative approach to the single-stage AC/DC power conversion. The topology is derived from the well-known three-to-three AC/AC matrix converter. It has a low-pass LC filter between the DC terminals and the DC source/load terminals, with no intervening impedance except for snubbers and wiring [53]. Both polarities of voltages and currents may be controlled during the bidirectional operation of the converter [54]. Moreover, the bidirectional AC/DC matrix converter could be further modified by replacing the LC filter with a HF transformer, and then inserting a four-quadrant-switch H-bridge between the HF transformer and the DC side, thus achieving a multi stage topology (which are discussed in Section 4.4.2).

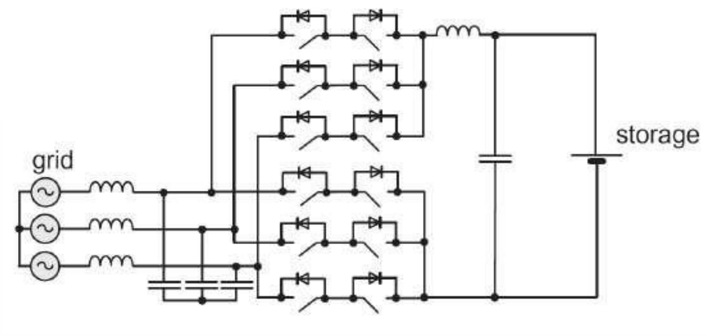

Figure 17 - Bidirectional AC/DC matrix converter [43]

By adding a Z-source network to the DC side of the bidirectional AC/DC matrix converter, a new topology of the matrix-Z-source bidirectional AC/DC converter could be derived (Figure 18) [55]. Thanks to its internal switch, it can achieve the voltage boost behavior for the inverter operation (switch set to position 1), used when the power has to be injected in the system. In the rectification mode (switch set to position 2), the converter can properly regulate the DC voltage.

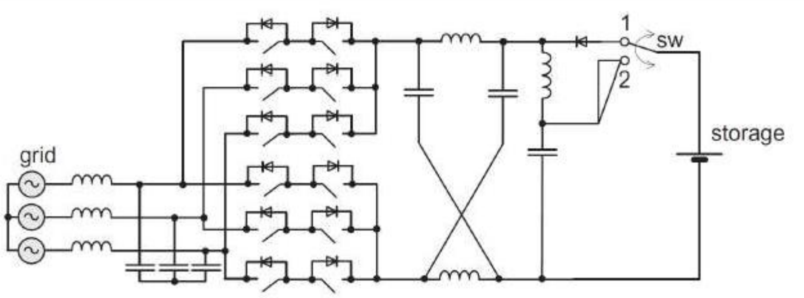

Figure 18 - Bidirectional AC/DC matrix-Z-source converter [43]

The single stage configuration presents several advantages: low device count, low cost, and reduced losses. However, this type of converters is limited to LV applications due to the lack of a voltage adaptation stage for reaching MV level.

Double stage

A two-stage interface converter (Figure 19) consists of a DC/DC conversion stage and a DC/AC or inverter stage. The DC/DC stage boosts the storage DC voltage to a level that is suitable for the direct interface of the DC/AC stage to the LV power system [56]. In general, the DC/DC stage topologies can be divided into two main groups: non-isolated and isolated. In the literature many non-isolated bidirectional topologies have been studied and proposed for the DC/DC stage, e.g.

half-bridge, Cúk, SEPIC, etc. However, at present the most practical topology for the DC/DC stage is the conventional bidirectional buck-boost topology.

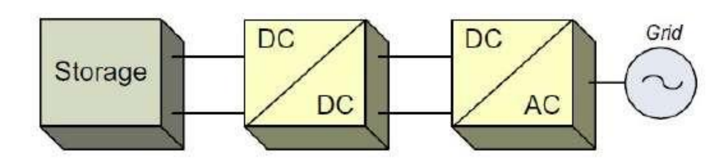

Figure 19 - Structure of a two-stage interface converter for energy storage [43]

The bidirectional half-bridge topology (Figure 20 a) is the most widely used solution due to its simplicity and relatively high efficiency (over 90%) [57]. The converter operates in buck mode when charging the energy storage and in boost mode when drawing energy from the storage device. A low component count and a simple structure result in a reliable and low-cost solution, thus making this topology the most popular one in many applications. However, the boost capability is limited, and it is not a fault-ride-through converter. Indeed, in the case of a short circuit in the DC-link between the two conversion stages, the energy storage results shorted as well. This problem can be solved with a double bidirectional half-bridge converter, as shown in Figure 20 b.

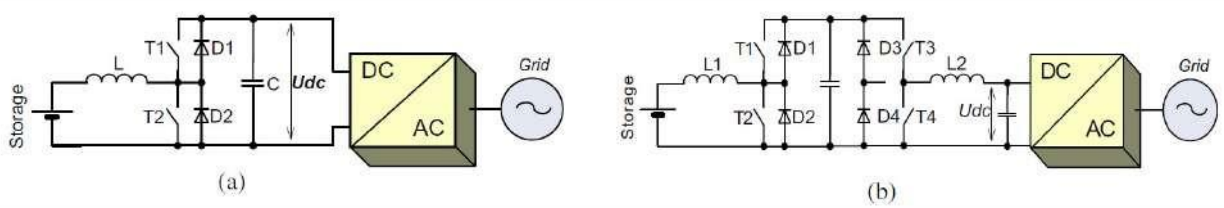

Figure 20 - Step up DC/DC converters for energy storage: bidirectional half-bridge (a), double bidirectional half-bridge (b) [43]

Quite similar to the bidirectional half-bridge converter is the bidirectional buck-boost converter (Figure 21 a). It can work as a buck or boost in both directions, depending on the control of its switches, making it a good solution for applications where voltage on the energy storage side can vary in a wide range (e.g. it is a good solution for supercapacitors). It shares the same advantages of the previous solution (low component count and simplicity), while presenting the reversed output voltage characteristic of the classical buck-boost converter [58], [59].

Similar bidirectional step-up and step-down functionality can also be achieved with the bidirectional buck-boost cascade converter. This topology is accomplished by cascading a buck and a boost converter, as shown in Figure 21 b. The proper operation is then achieved by controlling which switches are being used at each time. This version has more components than the bidirectional buck-boost converter. On the other hand, the components have lower electric and thermal stress, and the output voltage is not reversed. The most differences are in step-up operation, where the current rms value in the inductor, power switches and the output capacitor is about 33% greater in the bidirectional buck-boost converter. Thus, even if the buck-boost cascade topology has more components, a reduced size inductor and capacitors can be used, thus gaining back the cost increment [59], [60].

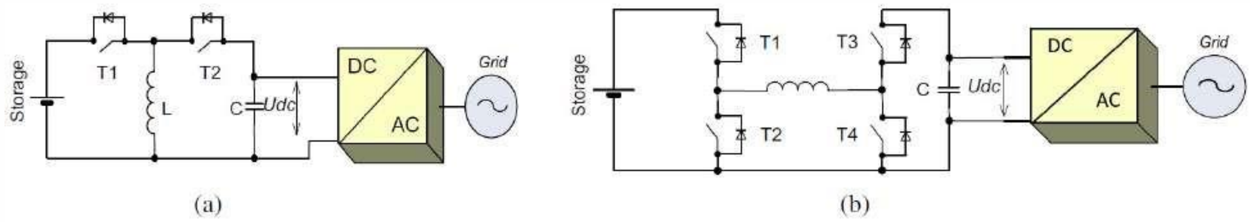

Figure 21 - Step-up/step-down DC/DC converters for energy storage: bidirectional buck-boost converter (a), bidirectional buck-boost cascade converter (b) [43]

Other variations in switches and passive components number, placement, and connection are possible, leading to many different additional topologies for non-insulated DC/DC converters that have both pros and cons. However, the presented ones are considered sufficient to highlight the large number of possible choices an ESS' designer has. Instead, it is significant to present some of the insulated converter topologies, since they are the base of the converters for MV applications with an integrated voltage transformation stage.

In some applications the isolation of the energy storage is required. In this case a medium frequency transformer together with appropriate power electronics has to be implemented. In general, four topologies and their variations can be considered in this case: a half-bridge, a full-bridge, a push-pull half bridge, and a push-pull full bridge topology [61], [62]. However, the push-pull half-bridge topology has quite low efficiency and suits best for low power applications. Therefore, it is excluded from the following.

The most widely used solution is the bidirectional buck-boost converter combined with a dual active bridge (DAB), as shown in Figure 22 [63], [64]. The bidirectional buck-boost regulates the input voltage of DAB and keeps it constant. This allows the DAB to work in its maximum efficiency operating point. The transformer integrated in the DAB provides additional voltage adaptation capability, which goes well beyond the levels achievable by a simple boost stage, and isolation. Thus, this solution is useful in the cases where a high boost ratio (such as for connecting a LV energy storage to a MV system) or isolation is required. The main drawback is the relatively high component count, which increases losses. Moreover, if such a solution is used for interfacing the ESS to a MV power system, the DC/AC converter must be designed for operating with the MV.

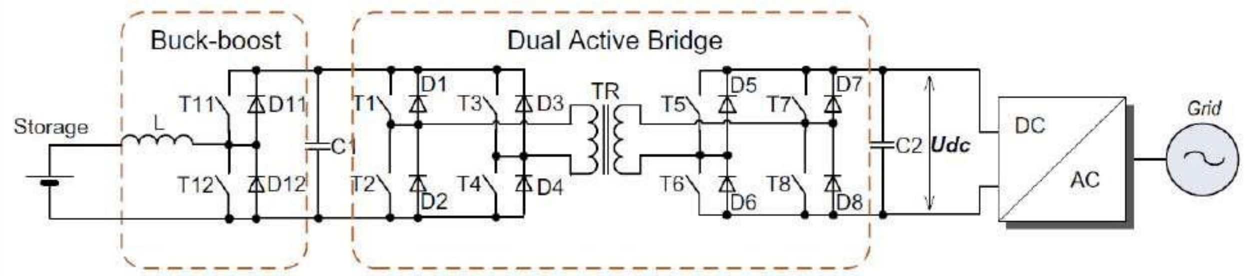

Figure 22 - Bidirectional buck-boost with DAB [43]

A good alternative to the DAB is a dual half bridge (DHB). This converter group can be divided into: voltage-fed (Figure 23 a) and current-fed (Figure 23 b) DHB [65], [66]. In general, the DHB uses half the switches than the DAB, while presenting bulkier DC capacitors and twice higher current in the switches [67]. Current-fed DHBs have several advantages over voltage-fed DHBs: they can achieve smaller current ripple for energy storage, they provide current mode control allowing the state of charge (SOC) estimation in a dynamic environment, thus energy storage performance and life cycle can be improved. Moreover, it can boost DC capacitor voltage on the transformer primary side to reduce current requirement for the isolated transformer, resulting in improved transformer efficiency [68], [69].

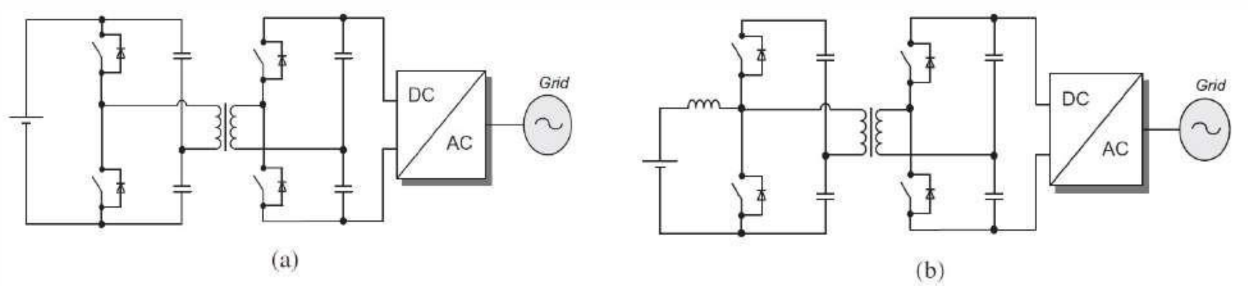

Figure 23 - Dual half-bridge converters: voltage-fed (a) and current-fed (b) [43]

Table 2 - Comparison of isolated DC/DC converters [43]

Primary side	Secondary side	Efficiency	Application
Push-pull	Half-bridge	Charge 90%, discharge 87%	Low power
Half-bridge	Half-bridge	Charge/discharge 92-94%	High/medium power
Full-bridge	Full-bridge	Charge/discharge 95%	High/medium power

A comparison of the three considered isolated DC/DC converters, regarding efficiency and applications, is depicted in Table 2. The double stage technology presents several advantages when compared with the single stage configuration. One of the most important advantage relays on the fact that the double-stage technology allows for a DC distribution configuration, since a step-up DC/DC converter can be connected to each storage elements and connected in parallel. Thus, different storage elements can be connected to a single DC bus, allowing for the use of a single DC/AC converter module. However, if the instantaneous voltages at the outputs of the DC/DC converters are different circulating currents will appear, and this interferes with the operation of the overall system. Thus, the control system must be designed in order to prevent this drawback. This technology also allows avoiding the series connection of storage elements, since several DC/DC converter modules can be used in parallel to control independently each element. This procedure is more reliable than the series connection and allows for fault tolerant operation using redundant storage elements and DC/DC converter modules. These double stage topologies allow a better measure of the state of charge (SOC) of the different storage elements, being this an important advantage. This configuration has the disadvantage of requiring a high number of devices, although these devices have lower power rating. Finally, double stage configuration can be used for MV applications in DAB and DHB configurations.

4.4.2 Multilevel topologies

The general function of a multilevel voltage source converter is to synthesize a desired AC voltage from several levels of DC voltages. Initially, this power converters were mainly used in industry for AC drives [70], [71], [72]. However, due to their characteristics (such as low required ratings for solid state switching devices, very low output voltage distortions, and low switching frequency) have begun to be used for other kind of applications [73]. Multilevel power converters can be an important interface for the electrochemical energy storage systems, since capacitors, batteries, fuel cells or other storage equipment can be used as the multiple DC voltage sources. Indeed, as previously stated the single electrochemical cells are characterized by low voltages, making it possible to separately connect small series of cells to the multilevel converter, in place of connecting in series high numbers of cells to reach a voltage suitable for normal converters. During the last years many multilevel converter structures have been proposed. However, the most widely used and common topologies are the cascaded H-bridge multilevel inverter, the neutral point clamped multilevel inverter, and the flying capacitor multilevel inverter.

The cascaded H-bridge converter (CHB) structure was introduced by Baker and Banister through a patent in 1975 [74]. Subsequently, this structure has been extended for three-phase systems [75], [76], [77]. This structure is based on the series connection of several H-bridges, each with a separate DC source. Due to this configuration and the characteristics of the multilevel inverters, this structure is suitable for electrochemical energy storage systems. Figure 24 shows a three-phase cascaded H-bridge multilevel inverter proposed for ESS [78], [79], [80], [81]. The structure consists of a series connection of several storage elements each connected to its dedicated power converter module. This overcomes the disadvantage of series connected storage systems, where the fault in one element cause the failure of the entire system (until the element is replaced or bypassed). Another advantage is the possibility of building a transformer-less energy storage system for MV applications. In Figure 25 four possible converter cell structures are shown. In Figure 25a it is shown a structure where the energy storage unit is connected directly to the H-bridge. In such a way the converter module both generates an AC voltage and controls the charge and discharge of its energy storage unit. The second structure (Figure 25b) uses a double-stage scheme for the module, decoupling the control of storage and AC sides and allowing the AC section of the converter to operate better. The third structure (Figure 25c) uses an interleaved boost converter that allows reduction of the inductor current ripple (reducing its core size). Figure 25d shows the fourth structure, based on the dual active bridge. This structure is the one that allows to obtain both galvanic isolation and the use of significant lower voltage energy storage units compared with the total AC output voltage. Moreover, if properly controlled H-bridge multilevel converters have significant fault-tolerance levels, being able to continue operation also with faulty elements [82].

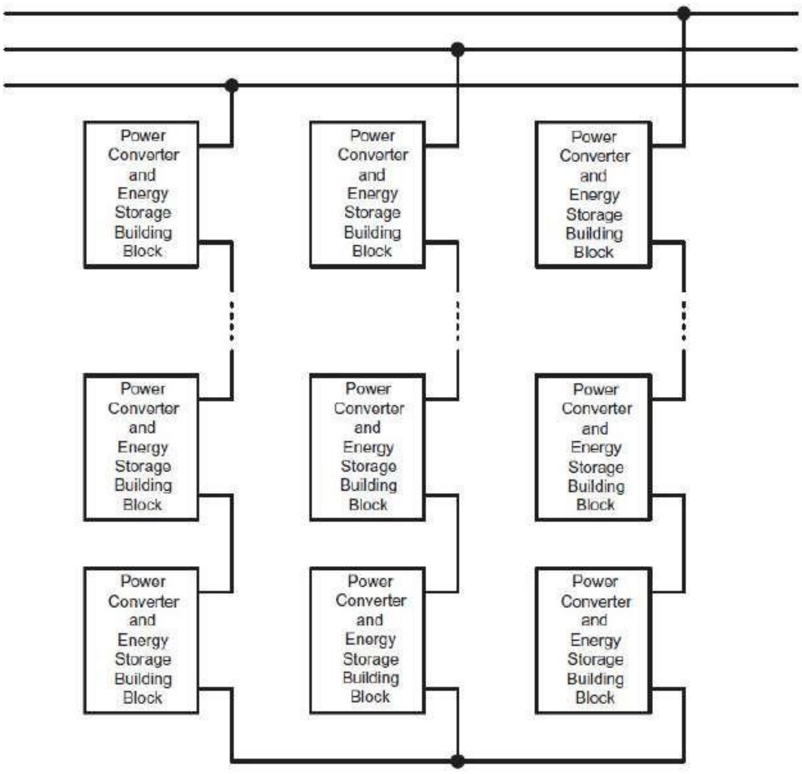

Figure 24 - Energy storage system based on the cascade H-bridge multilevel inverter [43]

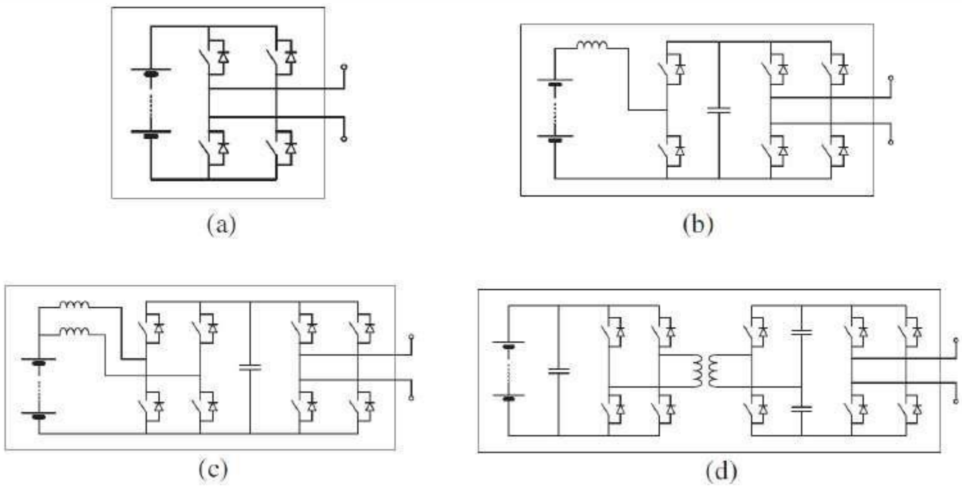

Figure 25 - Converter cell structure: (a) single-stage converter cell; (b) basic double-stage converter cell; (c) interleaved converter cell; (d) isolated converter cell [43]

The neutral point clamped (NPC) multilevel inverter proposed by Nabae, Takahashi and Akagi in 1981 [70] was basically a three-level diode clamped inverter. However, in the years several new structures, derived from this and presenting more voltage levels, have implemented. The base concept on which this type of converters is built is the use of a series string of capacitors to divide the DC side voltage into several levels. This also means that a charge-balancing control system for the capacitors is required, which is one of the major disadvantages of this topology. Figure 26 shows the structures of a single-stage grid connected NPC converter and of the Active Neutral Point Clamped (ANPC) converter [83], [81], [84]. Due to the additional switches, the ANPC has better loss distribution among the devices, allowing for a higher semiconductor switch utilization [85]. Storage systems based on the diode clamped multilevel inverter with a two-stage converter structure were also proposed by [86] and [87] (Figure 27a). In [81] a structure based on the ANPC using galvanic isolation is presented (Figure 27b). An alternative topology to the NPC was introduced by Meynard and Foch in 1992, with the flying capacitor multilevel inverter (FC) [88]. The structure is similar to an NPC, but uses capacitors in place of the clamping diodes to divide the input DC voltage. In Fig. 18 a three-phase flying capacitor multilevel inverter is represented [83].

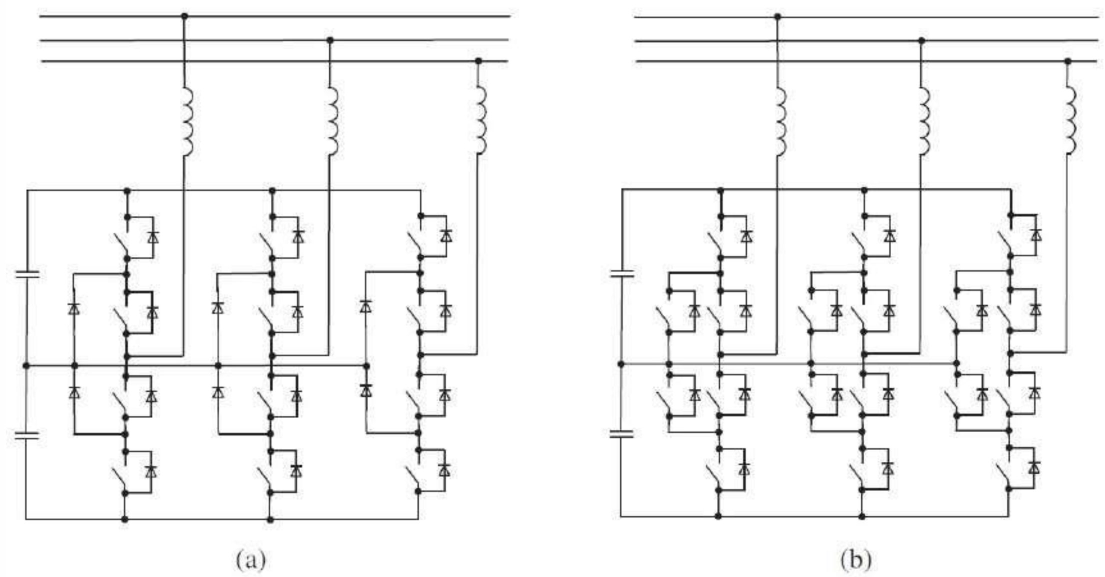

Figure 26 - Energy storage system based on a single multilevel converter stage: (a) NPS; and (b) ANPC [43]

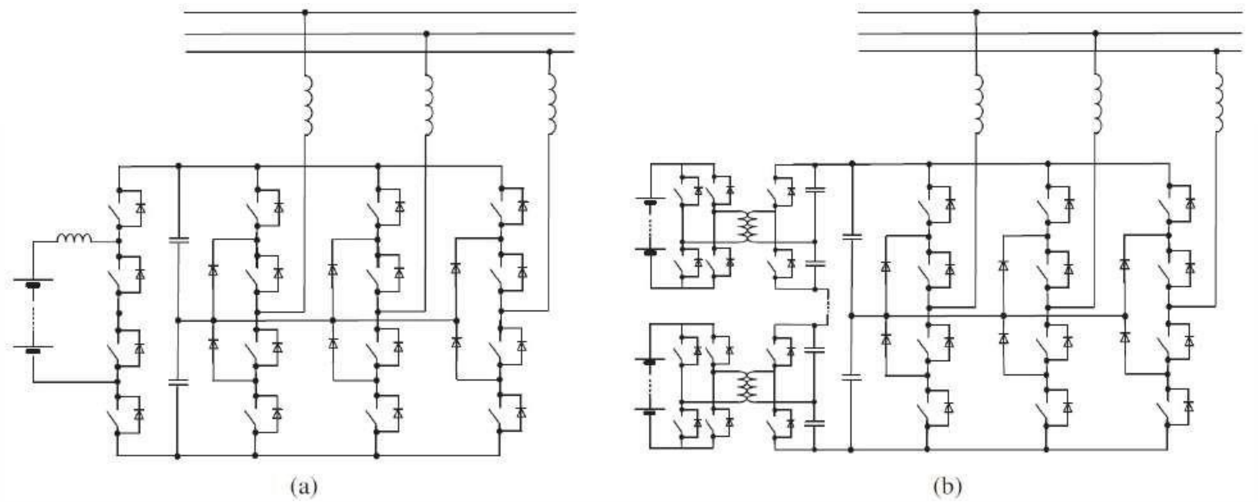

Figure 27 - Energy storage system based on a two stage multilevel converter: (a) without galvanic insulation; and (b) with galvanic insulation [43]

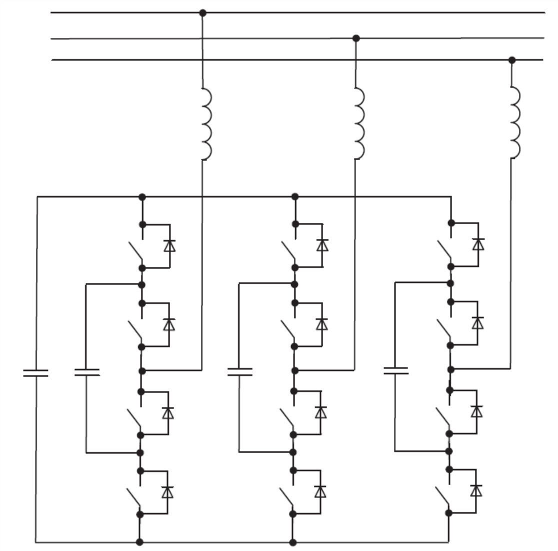

Figure 28 - Three-level flying capacitor multilevel converter [43]

Based on the previous multilevel structures, a hybrid converter was proposed through a patent in 2002 [89]. The modular multilevel converter (MMC) is based on the combination of the cascade H-bridge converter and the flying capacitor converter. It consists of a series connection of identical modules based on half-bridge cells and an inductor (Figure 29). Due to his structure, this converter is suitable for MV applications [90], [91], [92]. Three different possible converter cell structures have been presented at present [93]. Figure 30a shows the structure with the reduced number of active components. The second structure is an extension of the first one, where an interleaved boost converter is used to reduce the inductor current ripple (Figure 30b). The third structure (Figure 30c) is based on the dual active bridge converter, allowing high efficiency and high boost ratios to be achieved.

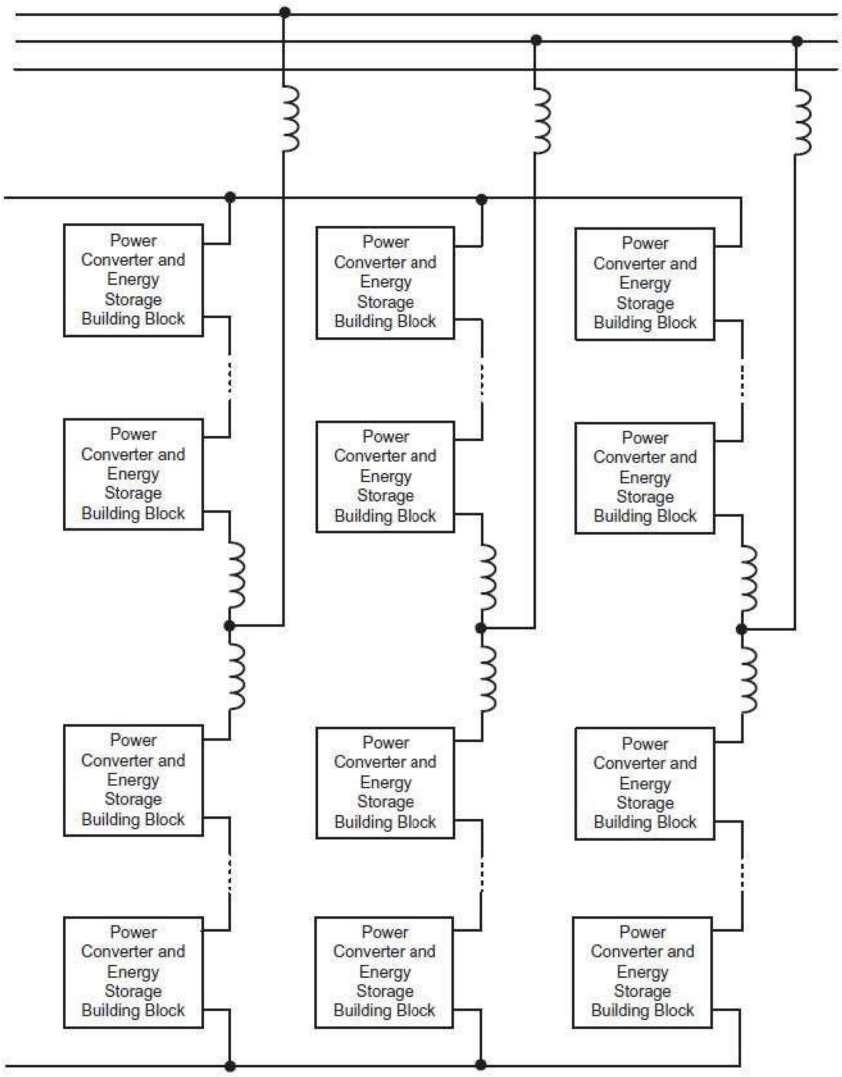

Figure 29 - Energy storage system based on a modular multilevel converter [43]

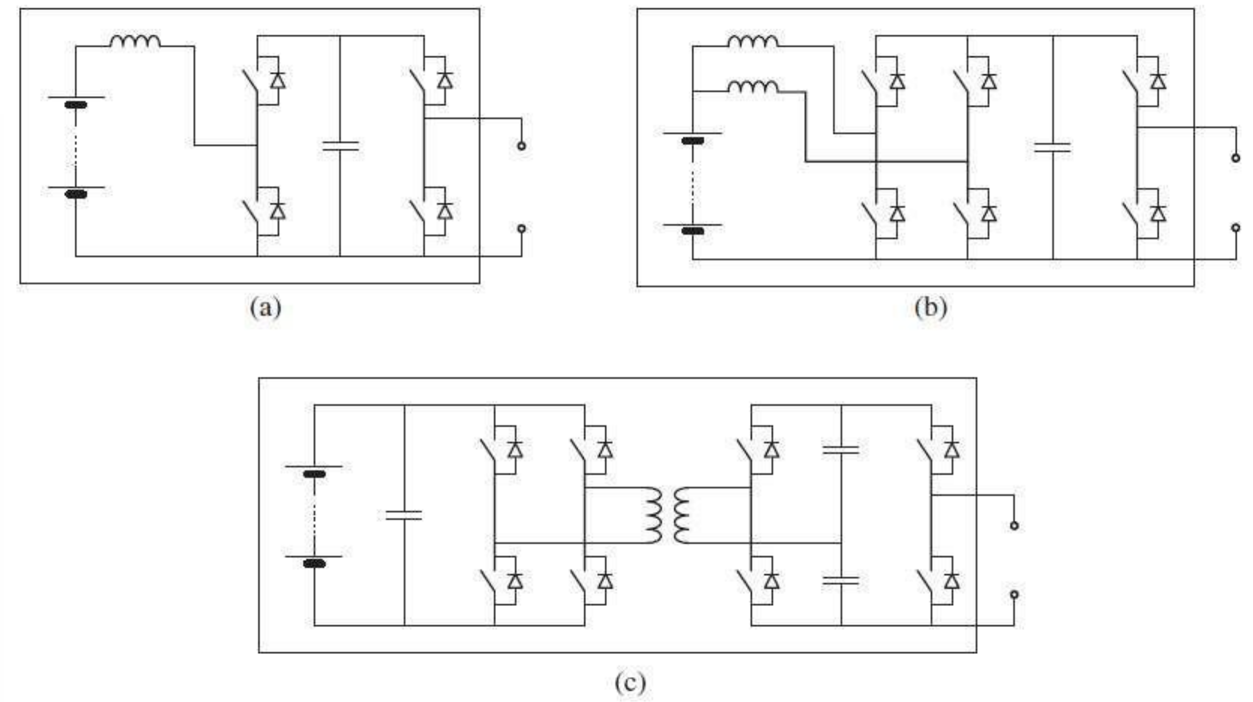

Figure 30 - Converter cell structure (a) basic double stage converter cell, (b) interleaved converter cell, and (c) cell using a converter with isolation [43]

Multilevel topologies present several advantages. The cascaded H-bridge converter structure and the modular multilevel converter have a modular structure, which allows to reduce manufacturing cost. Moreover, the redundant levels can be used to increase reliability, to achieve a better state of charge (SOC) tracking for each storage element, to reduce AC voltages' harmonic pollution, and present low electromagnetic interference output. The increased cost due to the increased number of switches is usually considered as a disadvantage, despite being able to use lower rated (thus cheaper) switches. Another disadvantage is the high ripple present in the storage elements. Analyzing the advantages and disadvantages between the several multilevel topologies, the CHB and MMC topologies are characterized by modularity, small output filter, good failure management in systems with a high number of cells. However, they present disadvantages like second harmonic current ripple on storage cells, and high number of devices. The MMC also presents the disadvantage of current circulation in each phase. The NPC presents as advantages a high efficiency and a low cost, while having as a disadvantage the unequal loss distribution in devices and the limit to maximum three levels. The ANPC allows to overcome the problem of the unequal loss distribution in devices, at the price of an increased number of components. The FC presents as advantages the modularity of active devices, a smaller output filter, and a substantial gain in equal loss distribution. However, it requires big flying capacitors and a dedicated control system for their management. Finally, due to their modular structure multilevel converters can be easily used for interfacing ESS with MV systems, by installing a sufficiently high number of series connected stages.

4.5 Examples of existing Industrial Storage Systems

4.5.1 Industrial Storage Systems (ISS) in Germany.

In this section the evaluation of the results of a research about present ISS in Germany is given [12]. The analyzed dataset contains only 196 ISS projects, thus being not fully representative of the entire German ISS market. Nevertheless, some useful information about the wide range of system designs that ISS cover can be inferred, as well as the capacity-dependent prices.

Power and capacity.

Figure 31 shows the wide capacity and power range of the single ISS projects. The majority of the projects is in the class below 100 kWh and 100 kW, although single projects have capacities around 800 kWh to 900 kWh and powers between 700 kW and 800 kW. Most ISS for the PV self-consumption have lithium-ion batteries and are relatively small, starting in the range below 10 kW / 10 kWh and end with a single system at 500 kW / 500 kWh. These projects are mainly installed by commercial businesses. The ISS for smart grid and renewable energy sources (SG / RES) integration, on the other hand, are often research projects within the distribution grid. They show mostly larger capacities and powers above 100 kWh, and often use lithium-ion batteries. Their size depends largely on the size of the PV or wind plant they are connected to. The projects of EV charging are both research and commercial projects for charging stations with 100 % renewable energy supply and buffer storage for fast charging stations (such a type of application is significant, and it is recalled in Section 6.4.2, page 74). Their system designs are mainly in between the self-consumption and SG/RES integration projects, although there is also one project with 200 kW / 600 kWh. These projects use mainly redox-flow and lithium-ion batteries.

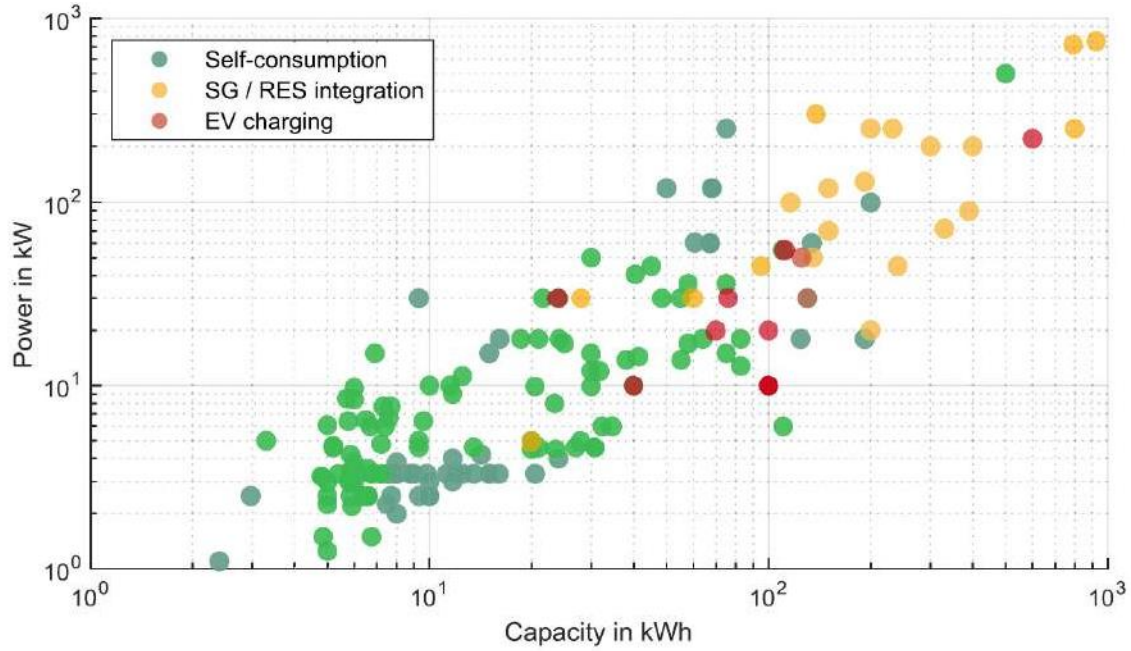

Figure 31 - ISS projects in Germany, sorted by capacity and power according to application [12]

Energy to power ratio and specific prices.

Figure 32 (left) combines the information on battery technology, application area, and the energy to power (E/P) ratio. The circle size indicates the installed battery capacity. The shown ISS projects cover a wide range of E/P ratios, up to nearly 11 h in the considered dataset. While most ratios are between 1 h and 6 h, six lithium-ion projects in applications of SG / RES integration, EV charging, and self-consumption have ratios below 1 h. The evaluated redox-flow batteries serve in SG / RES integration with E/P ratios of 2 h to 4.5 h and EV charging projects that are between E/P ratios from 2.5 h to 5 h, with the exception of one 10 h project. Figure 32 (right) shows the specific system prices incl. VAT for the 120 lithium-ion ISS that are operated to increase PV self-consumption. The prices were gathered from mid-2018 until the beginning of 2019, thus no development is shown here. Further, the circle size indicates the installed converter power of these projects. The lithium-ion ISS cover prices from 770 €/kWh to 2,200 €/kWh, while most of the systems are between 1,000 €/kWh and 1,500 €/kWh. Especially ISS in the capacity classes of HSS have a large price spread covering the smallest and largest specific price shown. The evaluated larger ISS have in average larger power and slightly lower price. However, the presented projects do not cover capacities larger than 140 kWh. Price information about the other systems are not available in the source [12].

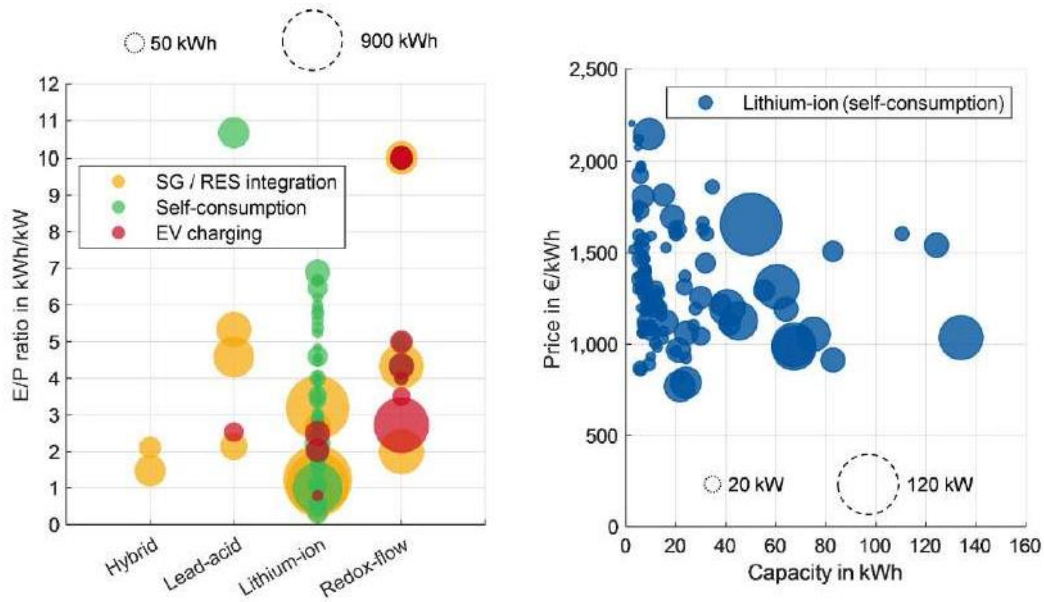

Figure 32 - ISS projects in Germany, sorted by battery technology and E/P ratio according to application areas (left), and specific prices of Lithium-ion ISS depending on the capacity (right) [12]

4.5.2 Energy storage database of Sandia National Laboratories, for the U.S. Department of Energy/National Nuclear Security Administration.

Regarding battery energy storage systems (BESS) installations and pilot projects, information (about power and energy rating, location, applications, owner, storage technology, and status) of installations located worldwide are contained in the database on energy storage installations maintained by National Technology & Engineering Sciences of Sandia, LLC (NTESS), operator of Sandia National Laboratories for the U.S. Department of Energy/National Nuclear Security Administration [94]. In the following only the active installations, with sufficient information, adopting electrochemical technology and power rating less or equal to 5 MW are considered. At the time of consultation done in [14] (in 2019), this resulted in a set of 466 projects.

The results in terms of services performed by the storage and their technology are displayed in Figure 33. What stands out from Figure 33 (a) is the fact that there the use cases are evenly spread. The most frequent services are six services: electric bill management, energy time shifting, frequency regulation, microgrid capability, renewable generation shifting, and renewable capacity firming. On the other hand, Figure 33 (b) clearly shows that lithium-ion technology (in all its variants) is by far the most common solution. Moreover, Figure 34 shows that BESS are often deployed as multifunctional systems, with nearly half of them being used for both commercial and technical services. Such results strengthen the decision to evaluate also the possible ancillary services for these systems, which will be done in Activity 5.4 of the present Research Project.

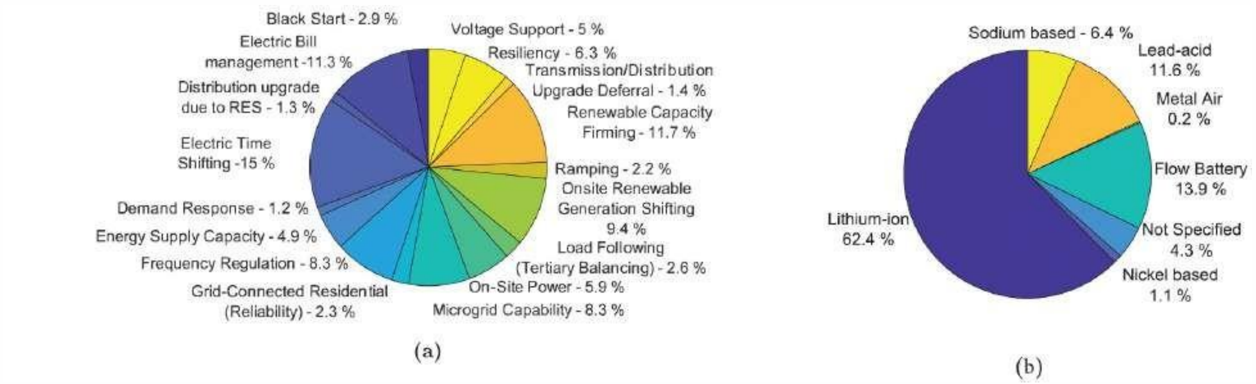

Figure 33 - Energy storage applications (a) and technologies (b) [14], [94]

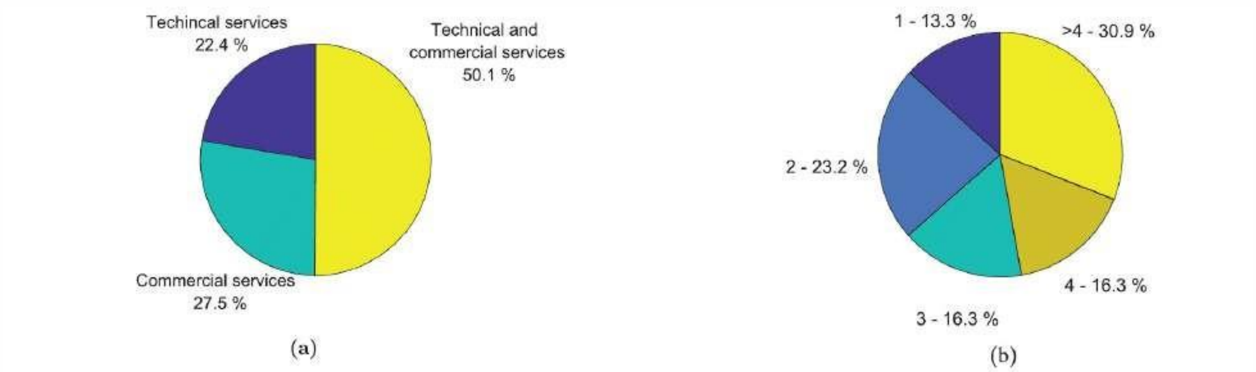

Figure 34 - Percentage of battery ESS installations performing technical and commercial services (a) and number of services performed by each single installation (b), [14], [94]

4.5.3 Energy Storage Systems in Italy

The section of ANIE (i.e. the Italian National Federation of Electrotechnical and Electronic companies) dedicated to renewable energies periodically produces a report about the numbers of energy storage installations in Italy that are combined with renewable energy systems [95]. On September 2019, the Italian TSO database lists 22.774 installed storage systems. The total power of the installed storage systems is 103 MW, while the maximum used capacity is 222 MWh. The monthly data show a fluctuating but positive trend in the third quarter (Q3). Indeed a rising trend can be find in terms of number of storage systems installed (+ 12% in Q3 compared to Q2, while -14% in Q2 compared to Q1), in terms of power (+ 19% Q3 / Q2; -7% Q2 / Q1), and in terms of capacity (+ 134% Q3 / Q2; -21% Q2 / Q1). Almost all of the storage systems (97%) have power <20 kWh, and are combined with residential-sized photovoltaic systems. Regarding their technical configuration most of them are connected on the renewable generator side, in direct current (58%). Up to 13% of the energy storage systems are installed on the AC side of the renewable generator, while the remaining 29% of them are installed upstream. Lombardy is the region with the largest number of installed systems (7,524 ESS for 30.1 MW total power and 57.6 MWh total capacity), followed by the Veneto Region (3,397 ESS for 15.2 MW total power and 24.8 MWh total capacity). Third and fourth place belongs to Emilia Romagna Region (2,594 ESS corresponding to a power of 12.3 MW and a capacity of 30.9 MW) and to Piedmont (with 1,708 ESS, corresponding to 8.1 MW and 13.0 MWh).

Regarding large scale energy storage systems, information can be found also on the Italian TSO site [96]. In particular, some pilot projects are in course, with the aim of installing LSS interfaced to the Transmission network. While such an application is outside the scope of this report, some information is given to provide an overview on the trends in ESS integration in Italy.

The plans for integrating ESS in the transmission system by Italian TSO started with the 2011 Development Plan for the Transmission Network (i.e. “piano di sviluppo della rete di trasmissione nazionale”). With such a plan a pilot project for installing LSSs was started, which led to the installation of three storage systems (SANC – “Sistema di Accumulo Non Convenzionale”) connected to the 150 kV sub transmission network: Ginestra SANC, power 12 MW and capacity 80 MWh, installed in Castelfranco in Miscano (BN); Flumeri SANC, power 12 MW and capacity 80 MWh; Scampitella SANC, power 10,8 MW and capacity 72 MWh. At present these LSS are operating in remote control, not only for delivering services like peak shaving and frequency regulation, but also for experimenting on innovative functions. The second big plan for LSS installation by the Italian TSO was set with the 2012-2015 Plan for the Defence of the Security of the National Electrical System (i.e. “Piano di Difesa per la Sicurezza del Sistema Elettrico Nazionale”). The plan aims at installing up to 40 MW of ESS, to improve the regulation margins for the transmission system. The project has been subdivided in two phases, where the first aims at building an experimental Storage Lab (for a total of 8 MW in Sicily and 8 MW in Sardinia) endowed with different storage technologies. At present 12.5 MW / 18,2 MWh of ESS have been installed, using 9,2 MW of Lithium-ion batteries and 3.4 MW of ZEBRA (Molten-salt) batteries. The experimental installation of Redox Flow batteries is in course, and the total 16 MW goal is planned to be reached integrating also supercapacitors. The second phase will be performed after the experimentations on the Storage Lab, using the most suitable technologies for the integration of the remaining 24 MW in the Italian TSO control systems.

5 Power quality issues

From a broad perspective, power quality is related with the management of the deviation of electrical system variables in respect to the normal operation. The latter can be represented in general by: voltage level fluctuation; frequency fluctuation; harmonic distortion; transient overvoltage; unbalance load; variable reactive loads.

The importance of power quality issues is increasing along with the increase in renewable sources exploitation at distribution level (e.g. production decentralization). Indeed, these sources are commonly interfaced to the grid by means of power conversion stages, which behave differently than conventional loads (either static or rotating ones). As a result of a disturbance in the system (short circuits, voltage dips, disconnection of power plants, or major variations in loads consumption) these energy sources can react by disconnecting themselves, possibly worsening the disturbance effects up to a general failure of significant sections of the power grid. Moreover, the converters non-linear behavior leads to the generation of harmonic distortion for the system, because their commutating operation is far from the sinusoidal variations expected by conventional power systems.

In regards to the specific application in study (charging stations and peer infrastructure), most of the above-mentioned issues can be ignored. In fact, these are problems that must be solved by the distribution system operator (DSO), either with modifications in the power system or by setting new standards for the users' interconnection. However, one specific issue is significant also for the user: the harmonic distortion.

Following approach used also for managing the other issues, the DSOs set limits for the harmonic currents that a user can inject in the grid. However, such limits are to be satisfied at the point of common coupling (PCC) between the DSO and the user, which is the electrical point where the user's power system is connected to the distribution one. This means that the harmonic distortion inside the user's system is an issue for the user itself, and may or may not be a problem also if the DSO limits are complied with at the PCC. Indeed, the composition of harmonic disturbances depends on several different factors besides the harmonic distortion sources, like the phase of the disturbances, the power system impedances, the presence of filters, and so on.

While an in-depth analysis of such a phenomenon is not in the scope of this document, a brief explanation about the possible harmonic disturbance sources that can be introduced in a modern port electrical infrastructure can be given. Reference is made to the power system components presented in the previous sections, i.e. ship charging stations (shore connection apparatuses) and ESS.

5.1 Shore connection systems

As mentioned in Section 3, standard shore connection systems can either be at 50 or 60 Hz, depending on the frequency used by the ship power system. Such a distinction is relevant for large ships, which may be berthed to different ports in different countries during their operations, thus making it important to have an interface able to provide to both standards.

Regarding small ships and boats, their area of operation is usually limited, thus making it convenient to design them using the same frequency standard as the land power grid, to avoid unnecessary conversion stages in the shore connection apparatus. However, the interest in DC shore connections is rising, due to both the introduction of onboard ESS (which are inherently DC systems) and other advantages related to the DC distribution onboard exploitation [97].

Thus, from the harmonic disturbance point of view it is useful to subdivide the shore connection apparatuses in AC ones at line frequency (i.e. 50 Hz in the considered area), and the others (AC ones at different frequency in respect to the land power grid, DC ones).

AC shore connections at line frequency do not present any issue in regards to harmonic distortion, as they lack power electronics converters. Indeed, the power system components are only the ones devoted to protection (like breakers, or safety equipment) and to the possible need of voltage adaptation (transformers). There may be an issue of harmonic disturbance propagation by means of such shore connection systems, if the berthed ship has onboard converters. However, such an issue cannot be managed from the port side without knowing all the possible power system configurations of all the ships that may possibly be berthed in the future. Thus, also in this case a solution similar to the one used by DSOs can be applied: the ship owner must comply with the harmonic limits at the shore connection coupling point.

AC shore connection at different frequency in respect to the land power grid and *DC shore connections* share the same harmonic distortion issues in respect to the port power system.

Indeed, both of them are based on converters that have a rectifier as a first interface stage with the power system.

The most popular rectifier topologies [98] used in industrial applications are the following:

1. *6-pulse full-wave rectifier* fed by a three-phase two winding delta-wye transformer (Dyn11). Refer to Figure 38.
2. *12-pulse delta/wye parallel full-wave rectifier* fed by a three-winding, six-phase transformer with a delta primary along with a delta secondary and a wye secondary (Dd0yn11). Each three phase secondary feeds a 6-pulse full-wave rectifier, and each rectifier is connected in parallel with the load. Refer to Figure 39.
3. *12-pulse delta/wye series full-wave rectifier* fed by a three-winding, six-phase transformer with a delta primary along with a delta secondary and a wye secondary (Dd0yn11). Each three phase secondary feeds a 6-pulse full-wave rectifier, and each rectifier is connected in series with the load. Refer to Figure 40.
4. *12-pulse auto-xfmr half-wave rectifier* fed by a twelve-phase polygon auto-transformer. The rectifiers are connected in parallel with the load. Refer to Figure 41.
5. *18-pulse auto-xfmr full-wave rectifier* fed by a nine-phase polygon auto-transformer. The rectifiers are connected in parallel with the load. Refer to Figure 42.
6. *Active-Front-End (AFE) rectifier* topology feeding a load. Refer to Figure 43.

All the rectifiers but the AFE are built by means of uncontrolled diode bridges. In the figures are also shown AC line reactors and DC link chokes, when required by the specific topology for its correct operation.

The harmonic distortion caused by the converters depend on their operating condition, which in turn depends both on the supply system parameters and the load. To provide an insight about the effects of the converter on the system, both a specific load and a set of operating conditions have been considered. The loads consist of a capacitor bank rated at 63.6 uF per kW of load, and a constant power load on the DC side, rated at 160 kW. Such a load can model an AC drive, like it is shown in the figures. However, in most of the cases considered in this research project the load will be another converter (an inverter in the case of an AC 60 Hz shore connection, or a DC/DC converter for managing the ESS recharge in the other cases), which can be modeled in the same way. Regarding the operating condition, these are:

a) Fed by a 500 kVA, 480V, 5% transformer source impedance with balanced voltages and no voltage distortion (Figure 35).
b) Fed by a 500 kVA, 480V, 5% transformer source with 1% unbalanced voltages and no voltage distortion.
c) Fed by a 500 kVA, 480V, 5% transformer source with balanced voltages and 3% of 5th harmonic voltage distortion at 0° phase angle with respect to the line-to-neutral voltage waveform (Figure 36)
d) Fed by a 500 kVA, 480V, 5% transformer source with balanced voltages and 3% of 5th harmonic voltage distortion at 180° phase angle with respect to the line-to-neutral voltage waveform (Figure 37).
e) Fed by a 500 kVA, 480V, 20% generator source with balanced voltages and no voltage distortion. No load conditions are the same as Figure 35.
f) Fed by a 500 kVA, 480V, 20% generator source with 1% unbalanced voltages and no voltage distortion.
g) Fed by a 500 kVA, 480V, 20% generator source with balanced voltages and 3% of 5th harmonic voltage distortion at 0° phase angle with respect to the line-to-neutral voltage waveform. No load conditions are the same as Figure 36.
h) Fed by a 500 kVA, 480V, 20% generator source with balanced voltages and 3% of 5th harmonic voltage distortion at 180° phase angle with respect to the line-to-neutral voltage waveform. No load conditions are the same as Figure 37.

In theory, when the 5^{th} harmonic current passes through a delta-wye transformer a phase shift of 180 degrees is applied, leading to a shift also in the voltage distortion phase angle. Since both of these cases can happen in real applications, the "worst case" conditions of 0° and 180° phase angles for the 5^{th} harmonic have been both considered. Conversely, the reason for using a magnitude of 3% for the 5^{th} harmonic voltage comes from the IEEE Std 519-2014 Section 5.1 [99], which recommends that no single voltage harmonic be greater than 3% of the fundamental in industrial applications, for voltages between 1 and 69 kV (such limit is increased up to 5 % for voltages below 1 kV).

The cases e, f, g, and h imply the supply by means of a generator, modeled by means of its sub-transient reactance. This is interesting, because in many applications there is a back-up generator for supplying the loads in absence of the grid supply.

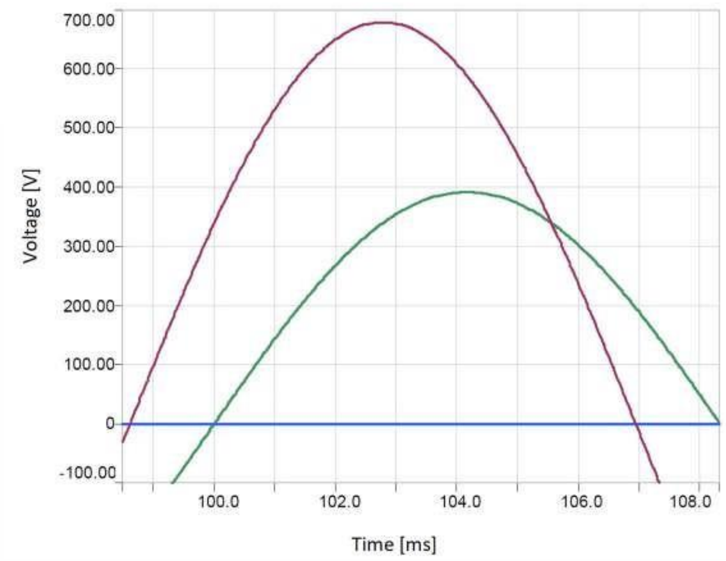

Figure 35 - Resulting line-to-neutral voltage (green) and line-to-line voltage (purple) with no 5th harmonic distortion (blue) [98]

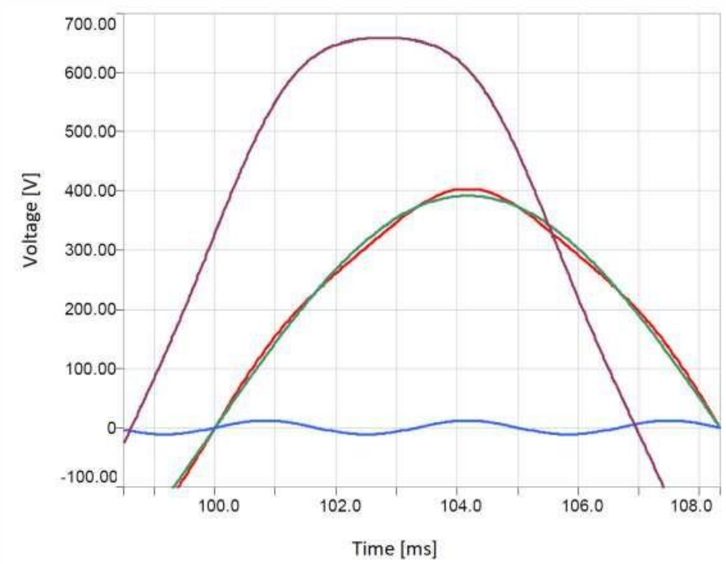

Figure 36 - Resulting line-to-neutral voltage (red) and line-to-line voltage (purple) with 5th harmonic distortion at 0° phase (blue), undistorted line-to-line voltage in green [98]

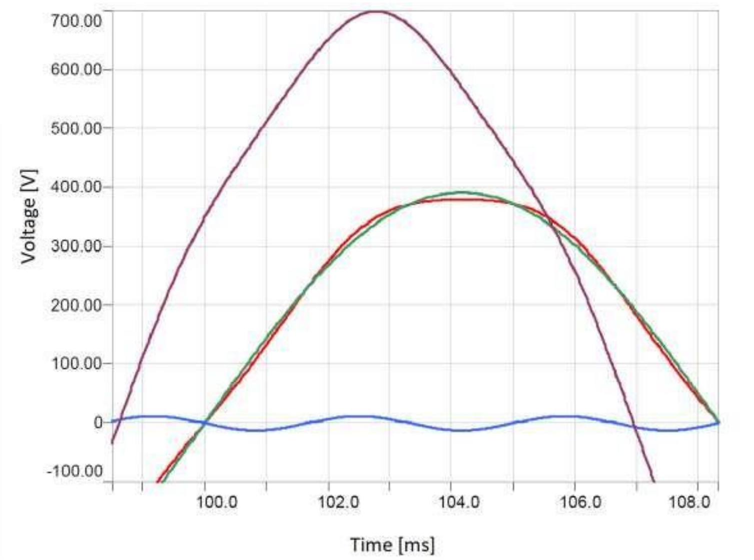

Figure 37 - Resulting line-to-neutral voltage (red) and line-to-line voltage (purple) with 5th harmonic distortion at 180° phase (blue), undistorted line-to-line voltage in green [98]

The operating conditions are collected in Table 3, where the impedance of the source (%Z), the percentage of voltage supply unbalance (%Vunb), the percentage of 5th voltage harmonic (%V5) and its phase angle (V5 theta) are shown. These values are also recalled in the first columns of the tables given within each rectifier topology figure, to allow an immediate comprehension of the cases.

Table 3 - Operating conditions for the rectifiers [98]

Operating condition	%Z	%Vunb	%V5	V5 theta
a	5	0	0	0
b	5	1	0	0
c	5	0	3	0
d	5	0	3	180
e	20	0	0	0
f	20	1	0	0
g	20	0	3	0
h	20	0	3	180

The key parameters regarding harmonic distortion for the converter topologies here considered are shown in the figures of the topologies, in the tables below the diagram. These are:

- Current total harmonic distortion, **Ithd**, at the secondary of the 500 kVA source (transformer or generator);
- Voltage total harmonic distortion, **Vthd**, at the secondary of the 500 kVA source (transformer or generator);
- Total RMS current, **Ipri**, into the rectifier circuit transformer (from the 500kVA source transformer or generator);
- Total PF of Ipri, **PF**;
- Total RMS current, **Id**, or **Iy**, into each 6-pulse rectifier bridge;
- % Unbalance of the total RMS currents, % **Iunb**, feeding each 6-pulse rectifier bridge in the topology;
- Average DC bus voltage, **Vdc**, feeding the load.

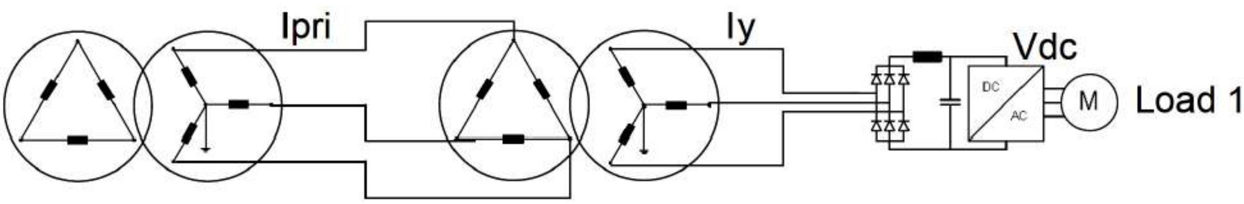

%Z	% Vunb	% V5	V5 theta	Ithd	Vthd	Ipri	PF	Iy	Vdc
5	0	0	0	26.0	2.8	213	0.935	211	612
5	1	0	0	25.2	2.9	221	0.932	212	612
5	0	3	0	28.2	2.0	213	0.934	212	616
5	0	3	180	24.1	5.2	213	0.935	211	609
20	0	0	0	21.6	9.5	219	0.932	217	587
20	1	0	0	20.9	9.7	225	0.931	218	587
20	0	3	0	23.1	7.8	218	0.933	217	591
20	0	3	180	20.4	11.5	218	0.930	217	584

Figure 38 - 6-pulse full-wave rectifier (config. 1), system topology and main parameters [98]

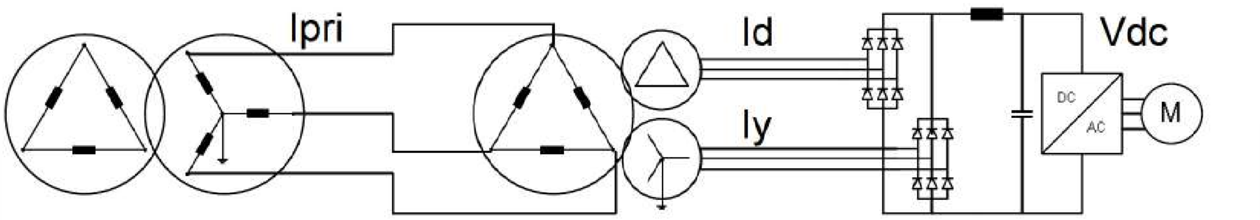

%Z	% Vunb	% V5	V5 theta	Ithd	Vthd	Ipri	PF	Id	Iy	% I unb	Vdc
5	0	0	0	6.2	1.5	207	0.964	108	108	0.1	615
5	1	0	0	6.7	1.5	215	0.958	104	108	3.7	615
5	0	3	0	8.0	3.1	207	0.963	93	122	27.7	615
5	0	3	180	8.0	3.0	207	0.963	122	93	27.6	615
20	0	0	0	4.9	4.7	212	0.962	110	110	0.0	597
20	1	0	0	5.0	4.9	218	0.958	108	111	2.6	597
20	0	3	0	6.0	5.2	212	0.961	99	121	20.0	597
20	0	3	180	6.0	5.2	212	0.961	121	99	19.9	597

Figure 39 - 12-pulse delta/wye parallel rectifier (config. 2), system topology and main parameters [98]

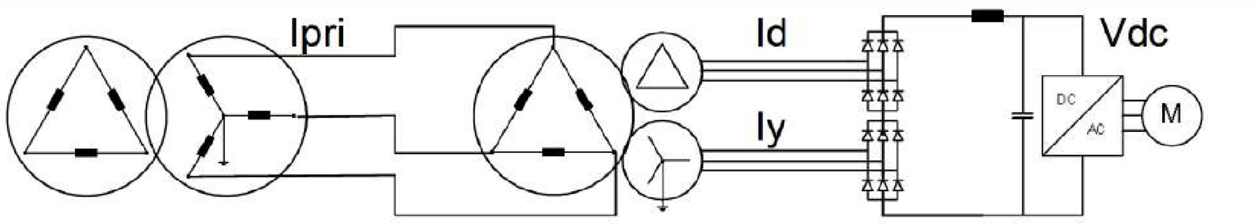

%Z	% Vunb	% V5	V5 theta	Ithd	Vthd	Ipri	PF	Id	Iy	% I unb	Vdc
5	0	0	0	7.2	1.7	207	0.975	210	210	0.0	608
5	1	0	0	7.5	1.6	214	0.969	203	210	3.2	608
5	0	3	0	8.2	3.3	207	0.974	209	211	1.0	608
5	0	3	180	8.2	3.3	207	0.974	212	209	1.0	608
20	0	0	0	5.4	5.4	212	0.975	214	214	0.0	594
20	1	0	0	5.5	5.4	217	0.972	210	214	2.2	594
20	0	3	0	6.3	5.9	212	0.975	213	215	0.9	594
20	0	3	180	6.3	5.8	212	0.975	215	213	0.9	594

Figure 40 - 12-pulse delta/wye series rectifier (config. 3), system topology and main parameters [98]

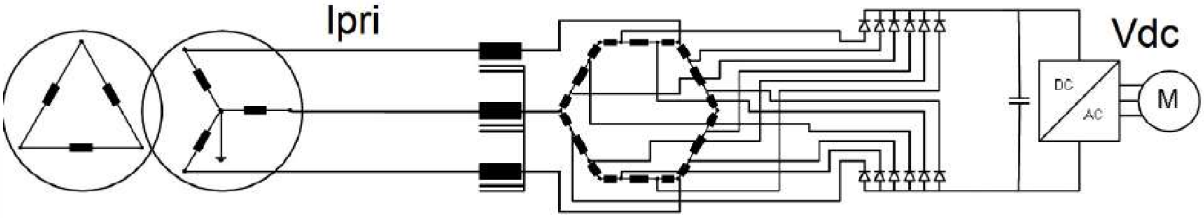

%Z	% Vunb	% V5	V5 theta		Ithd	Vthd		Ipri	PF								Vdc		
5	0	0	0		7.0	1.6		199	0.971								637		
5	1	0	0		8.5	1.7		211	0.963								637		
5	0	3	0		9.8	2.9		199	0.969								637		
5	0	3	180		10.5	2.9		200	0.969								637		
20	0	0	0		5.3	5.0		203	0.973								623		
20	1	0	0		5.9	5.2		210	0.969								623		
20	0	3	0		6.8	5.3		203	0.972								623		
20	0	3	180		7.4	5.1		204	0.972								623		

Figure 41 - 12-pulse auto-xfmr half-wave rectifier (config. 4), system topology and main parameters [98]

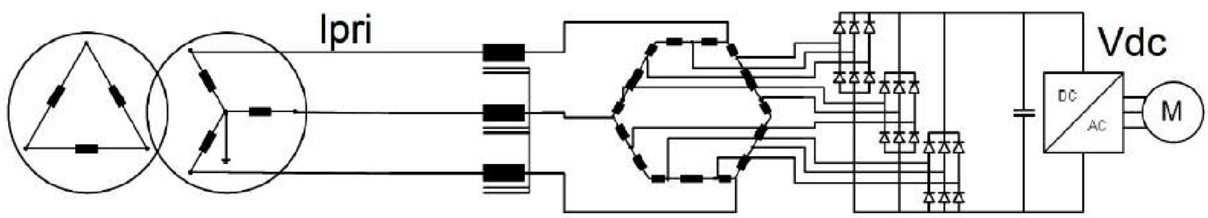

%Z	% Vunb	% V5	V5 theta		Ithd	Vthd		Ipri	PF								Vdc		
5	0	0	0		4.3	0.6		198	0.970								651		
5	1	0	0		7.4	1.0		211	0.960								651		
5	0	3	0		6.2	2.9		198	0.968								651		
5	0	3	180		8.0	2.7		200	0.967								651		
20	0	0	0		2.7	2.6		203	0.971								635		
20	1	0	0		4.3	2.7		210	0.966								635		
20	0	3	0		4.9	3.5		203	0.970								636		
20	0	3	180		5.5	3.1		204	0.970								635		

Figure 42 - 18-pulse auto-xfmr full-wave rectifier (config. 5), system topology and main parameters [98]

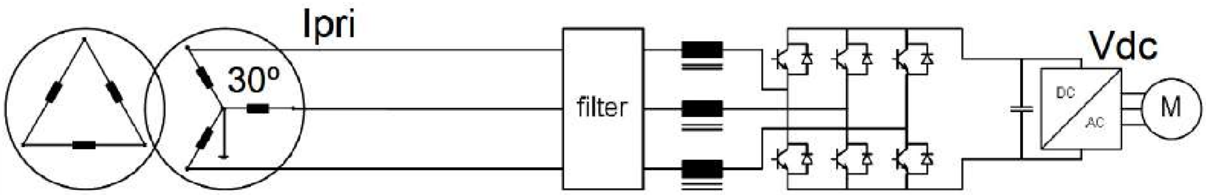

%Z	% Vunb	% V5	V5 theta		Ithd	Vthd		Ipri	PF								Vdc		
5	0	0	0		2.4	0.3		193	0.997								717		
5	1	0	0		2.2	0.3		198	0.998								717		
5	0	3	0		3.7	2.8		192	0.997								717		
5	0	3	180		3.8	2.8		192	0.997								717		
20	0	0	0		1.8	0.9		195	0.994								717		
20	1	0	0		1.6	0.8		199	0.994								717		
20	0	3	0		3.0	2.5		194	0.993								717		
20	0	3	180		3.1	2.4		195	0.993								717		

Figure 43 - Active Front End (AFE) rectifier (config. 6), sysem topology and main parameters [98]

Note that the popular 12-pulse delta/wye parallel rectifier, i.e. the topology #2 shown in Figure 39, is very sensitive to 5th harmonic voltage distortion. With no voltage distortion present, each bridge draws about 106 A_{rms}. With just 3% distortion present, the current sharing between the two rectifier bridges can become unbalanced by ~28%. One bridge draws about 91 A_{rms}, the other draws about 120 A_{rms}. As the distortion increases, so does the imbalance in the currents. The cause of the current unbalance between the bridges is due to the difference in the peaks of the voltage waveforms feeding the two diode bridges. If the voltage waveform feeding the primary has a flattened top due to the 5th harmonic peak subtracting from the fundamental peak, the voltage waveform appearing at the delta secondary terminals will be identical. However, the voltage waveform appearing at the wye secondary terminals will be different due to the 5th harmonic adding to the peak of the fundamental (Figure 44). This results in the delta bridge receiving a voltage with a peak at 0.97 times the fundamental, and the wye bridge receiving a voltage with a peak at 1.03 times the fundamental. The bridge with the higher peak voltage will draw the larger amount of current since the bridges are in parallel. Figure 45 shows how this is switched when the phase angle of the 5th harmonic changes 180°. [98]

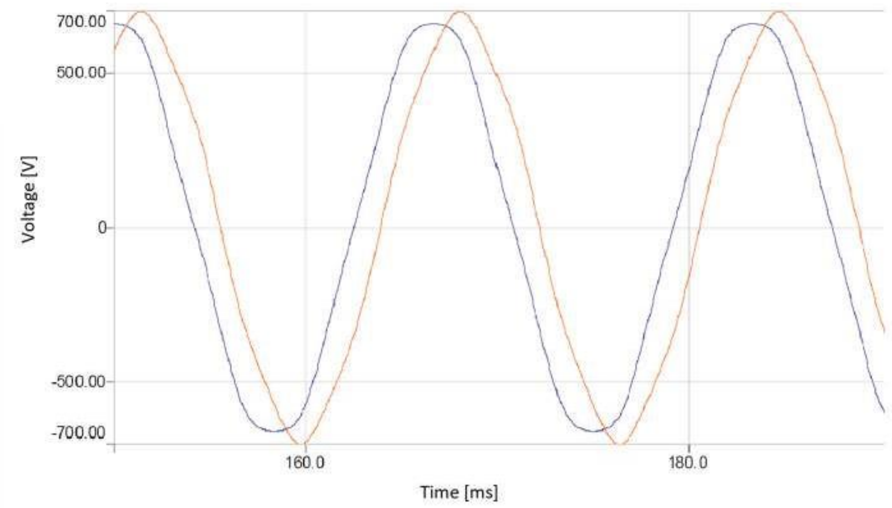

Figure 44 – Effect of 3% of 5th harmonic voltage distortion at 0°. Delta secondary is blue, wye secondary is orange. [98]

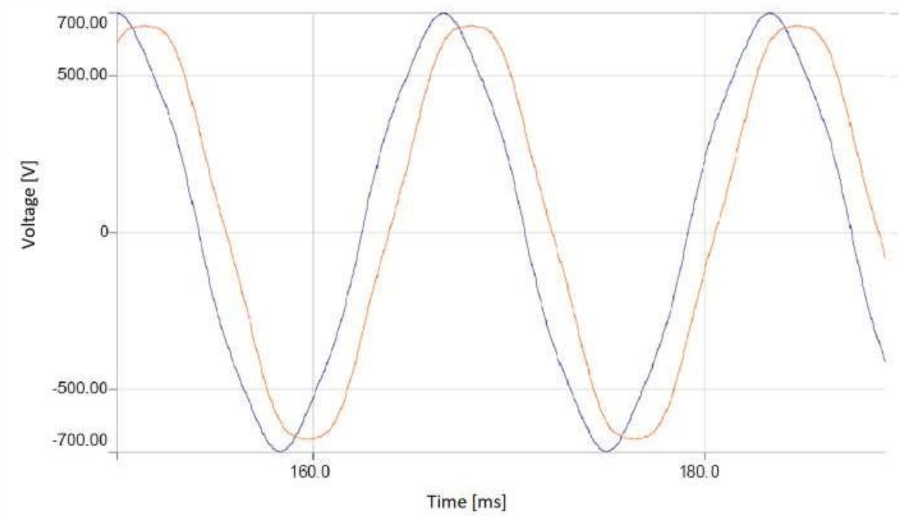

Figure 45 – Effect of 3% of 5th harmonic voltage distortion at 180°. Delta secondary is blue, wye secondary is orange. [98]

As can be easily seen from the results, each topology provides different performance in terms of current and voltage THD levels, as well as other specific parameters. In Table 4 are summarized the results for the considered converters in two of the grid-connected conditions. From the results it is evident how the simplest configuration (config. 1, i.e. the six-pulse full-wave rectifier) offers very low performance in terms of harmonic distortion. Conversely, the two 12-pulse configurations with isolation transformer (config. 2 and 3) allows to attain good performances, while still using uncontrolled components for the rectifier. While the two auto-transformer solutions (config. 4 and 5) perform satisfactorily on the harmonic distortion point of view, they lack the galvanic isolation (which may be an issue in some cases) and increase costs without delivering substantially better results. Finally, the AFE configuration (config. 6) provide the best results in terms of harmonic distortion, but requires controlled devices to be exploited (thus leading to the need of a control system and other auxiliaries). However, it also allows to control the output voltage independently from the input one, while the other configurations cannot. The latter function is not required for AC shore connection, since an inverter will be required to recreate the sinusoidal AC voltages, which is a controlled converter by itself. On the other hand, the output voltage control function is significant for the DC shore connection, because it allows to deliver to the ship the correct voltage regardless of the voltage variation at the AC input, without the need of additional DC/DC conversion stages.

Table 4 - Comparison of the converters in terms of harmonic distortion in the best and worst grid-connected operating conditions

	Operating condition a)		Operating condition b)	
Configuration	**Ithd %**	**Vthd %**	**Ithd %**	**Vthd %**
1	26.0	2.8	24.1	5.2
2	6.2	1.5	8.0	3.0
3	7.2	1.7	8.2	3.3
4	7.0	1.6	10.5	2.9
5	4.3	0.6	8.0	2.7
6	2.4	0.3	3.8	2.8

5.2 ESS interface converters

The power electronics converters dedicated to the ESS interface with the power system can be built with different technologies. In regards to converters dedicated only to the recharge of the storage systems (for systems where the charge and discharge of the ESS are made by different converters, e.g. in UPSs), they are interfaced to the grid by means of a rectifier stage. Thus, it can be made reference to the discussion depicted in the previous section, applying the same considerations made for DC shore connections. Conversely, for ESS that use the same converter to exchange power with the grid (charge and recharge), different configurations are possible, as depicted in Section 4.4 (page 27). In general, all these converters use controlled semiconductor devices that switch on and off several times in a single AC input period, thus being able to present a quasi-sinusoidal current absorption. An example of such an operation can be made by showing the current absorption of an AFE, when different input filters are used [100]. Figure 46 uses a simple inductance as input filter, while Figure 47 adds a capacitor, and Figure 48 uses a full LCL filter. As can be easily seen, the input current of an AFE is quasi-sinusoidal, being present only a high frequency ripple. Such a ripple is caused by the controlled power electronics switches operation, and it causes an oscillation at the frequency of commutation used by the converter. Being such a frequency usually high (in the order of the kHz), it is easy to remove it by means of filtering stages. In fact, such a behavior is visible in the figures, where the current becomes more and more sinusoidal as the filtering stage complexity rises. It is to be noticed that the LCL filter is the most used one for AFE applications, leading to the conclusion of considering such converters as absorbing sinusoidal currents (thus causing no issues in terms of harmonic distortion). Other types of converters may have different specific behavior. However, all of the conversion technologies presented in Section 4.4 operate with a high commutation frequency, leading to the same considerations made for the most common AFE ones.

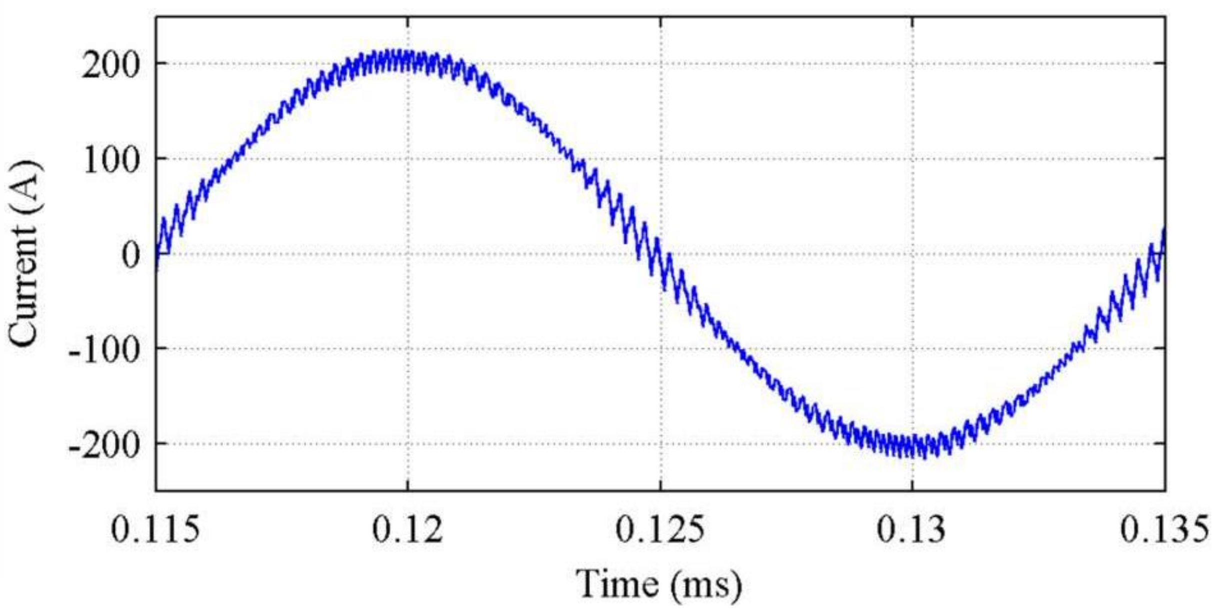

Figure 46 - Grid current waveform for an AFE with an L filter [100]

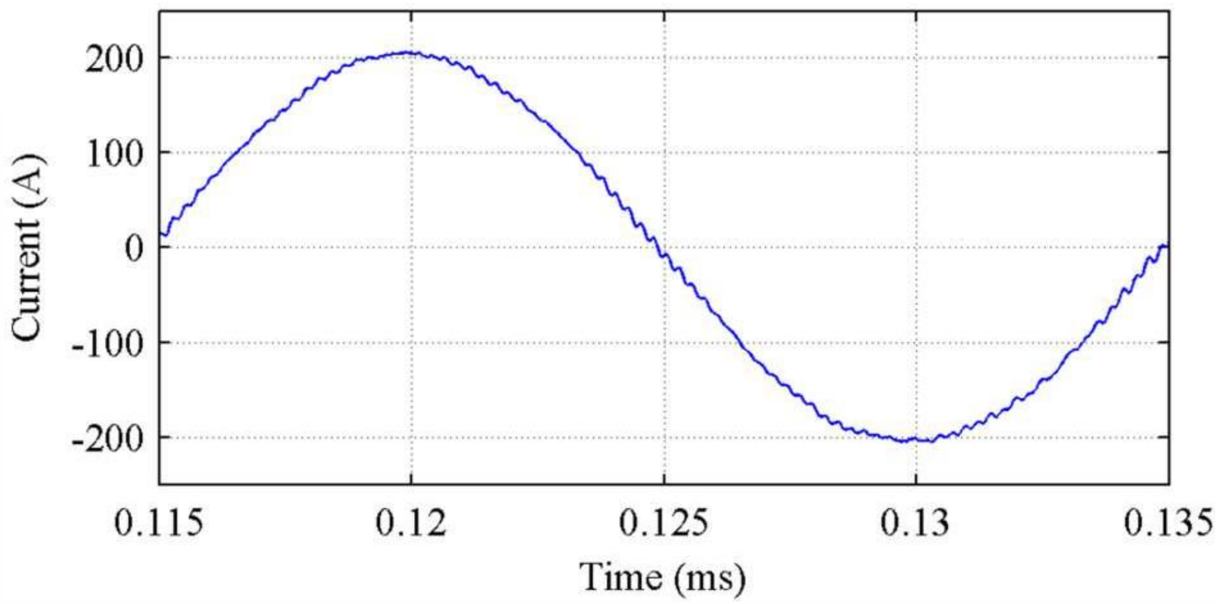

Figure 47 - Grid current waveform for an AFE with an LC filter [100]

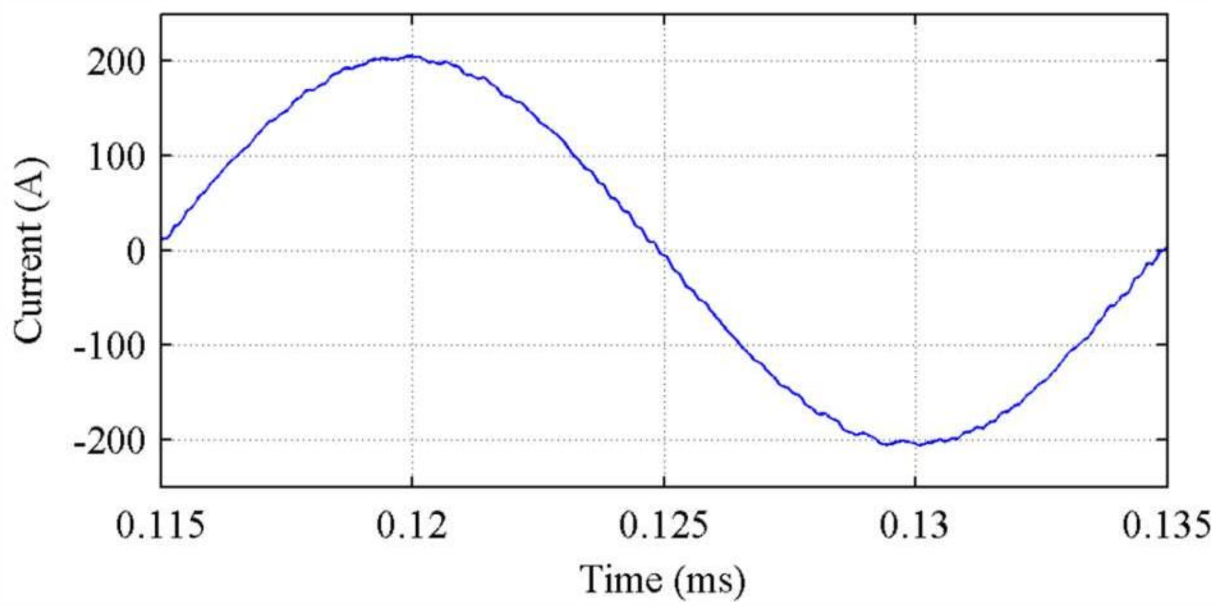

Figure 48 - Grid current waveform for an AFE with an LCL filter [100]

6 Integration among shore connection apparatus (charging station), energy storage system, and port electrical infrastructure

6.1 Introduction

The correct exploitation of a more environmentally friendly transport system involves the analysis of the overall infrastructure in which it has to be integrated. Indeed, it is worth nothing to have a ship capable of sailing using the energy stored in its onboard ESS, if it is recharged from the shore by using nonrenewable energy. Similarly, if the port infrastructure is unable to supply the required energy to allow the ship operation throughout its daily routine, at a certain point the onboard ESS will be depleted and it will be necessary to rely on the onboard Diesel generators. This means that the achievement of a lower environmental impact for the ship involves not only the design of a new ship, but also modifications to the port electrical infrastructure. Being these elements strictly interrelated, it is necessary to develop a methodology able to take into account all the significant variables and data.

A methodology to integrate all these different elements altogether has been developed, and it is shown in the design process of Figure 49. In the depicted figure, the overall design process is subdivided in three macro areas (sub-processes). These sub-processes have been defined only for the sake of a simpler textual exposition, relating each of them to one of the sections in the following text (defined by their section number in Figure 49).

The process starts from a set of input data and from a set of design choices, both clearly identified in the figure. The former regard the ship power system and its daily operative profile, as well as all the information known about the port power system, its loads, the land power grid feeding it, the presence of energy sources in the port premises, and its possible future modifications. If the integration in the port of an ESS is foreseen also for other applications besides the ship feeding (e.g. ancillary services), it has to be known. Then a set of design choices must be made, regarding the onboard ESS recharge concept (e.g. who recharges it? how many times a day? recharge at berth by shore connection or by DGs during sailing? etc.) and regarding new energy sources that can be integrated in the port (possibly renewable ones).

The developed methodology has some feedback links, making it necessary to define the initial values for some of the data in order to start the design process. An evident example is given by the “shore power characteristics” item, which is one of the outputs of the design process, as well as an input for defining the “ship daily energy consumption profile”. In such a case, a first guess has to be made, and the process has to be run iteratively until a feasible solution is found.

In the following, the application of the Figure 49 methodology is described, by means of a case study. It has to be noticed that the application of the design process to the case study here presented is simplified, depicting only the results attained using the correct final values of guessed data, in place of the full iterative design process. Anyhow, it offers results that are sufficient for its aims, showing how to integrate a ship with the port recharging infrastructure, for boosting the environment-friendliness in maritime transport.

The presented results do not take into account details like the efficiency losses of the converters, or the efficiency of the specific ESS used for the ship. This is because some of the required data will be finalized only at the end of the design activity, performed in the WP3 of this research project. However, the proposed methodology is valid, and new results can be calculated when additional data will be available. Moreover, the proposed methodology is sufficiently flexible to take into account for different levels of accuracy and design detail, and act accordingly.

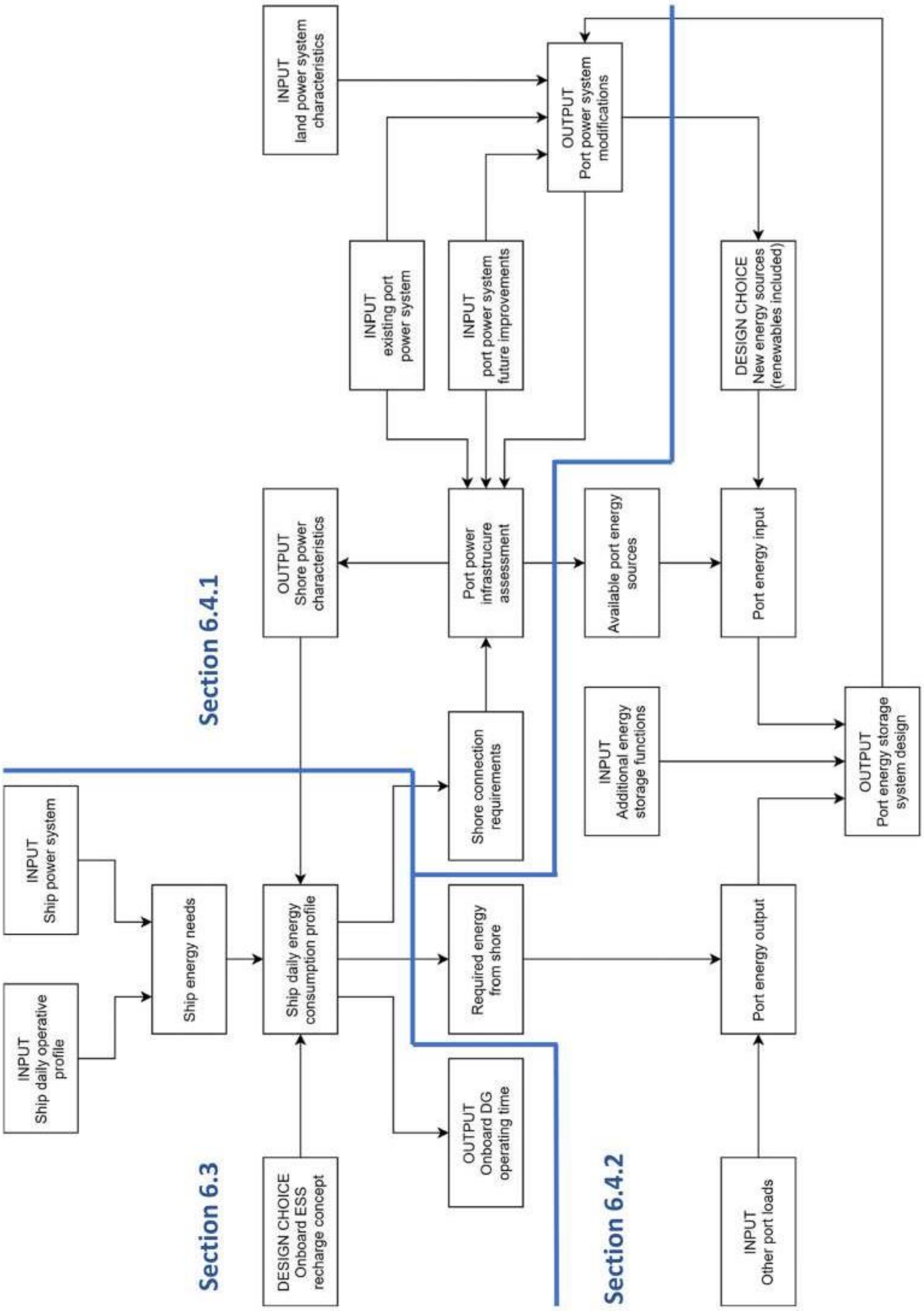

Figure 49 – Methodology developed for the integration of shore connection apparatus, energy storage system, and port electrical infrastructure; Includes the subdivision in sub-processes and the reference to the related Deliverable sections.

6.2 Case Study

The Case Study presented in this report is an example of the possibilities given by an integrated use of ESS. In particular, by considering the ESS presence as a given, it is possible to design a system that is able to fully take advantage of their presence. It is relevant to notice that the design of the recharging infrastructure for a ship is strictly dependent on the operative profile of the latter. In other words, it is necessary to understand the onboard energy needs, for establishing the most convenient infrastructure for supplying it. Particularly, the operative profile is here obtained by analyzing power system data and route characteristics, as expressed in the following. Regarding the route, reference is given to the Brestova-Porozina route (refer to document "*Identification of research area, referent lines and referent ships*"), and thus to the two ports described in Section 2.1 (page 5). Although the route is described in the referred document, a brief recall is given here. Each crossing from one port to the other lasts 35 minutes, subdivided into 15 minutes for the sea navigation plus 20 minutes for the maneuvering in port (10 for each). The ship then waits at berth for additional 15 minutes, leading to total 50 minutes for each trip. In summer, the ferry operates up to 16 trips/day [101].

The presented case study is referred to one of the proposed architectures for the bi-directional Ferry, i.e. a series hybrid configuration endowed with an electrical propulsion system, an integrated power system with Diesel generators, an energy storage system, and a shore connection. Such a configuration is referred as "DE – Hybrid with Shore Connection" in the project work document "*Preliminary Considerations on Machinery Configurations*". More in detail, the bidirectional ferry under study presents a series-hybrid DC power system (Figure 50), where the electrical propulsion motors (EM) can be supplied either by the synchronous Diesel generators (DGs) or by the battery pack (BP). Power electronics converters are used to interface the subsystems: AC-DC rectifiers (converters 1 and 3) are used for powering the DC bus (1000 V) by means of the AC DGs; whereas DC-AC inverters (converters 4, 5, and 6) are installed for supplying the AC loads. The shore-connection (SC) system is depicted in a dashed box, to highlight its installation on the berth (the AC-DC power rectifier number 2 is to be intended as part of the port infrastructure). For what concerns the power system data, only the most significant power figures are given. In particular, each DG provides up to 800 kW, whereas the two electrical machines EM request a total power of 480 kW during the sailing and 200 kW in maneuvering operations. The hotel load (i.e. LVAC users) is 80 kW, while the BP capacity is 750 kWh. The BP capacity is higher than the one defined by WP3 activities (which is 500 kWh), and the shore connection power is considered as a variable in this study. This is because the WP4.1 case study was chosen and analyzed before fixing such data for the ship in WP3. However, the results are able to provide useful insights for the designers, and the methodology can be easily applied to the WP3 dataset, when all the relevant information will be available.

item	description
BP	battery pack
BC	battery charger
SC	shore connection
DG	diesel generator
EM	electrical motor

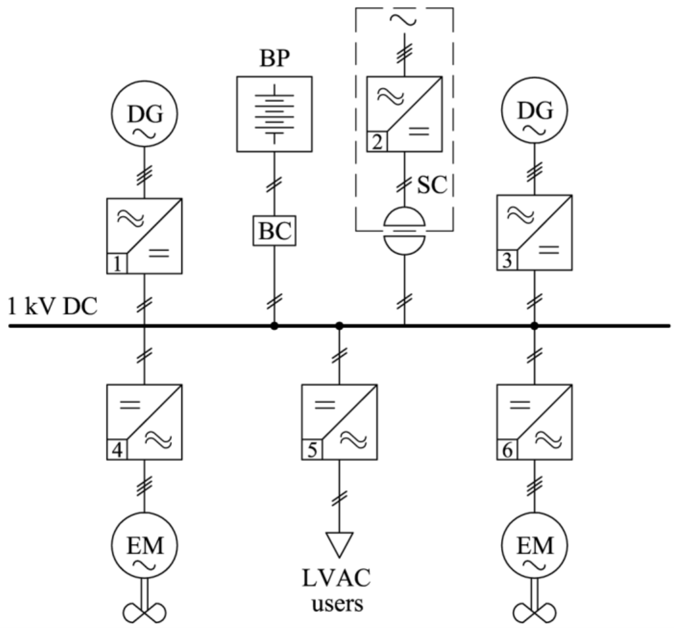

Figure 50 - Bidirectional ferry onboard DC power system [1]

The energy balance can be determined by taking into account the routes scheduling and the power system data expressed so far. Such a balance is a significant input data to correctly design the recharging platform. For defining the energy demand, it is convenient to split the ship behavior in its operative modes. During the sea navigation (i.e. 15 min = 0.25 h), the requested energy amounts to 140 kWh. This is given by the simultaneous application of the 480 kW propulsion power and the 80 kW hotel load. The 10 min maneuvering phase is applied two times for each route (one at each port, thus a total of 0.33 h), using 200 kW for the EM and 80 kW for the hotel load. Therefore, 94 kWh is the required energy. Finally, at berth only the hotel load is applied, leading to 20 kWh required energy (80 kW for 15 min). By summing the three terms, the total energy for a single route is 254 kWh.

While the specific results presented below are valid only for the case study, the same methodology can be easily applied to another ship configuration and/or another route.

6.3 Recharging solutions

Considering the Case Study in analysis, two proposals have been made for lowering the vessel's environmental impact during its operation. Both of them leverage the shore connection energy supply to lower the running hours of the onboard Diesel generators (DGs). The first solution uses a Low Voltage AC (LVAC) shore connection, for recharging the ship at night. Conversely, the second uses a Medium Voltage AC (MVAC) shore connection, to supply the ship both during the berthing period and at night.

6.3.1 Combined recharging from DGs and LV-SC

This configuration is aimed at using a single DG for powering the ship and at the same time recharging the BP during navigation, while the stored energy is used for maneuvering and berthing. Moreover, during the night stop at berth, a LV SC is used to completely recharge the battery. During the sailing, one DG is used to supply both propulsion and hotel loads, while at the same time recharging the ESS. Indeed, the installed DG can provide up to 800 kW, while the propulsion and hotel loads totals a lower value (480 + 80 kW respectively). This means that the remaining power can be used for recharging the onboard battery, thus reducing the emissions near the coast and in port with beneficial effects on the environment and the population. Additionally, by increasing the load on the running DG it is possible to make it operate near its highest efficiency point.

Two cases can be set, depending on the power used for ESS recharge:

a) Load the DG up to 100 % rated power (aim for the DG's maximum achievable power);
b) Load the DG up to 85 % rated power (aim for the DG's maximum efficiency point).

In case a), the power available for recharging the ESS is equal to 240 kW, which means that a total of 60 kWh can be stored during each 15 minutes navigation period. Conversely, in case b) only 120 kW are available, thus leading to recharging the ESS for 30 kWh in each navigation period. During maneuvering and ship at berth conditions, the onboard ESS needs to supply the ship, while the onboard DGs are shut off. The total required energy in such operations is equal to 114 kWh (i.e. 94 kWh for maneuvering plus 20 kWh at berth).

In case a), by taking into account the 60 kWh provided by the DG during the navigation, the resulting energy balance is -54 kWh for each route. This means that it is not possible to sustain such an operation throughout the entire daily routine. Indeed, supposing the battery to be totally charged at the start of the first route due to the night charging, and having it a capacity of 750 kWh, the ESS becomes totally empty after 14 routes (i.e. 54 x 14 = 756 kWh). As previously observed, each route takes 50 minutes, but 35 of them are related to port operations. Therefore, in case a) up to 14 routes can be provided with zero emission maneuvering and berthing operations, with the DG running only during navigation, while two routes have to be totally powered by the DG.

In case b) the DG can recharge the BP for only 30 kWh during navigation, leading to a 84 kWh energy discharge at the end of each trip. The energy stored in the system at the start of the day (the 750 kWh recharged by night) can last only up to 9 trips, leaving 7 routes to be performed with DG running.

At the end of the working day, in both cases the LVAC shore connection completely restores the ESS stored energy. Since the battery capacity is 750 kWh, a low voltage three-phase AC SC can be sized by assuming 160 kW as rated power and 400 V as line-line voltage (AC phase current equal to 230 A, DC side maximum current 160 A @ 1 KV). By means of such LVAC SC, the onboard ESS is completely recharged in less than 5 h. It is relevant to notice that at present there are LV shore connection apparatuses able to deliver up to 1000 A @ 400 V to the ship (equal to more than 500 kW, depending on the load power factor), as highlighted in Section 3.2 "*Low power shore connection*" (page 15). However, such a high power would require significant modification to the port infrastructure. It has been thus deemed useful to limit the power of the LV-SC to a lower power level, while using the MV-SC (described in the following) for the higher power delivery.

6.3.2 Fast recharging from MV-SC

The second configuration foresees the installation of a high power (750 kW) Medium Voltage Shore Connection in one of the two ports. Such an infrastructure can offer a partial fast-recharge during the 15 minutes berthing of the ship, storing up to 187 kWh in the onboard BP.

Two configurations for the recharge infrastructure can be considered:

c) Fast recharge in only one port;
d) Fast recharge in both ports.

In case c) the shore connection can do a fast recharge every two complete routes. This means that each 187 kWh recharge is coupled with a 508 kWh discharge (two trips each consuming 254 kWh). The 750 kWh stored in the BP at the start of the day is thus depleted in nearly 5 trips, due to the net energy loss of 320 kWh each 2 trips. Thus, the other 11 trips to complete the daily routine have then to be performed with the DG running. It is worth noticing that the performed calculation is approximated, because it does not take into account the real charges and discharges that are caused by the ship operation. Indeed, more information can be attained by producing a graph representing the energy stored in the battery and the sequence of operations that are done on them. Such a graph is shown in Figure 51, where the trips are identified by an increasing number, and the recharge operation by a capital R. As can be seen by analyzing the figure, the DG needs to be started during the fourth trip, to provide the 79 kWh that are missing from the ESS. Then, from the fifth trip onwards the contribution of the ESS to the ship operation is minimal, since it can only provide 187 kWh in respect to the 508 kWh consumed by the ship between two recharges. Such a result is more detailed in respect to the approximated evaluation made in the previous paragraph using only the total energies. However, the results are similar to the ones attained with the simplified evaluation. Thus, the previous approach is deemed sufficient for a preliminary study aimed at providing information to the designers in regards to the system architecture (for ship, port, and shore connection) to be selected and analyzed in depth in a later design stage.

Case d) infrastructure allows to recharge at each port, thus reducing the net energy loss down to 67 kWh for each trip (187 kWh recharge – 254 kWh consumption). In this case the energy store in the ESS at the start of the day can last up to 11 trips, leaving only 5 trips left to be powered by the DG. In this case it is also possible to trace a graph regarding the ESS charge and discharge operations during the ship work day. From Figure 52 it is clear that the DG needs to be started only during the ninth trip, to cover a 40 kWh deficit. Then, from the tenth trip onwards the DG is used during the navigation, to provide nearly 25 % of the required energy.

At the end of the working day, in both MV-SC cases the shore connection is used to completely restore the ESS stored energy. Given the large power available due to the MV shore connection, there are no issues for totally recharging the BP in the 10 hours of night berthing.

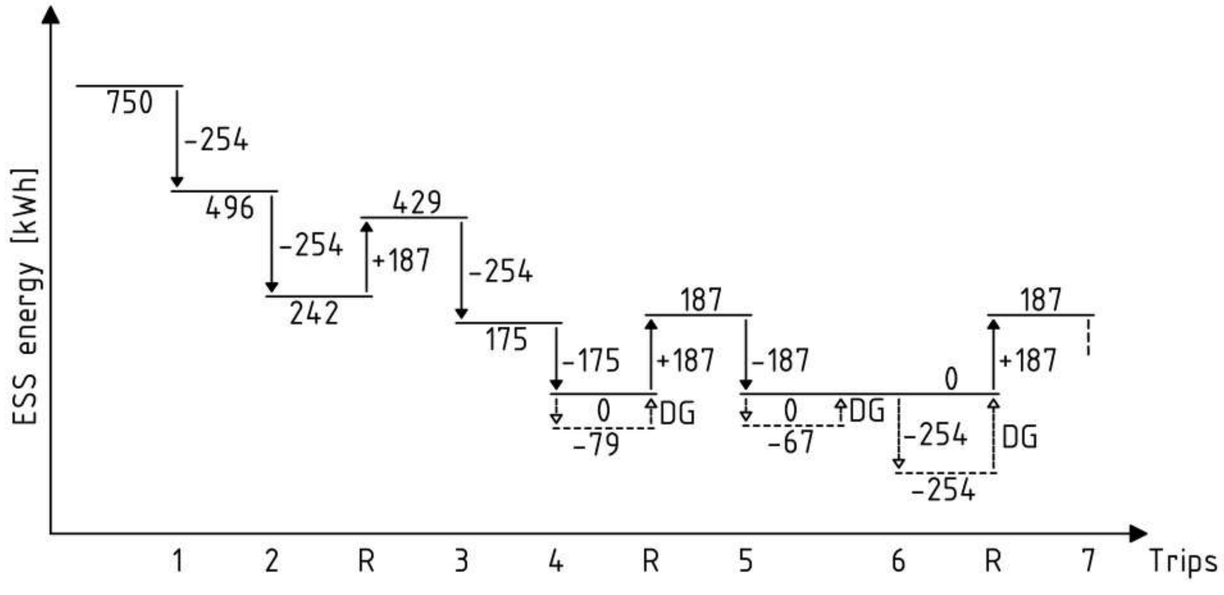

Figure 51 - Energy stored in the ESS, consumption and recharge (R) during a working day, single MV-SC (case c)

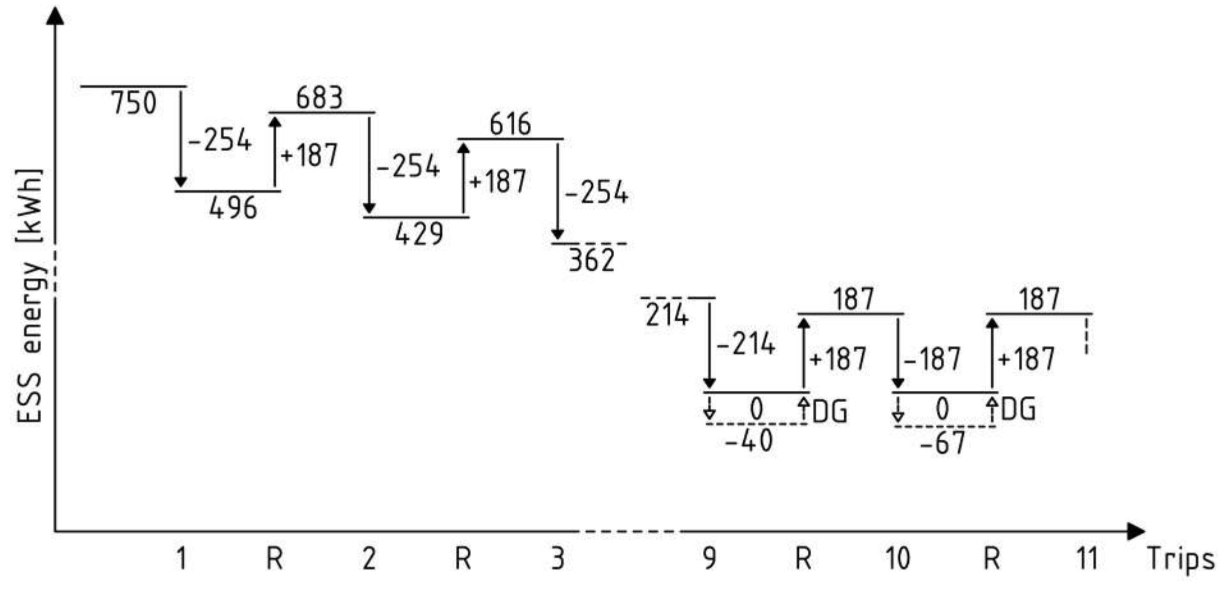

Figure 52 - Energy stored in the ESS, consumption and recharge (R) during a working day, double MV-SC (case d)

6.3.3 DG operating time

As previously mentioned, one of the advantages of integrating an ESS onboard a ship is the reduction in the DGs' running hours. Besides the direct reduction in environmental impact given by the reduction in gaseous pollutant emissions, the ESS navigation leads to additional indirect advantages in terms of pollutant emissions reduction. Indeed, the reduction in DGs' running hours leads to an increase of the maintenance intervals in terms of number of routes performed by the ship. Hence, all the related pollution is reduced as well.

For the first configuration (i.e. combined recharging from DG and LV-SC), the DG is used during the navigation (15 min) for 14 trips in case a), and for 9 trips in case b). The remaining trips (2 in the first case, and 7 in the second) are performed with DG running in both cases.

Thus, for case a) the running time of the DG is 210 min during the ESS assisted trips (14 trips * 15 minutes of operation each trip), and it is equal to 100 min for the DG operated ones (2 trips * 50 minutes operation). Consequently, the DG run for a total of 310 min (i.e. 5 h and 10 mins) during the 14 working hours of the ferry in a day. In other words, the bidirectional ferry boat works for nearly 9 hours in zero emission mode (i.e. 64% of total operating time).

In case b) the ESS assisted trips are lower (i.e. 9). The result is a 135 minutes DG operation time when energy can be taken from BP, and up to 350 min of DG operation in the remaining 7 trips. The result is 485 min (nearly 8 h) of DG operating time during the 14 working hours of the ferry in a day. Thus, the bidirectional ferry boat works for nearly 6 hours in zero emission mode (i.e. 43% of total operating time).

For what concerns the second configuration (i.e. fast recharging with MV-SC), the two analyzed cases have a bigger difference in terms of carbon-free navigation time, in respect to the previous configuration.

The case c), which is the fast-recharge in only one port, leads to a total of 550 min of DG operation. This means that the DG have to be running for up to 9 h during the 14 working hours per each day. In terms of zero emission operation, it results in only a 36% of total operating time (nearly 5 h), which is the lowest result found in this case study.

On the other hand, in case d) the DG runs for about 250 min in each day (slightly more than 4 h). This results in nearly 10 hours of zero emission operation, which is 71% of daily operating time. Such a result is the highest among all the examined cases.

6.4 Integration with the port electrical infrastructure

The two solutions here analyzed provide good results in terms of reduction of DG running hours. However, to achieve such results it is necessary to install in the port the required shore connection apparatus, to recharge the ship's onboard ESS. Thus, in this section the technical aspects related to the integration of the charge station with the port electrical infrastructure are discussed. The most significant data about the ports electrical infrastructure is depicted in Section 2.1 (page 5) , thus here only the relevant information is recalled.

6.4.1 Shore power and port infrastructure integration

LV-shore connection

Starting with the first proposed solution, i.e. the LV-SC, its low power makes its integration possible in both of the ports of the route (Brestova and Porozina) with only a reduced amount of power system modifications. In fact, in Brestova the existing transformer installed in the MV/LV transformation substation has a size that is insufficient for this application (50 kVA rated power, while the LV-SC requires up to 160 kW). However, the existing substation can accommodate a bigger transformer (up to 250 kVA), which means that it is possible to provide the required power to the LV-SC by only changing the electrical machine and the switchboard in the substation, in addition to installing the shore connection apparatuses. Conversely, while the existing situation in Porozina is similar to Brestova one, the DSO has planned an overhaul of the power system in such an area. Indeed, in the future a new substation will be created in Porozina, able to supply up to 400 kW to its loads. Such power is sufficient for supplying the LV-SC, greatly reducing the impact of the recharging infrastructure integration in the port (since the port owner has only to install the shore connection apparatus and its protections). The integration of the LV-SC in both ports makes it possible to provide the shipowner with more flexibility in terms of night berthing of the ferry. However, it is also possible to install the LV-SC only in Porozina, to take advantage of the future investments of the local DSO and thus minimize the costs related to the integration of the LV-SC in the port infrastructure. This means that the ship can only be berthed at night at Porozina port, which is only a minor management issue.

MV-shore connection

Given the data about the electrical power system of the ports, it is clear that the second proposed solution (the 750 kW MV-SC) requires deeper modifications (and thus larger investments) to be integrated in the port infrastructure.

Starting from the Brestova port, it is small and distant from big residential areas, and its present power grid is dimensioned for supplying a maximum of 50 kVA. The possible power increase to 250 kVA, which is sufficient for the LV-SC integration, is still not enough for supplying the port loads and the 750 kW shore connection. It is thus required to define another viable solution for integrating such high-power shore connection in this context. A possible solution is the building of a new substation, to exploit the 2 MW capability of the existing MV line. This will make it possible to buy green energy from the Croatian energy market for supplying the port. The investment will be substantial, being necessary to install the MV-SC apparatus and the new substation

Regarding the Porozina port, both the actual (50 kW) and the future (400 kW) available power from the DSO substations are insufficient for the MV-SC supply. Thus, if the MV-SC is to be installed in this port, it is necessary to build a new electrical substation dedicated to the port power supply. Indeed, in such a way it becomes possible to have a direct connection to the existing MV power line, which is suitable for transporting 3.5 MW more than the present load. The investment will be significant also in this case, being necessary to build a new substation for the port, as well as acquiring the MV-SC apparatus. Regarding the night charge capability, if the shore connection is installed in a single port, there is less flexibility available for the shipowner. Indeed, the ship will need to be berthed in the specific port for assuring the night charge of the ESS. Conversely, if both ports are endowed with MV-SC, there are no issues in this regard. Another possibility for the case with only one MV-SC is the installation of a LV-SC in the other port, to only provide the night recharge (if needed).

6.4.2 Integration of renewable energy sources and energy storage systems

While the environmental impact of the first proposed configuration (*Combined recharging from DGs and LV-SC*) is directly related to DG power and the onboard BP capacity, different considerations can be made for the second configuration (*Fast recharging from MV-SC*). In the latter case the amount of energy coming from the land power grid is significant. In fact, the ship stores up to 3555 kWh (7 fast recharges plus one slow one in the port where the ship is berthed at night, and 8 fast recharges for the other) in case d) using the MV-SC, which is a lot more than the 750 kWh of the night charge coming from the grid in both cases of the LV-SC. Thus, the fast-recharge solution performance in term of pollutant emissions reduction is directly tied to the energy mix used for producing the electrical energy supplied to the ship's BP through the charging station. Such a fact promotes the definition of contracts with green electrical energy producers, to improve further the environmental friendliness of the proposal.

A smart idea to reduce the pollutant emissions related to operation of the ferry is the exploitation of locally installed renewable energy sources for powering the SC. Particularly, both photovoltaic (PV) systems and wind turbines can be suitable sources for producing carbon-free energy in Brestova and Porozina ports. Given the small area available, the production variability, and the specific characteristics of these technologies, it is clear that the direct supply of the SC by means of these sources is not possible. Thus, it becomes necessary to install an ESS in the port premises, to store the energy during the renewable energy source operation. Then, it is possible to transfer such energy to the ship at berth through the SC. Such a solution is in fact coherent with several installations of ESS in Germany, which are aimed at improving the renewables consumption in commercial/residential applications (refer to Section 4.5.1, page 42).

As can be seen from Figure 49, the design of the port ESS takes into account the ship needs, the port needs, the renewables production, and the land power system. In this specific case, being the port power requirements very low in respect to the ship's needs, it has been decided to use the latter as the base of the analysis, thus ignoring the other ports loads (the related input shown in Figure 49 has been set to zero). Given the ship's need in terms of daily energy consumption profile (numerosity, duration, and power of the recharges), it has been possible to consider the available port energy sources to define the required land ESS size. Finally, the renewable energy sources have been sized to provide the daily energy request of the port ESS, closing the design loop.

LV-SC with ESS

In the case of LV-SC the integration with port ESS can be used to store the energy produced during the day by renewable sources, to recharge the ship's BP during the night. This allows exploiting PV panels production, which is tied to the sun presence, as well as to store the wind energy produced during the day. Given the required energy storage capacity and the available time for the recharge during the day (the ship is not connected to the LV-SC for at least 14 hours per day, during its operation), the required power for the daily recharge is nearly 50 kW. This is a worst-case value that does not take into account the wind power production during the night. Such a power level is easily achievable with PV and/or wind generators within the available spaces in both ports. In particular, it is required nearly 325 m^2 of available area for a full PV system, while a single wind generator can reach the same power with a 16 m diameter rotor. It is worth noticing that a mixed solution will surely be the best option for the system, to both reduce the occupied spaces and exploit the different productivity characteristics of both PV and wind generators. Moreover, it has to be noticed that 50 kW is a power level that is still suitable for the direct connection to the existing ports' power grid, thus allowing to compensate for the days when the renewable energy sources have low production by means of grid supplied energy. A notional scheme of such a proposal is shown in Figure 53.

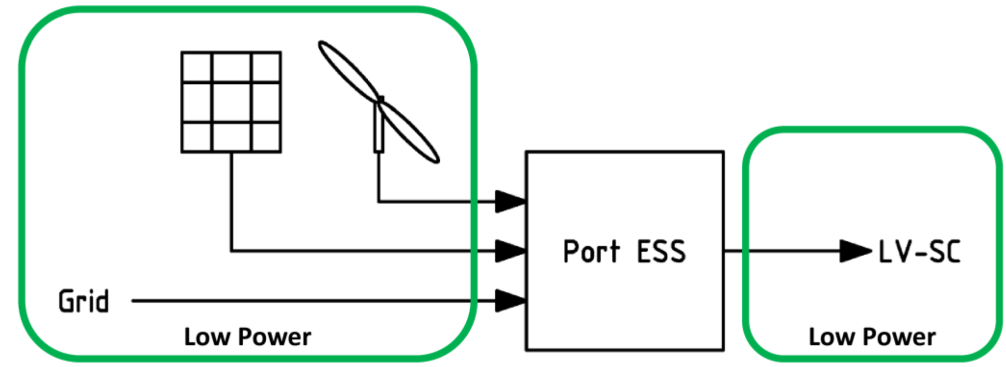

Figure 53 - Integration among ESS, renewable sources, grid and LV-SC

MV-SC with ESS

Regarding the MV-SC applications, the ESS integration in the port can be performed in different modes, depending on the specific function it is sought. Obviously, by means of a proper design, it can also provide all of them at the same time.

The first mode is similar to the one already described for the LV-SC. The port ESS stores energy from the renewable sources during the day, to enable the night charge with green energy (Figure 54). The same considerations made previously for the LV-SC still apply. In this case the high-power electrical infrastructure is still needed to power the MV-SC. However, part of the electrical energy is surely green (the 750 kWh stored for the night recharge), while the daily fast recharges have to be sourced by a suitable green energy producer on the electricity market.

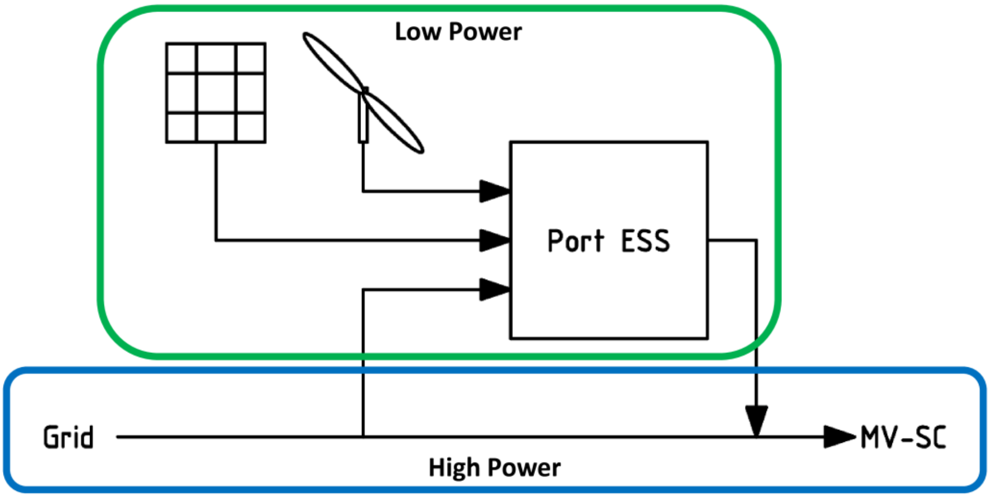

Figure 54- Integration among ESS, renewable sources, grid and MV-SC; first mode.

The second mode is the use of the port ESS to store energy coming from the grid during the periods in which the ship is not berthed, and then inject such energy in the onboard BP during the 15 minutes berthing period (Figure 55). In this case the 185 kWh @ 750 kW injected during the fast charge can be slowly charged during the ship's absence. Using 70 minutes as an approximated value for such a time, the required power results in less than 160 kW. Such a power is suitable for the Porozina port future electrical infrastructure, thus allowing to integrate an MV-SC without building a new substation. Regarding Brestova, such power is achievable by means of the port power system modifications already described for the LV-SC integration. In such a way a high-power interconnection to the land power grid is no more necessary, making it possible to install the MV-SC in both ports with limited impact (the same of LV-SC, plus the ESS). In this case all the power comes from the grid, which means that the only way to furtherly reduce the environmental impact is to source the energy from a green energy producer.

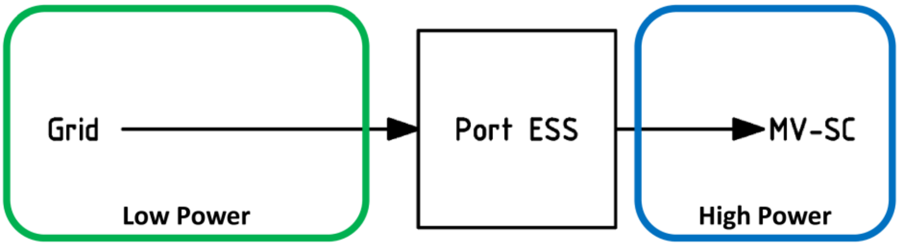

Figure 55 - Integration among ESS, renewable sources, grid and MV-SC; second mode.

It is also possible to provide both these operating modes altogether, by using renewable sources installed in the port premises to reduce the energy quota to be taken from the land power grid. In such a way the local renewable energy sources store their power in the port ESS throughout all their production periods, and the remaining energy quota can be taken from the grid (possibly from a green energy producer) if needed, furtherly reducing the required power for the grid interface. The notional scheme of such integrated solution is shown in Figure 56.

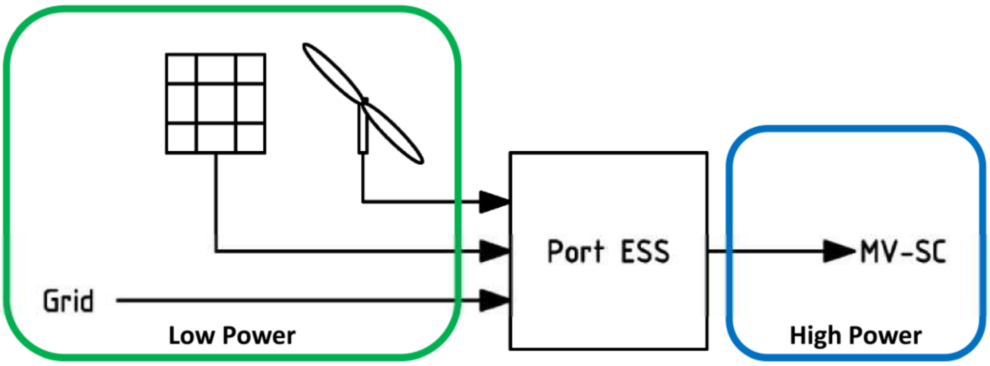

Figure 56 - Integration among ESS, renewable sources, grid and MV-SC; full integration.

6.5 Most suitable ESS technologies for the integration in the port infrastructure

Regarding the ESS to be installed into the port power system to enable the integration among, shore connection, port infrastructure, and renewables sources, a distinction has to be made among the two main use cases presented above. Indeed, the ESS technology suitable for the slow-charge solution has the scope of efficiently store energy during the day and then slowly recharge the ship by night, thus being aimed at optimizing the port self-consumption in terms of renewable energy. As it is obvious, this means that a single slow low power charge and a single low power discharge is performed once a day. Conversely, the fast-charge solution needs to be tailored for performing fast bursts of high-power discharges, multiple times a day. In such case the energy is stored in the ESS when the ship is sailing or berthed at the other port, which means that there is a lot less idle time for this use case. Thus, self-discharge becomes a minimum issue, but higher recharge rate is instead required (for assuring the full capacity availability at ship arrival) and the end of life for the ESS is reached in less time (since more cycles are performed in each working day in respect to the slow charge solution). In this section reference is made to the energy storage technologies presented above, in Section 4.2 (page 21).

6.5.1 Ship slow charge (LV-SC)

In this use case the *lead-acid* batteries seem to be the most ideal solution. In fact, the present very good cycle efficiencies, allowing to reduce the energy loss involved in the charge/discharge process. Moreover, they require low maintenance and have a low capital cost. Their low cycling life is not an issue, since in this application it is expected to have a single cycle per day at maximum. Thus, their medium life of 2500 cycles will allow at least 7 years of continuous daily operations, before some of the modules start failing. Also, the slow charge and recharge cycling here supposed also put them in the best conditions for reaching long life. The low energy density is not an issue since in land-based applications the space for the batteries can be easily found. Indeed, 750 kWh of lead acid batteries will require nearly 15 m^3 (given their volumetric energy density of 50-60 Wh/l), making them installable in a single 20’ container (internal volume of just above 30 m^3) considering also the required ventilation and safety systems.

Sodium-sulfur batteries, while being a good candidate and being used at present for similar applications, present significant drawbacks in terms of costs and management issues in respect to lead batteries. In particular, the achievable advantages (longer life, no self-discharge, and higher energy density) do not seem to be enough to overcome their disadvantages in this application.

Redox flow batteries may be a good solution due to their higher life expectation in respect to lead-acid ones. However, the increase in costs and the dangers related to their operating concept is not justified by any other benefit in this specific application. Indeed, the possibility of swapping the exhaust electrolytes with charged ones for instantly recharge the ESS is not required in the considered use case, and the required capacity is not so high to make this kind of battery advantageous in terms of total volume. One particular use case can be the installation of several separated reagent tanks, that can be charged when the energy from the local renewables is available and then stored for the days in which the renewables are not productive, thus lowering the quota of energy bought from the grid. However, the complexity of such solution seems to be too high for this application, and the related hazards are not justifiable.

Regarding *lithium-ion* batteries, in this use case the only relevant advantage in respect to lead-acid ones is the significantly longer life (more than 10000 lifecycles). All the other pros of such technology are not exploited by the LV-SC concept of operation. Thus, the choice of using lithium-ion batteries must be done on a cost base, considering a long-time application where their life expectancy of more than four times the lead-acid batteries can lead to possible long-term savings.

Finally, *flywheels* are not suitable for such applications, given the high self-discharge rate that makes both the storage of energy throughout an entire day and the slow charge of the ship by night unfeasible.

6.5.2 Ship fast charge (MV-SC)

Lead-acid batteries low number of maximum cycles makes them not suitable for the specific application, because the MV-SC requires to perform the ship recharge several times a day, leading to a very short operative life. Moreover, the fast discharge due to the high-power shore connection will further reduce their life, being such technology more suited to slow charges and discharges.

Similar considerations can be made for the *sodium-sulfur* batteries, whose higher number of achievable cycles is still not enough for their convenient exploitation (5000 cycles will only last up to 2 years, given the 8 discharges/day of the case study). The high efficiency and the almost zero self-discharge advantages are still not enough to recommend their use.

The life expectancy of *redox flow* batteries (above 10000 cycles) makes them a possible candidate for this application. However, their low efficiency (75 %) for high load conditions, their complexity, and the hazards related to their use makes them less interesting than other technologies here considered.

Lithium-ion batteries are the most suitable electrochemical energy storage technology for the MV-SC application. In fact, their long lifetime (above 10000 cycles for the LiFePO4 ones) makes them suitable for the high number of daily cycles (7 fast recharges plus one slow one in the port where the ship is berthed at night, and 8 fast recharges for the other), allowing to reach up to 3.5 years of continuous full charge/discharge operation. Obviously, in the real application such a figure will be higher, because the ship does not perform 16 trips a day for all the 365 days a year have, and also because a sufficient oversizing factor will be set for the battery pack sizing. Indeed, by oversizing the ESS it will be possible to lower the relative amount of discharge caused by the ship's fast-charge operation, thus making each operation count only as a partial cycle. The high efficiency allows for reduced losses in the several charge-discharge operations, while the fast response rate is good for maximizing the amount of energy that can be delivered to the ship during the berthing time. Finally, their high energy density allows to store all the fast charge energy (185 kWh) in just more than half a cubic meter. By adding the auxiliary systems and the power converters, it can be estimated that such an amount of energy can be stored in just above 1 m^3. As an example, the LG Chem ESS R1000 occupies 1 m^3 and weights 1350 kg, for storing 166.4 kWh and providing all the required conversion, control, and management apparatuses (refer to the R1000 product in the attached LG Chem datasheet). Considering the night charge needs, its 750 kWh can be stored in just 2.3 m^3, which is more than 6 times less the volume required for storing the same amount of energy in a lead-acid battery pack. Since the cost of lithium-ion batteries is reducing more and more as the time goes by, as depicted in Section 4.2.1 (page 21), it is also possible to design an oversized battery pack. Such a pack will then be able to store more energy, thus allowing to optimize the renewables use for the port system, and also sell ancillary services to the grid (with additional revenues for the port). Moreover, by oversizing the ESS it will be possible to increase the expected ESS lifetime in regards to the ship recharge operations, as above depicted.

Flywheel energy storage is a technology that is promising for the MV-SC application. Indeed, their characteristics make them very good at storing and delivering high amounts of power in short times, with a good efficiency and nearly infinite number of charge discharge cycles. Their average energy density is not an issue for a land-based application, while their high self-discharge rate (up to 20% per hour) makes them useful only for the daily fast charge operations, but not for the night slow recharge. In this case, by properly designing and sizing the ESS system, it also becomes possible to sell ancillary services to the grid.

As a final comment on the MV-SC case, it becomes evident from the above discussion that a hybrid ESS solution may be the best for this application. In particular, by combining two technologies it becomes possible to exploit the advantages of each of them, and overcome their disadvantages by the presence of the other one. In the specific case, an interesting solution is the use of flywheels for delivering the daily fast charge capability, while managing the night recharge with renewable energy stored during the day by means of lead-acid batteries. In such a way, the high self-discharge of flywheels is less of a problem, because they are used for short periods of time in high power bursts, and their long life removes the costs of changing the batteries after a few years. On the other hand, the high efficiency and low self-discharge of the lead-acid batteries make them ideal for storing the large amount of renewable energy produced throughout the entire day, and slowly recharge the ship at night, allowing for greatly reducing the number of daily full cycles (and thus increasing their expected lifetime). A possible alternative for lead-acid batteries in such a hybrid ESS are sodium-sulfur batteries, despite the issues related to their high temperature working point. Or even lithium-ion batteries, if the flywheels presence leads to a lack in available spaces for their installation.

6.6 Final remarks on the integration among shore connection apparatus, energy storage system, and port electrical infrastructure

As previously mentioned, the reduction of the environmental impact of a marine route has to take into account several aspects, considering not only the ship, but also the ports and their neighborhood. The proposed methodology of Figure 49 (page 64) is aimed at that, and its use allows to avoid evaluation errors that are common if the approach in the design is not an integrated one. A clear example can be made referring to the case study results depicted in Table 5, where the percentage of the daily operation time in zero emission operation are collected for all the examined cases.

Analyzing the shown data, it is possible to make some remarks on the case study results, to highlight some important concepts that have a general validity:

- The proposed LV-SC is a good solution if the energy recovered from the DG during the navigation can be maximized, leading to a 64% of zero-emission time. However, operating the DG at max power leads to increased emissions in respect to operating it at maximum efficiency point, as well as more fuel and maintenance costs. On the other hand, the choice of making the DG work at its minimum consumption point surely allows for a higher fuel efficiency and lower maintenance, but it makes the zero-emission navigation quota drop by a significant amount (-21%).
- The proposed MV-SC leads to the best results in terms of zero emission navigation if both ports are endowed with the shore connection apparatuses. Though, it becomes the worst one when the shore connection is installed in only one port.
- In general, it can be stated that an LV-SC costs less than the higher power one, while leading to results that are in the middle ground among the best and the worst one. Thus, such solution may be the most balanced one in terms of DG operating times, while being yet to be evaluated in terms of total pollutant emissions.
- Due to the power size and the modifications to the port power system that are required by the MV-SC, it is clear that it is a costly solution. However, it leads to the best results if a significant infrastructural investment is done in both ports.
- It is worth remarking again how an MV-SC installed in only one port leads to higher costs and worst results than both LV-SC cases. Thus, it is better to make a significant investment for installing the MV-SC in both ports, or to invest significantly less to make the LV-SC and recharge using the DGs, rather than investing in the single MV-SC.
- The LV-SC with DG recharge at max-efficiency seems to be a solution able to balance low investment costs for the recharge infrastructure, low maintenance costs for the ship, and a good amount of zero emission navigation. Thus, it may be a solution that will be worth analyzing more in depth in the future.

Table 5 - Results in terms of zero emission navigation for the analyzed solutions

Configuration	Case	Daily zero-emission navigation quota
LV-SC	a) DG at max power	64 %
	b) DG at max efficiency	43 %
MV-SC	c) SC in one port	36 %
	d) SC in both ports	71%

The above remarks highlight the need of taking into account all the variables to have sufficient information to make the right choice, because it is not possible to draw a complete picture with only partial information.

Obviously, all these remarks have to be weighted on the basis of the energy mix of the power grid, the renewables production in the port, and the specific pollutant emissions of the ship's onboard DGs. Moreover, a complete design is needed for correctly sizing the renewable energy generation plants, the related land ESS, the required power converters, and their management system, as well as the detailed power system modifications to be done on the ports. However, such a design requires as an input more detailed data about the ship, which will be only available at the end of the design activity performed in WP3 of this research project, and more data about the port infrastructure (in respect to the one available at present).

Since the scope of this case study is to show how the developed methodology can be implemented, rather than developing a detailed design ready for implementation, the information depicted above are considered sufficient. Indeed, as previously affirmed it will be possible to evaluate new results when additional data will be available, also exploiting the proposed methodology flexibility to take into account for a higher level of accuracy and design detail.

The general conclusion that can be drawn from the case study is the need of comparing the solutions as a whole (ship design + ship operation + SC technology + port infrastructure) to allow choosing the right one for the application. This demonstrate why actions aimed at decreasing the environmental footprint of a transportation mean cannot be successful if they don't take into account the overall system where such transportation mean is to be used and integrated.

7 Conclusion

The report goal was to provide a general insight about the technologies available for introducing charging stations in existing port infrastructure, and then to define a methodology to design the overall system by correctly integrating all the available elements.

Such a goal has been reached by means of the several Sections of the report, whose main contribution can be summarized as follows:

- Section 2 presented the port infrastructure of the ports in study, considering in particular their electrical power system actual state and its possible future modifications. Specific attention is given to the Brestova and Porozina ports, since they are the ports of the Case Study route. However, also the port of Trieste has been briefly examined, because it is expected to include a more detailed study about this port in the final deliverables at the end of the project.
- Section 3 presents the actual high and low power shore connection apparatuses. These can be used, as they are or by taking their base technology and modifying it, to interface the ship to the port infrastructure, for recharging the onboard energy storage systems and achieve an improved environmental friendliness for the entire route.
- In Section 4 the energy storage systems topic is addressed. Specifically, the most significant energy storage technologies applicable to the study case are presented with their pros and cons, and a brief comparison among them is made. Then, the power converters usable for interfacing the energy storage systems to the electrical power system are presented, as well as a collection of existing examples of integration of energy storage systems in the power grid.
- Section 5 provides an overview about the power quality issues that can arise for the power system when power converters are introduced.
- The developed methodology for the correct integration among shore connection apparatus (charging station), energy storage system, and port electrical infrastructure is explained in Section 6, by means of a Case Study. The proposed methodology takes into account several different inputs to provide an integrated design of the overall infrastructure, with the aim of maximizing the effectiveness of the ship recharge and reduce as much as possible its environmental footprint. Remarks about the impact on the port in terms of available spaces and costs, and about the most suitable energy storage

technology are also made, by considering the two possible solutions developed for the case study: a low power low voltage shore connection, and a high power medium voltage one.

In general, the results of the study remark the need of designing, analyzing, and comparing the system as a whole (ship design + ship operation + shore connection technology + port electrical infrastructure), in order to have the correct amount of information to choose the best solution for the specific application. This also demonstrate why actions aimed at decreasing the environmental footprint of a transportation mean cannot be successful if they don't take into account the overall system where such transportation mean is to be used and integrated. Thus, such a conclusion highlights the strength of the inclusive approach promoted by this research project.

Reference

[1] D. Bosich, A. Vicenzutti and G. Sulligoi, "Environment-friendliness in Maritime Transport: Designing Smart Recharging Stations in North Adriatic Sea," in *2020 Fifteenth International Conference on Ecological Vehicles and Renewable Energies (EVER)*, September 2020, to be published.

[2] D. Bosich, R. Faraone and G. Sulligoi, "Modeling and Analysis of the Port of Trieste Electrical Distribution System," in *2018 IEEE International Conference on Environment and Electrical Engineering and 2018 IEEE Industrial and Commercial Power Systems Europe (EEEIC / I&CPS Europe)*, Palermo, 2018.

[3] M. Dalle Feste, M. Chiandone, D. Bosich and G. Sulligoi, "Evolution of the Trieste Port: a real-time system for a coordinated cold ironing," in *2019 IEEE International Conference on Environment and Electrical Engineering and 2019 IEEE Industrial and Commercial Power Systems Europe (EEEIC / I&CPS Europe)*, Genova, Italy, 2019.

[4] G. Sulligoi, D. Bosich, R. Pelaschiar, G. Lipardi and F. Tosato, "Shore-to-Ship Power," *Proceedings of the IEEE,* vol. 103, no. 12, pp. 2381-2400, Dec. 2015.

[5] G. Sulligoi, D. Bosich, A. Da Rin and F. Tosato, "An Examination of Mutual Influences Between High-Voltage Shore-Connected Ships and Port Earthing Systems During Phase-to-Ground Faults," *IEEE Transactions on Industry Applications,* vol. 48, no. 5, pp. 1731-1738, Sept.-Oct. 2012.

[6] G. Sulligoi, D. Bosich, R. Baldi and F. Tosato, "Limiting hull touch voltages in large power shore connection systems during phase-to-ground faults: A solution proposal," in *2013 IEEE Electric Ship Technologies Symposium (ESTS)*, Arlington, VA, USA, 2013.

[7] "Gigieffe," [Online]. Available: http://www.gigieffe.com.

[8] "Plus Marine Srl," [Online]. Available: https://www.plusmarine.com/.

[9] "Tesla supercharging," [Online]. Available: https://www.tesla.com/en_EU/support/supercharging?redirect=no. [Accessed 24 06 2020].

[10] V. Bucci, A. Marinò, D. Bosich and G. Sulligoi, "The design of a slow-cruising superyacht with zero emission navigation and smart berthing modes," in *2014 Ninth International Conference on Ecological Vehicles and Renewable Energies (EVER)*, Monte-Carlo, 2014.

[11] G. Torri, S. Casini, A. Piccin and D. Mondo, "Shore to Ship Power Supply Integrating Conventional and Distributed Generators Along with Storage," in *19th International Conference on Ship & Maritime Research, NAV Conference*, Trieste, Italy, 20-22 June 2018.

[12] J. Figgener, P. Stenzel, K.-P. Kairies, J. Linben, D. Haberschusz, O. Wessels, G. Angenendt, M. Robinius, D. Stolten and D. Sauer, "The development of stationary battery storage systems in Germany – A market review," *ELSEVIER Journal of Energy Storage,* vol. 29, no. 101153, 2020.

[13] D. Haberschusz, K.-P. Kairies, O. Wessels, D. Magnor and D. Sauer, "Are PV Battery Systems Causing Ramping Problems in the German Power Grid?," *ELSEVIER Energy Procedia,* vol. 135, pp. 424-433, 2017.

[14] M. Stecca, L. Elizondo, T. Soeiro, P. Bauer and P. Palensky, "A Comprehensive Review of the Integration of Battery Energy Storage Systems Into Distribution Networks," *IEEE Open Journal of the Industrial Electronics Society,* vol. 1, pp. 46-65, 2020.

[15] World Energy Council, "World energy resources 2016," Technical Report, London, U.K., 2016.

[16] X. Luo, J. Wang, M. Dooner and J. Clarke, "Overview of current development in electrical energy storage technologies and the application potential in power system operation," *ELSEVIER Applied Energy,* vol. 137, pp. 511-536, 2015.

[17] H. Chen, T. Cong, W. Yang, C. Tan, Y. Li and Y. Ding, "Progress in electrical energy storage system: A critical review," *ELSEVIER Progress in Natural Science,* vol. 19, no. 3, pp. 291-312, 2009.

[18] S. Alnaser and L. Ochoa, "Optimal Sizing and Control of Energy Storage in Wind Power-Rich Distribution Networks," *IEEE Transactions on Power Systems,* vol. 31, no. 3, pp. 2004-2013, 2016.

[19] IRENA, "Electricity storage and renewables: Costs and markets to 2030," International Renewable Energy Agency, Abu Dhabi, 2017.

[20] H. Ibrahim, A. Ilinca and J. Perron, "Energy storage systems—Characteristics and comparisons," *ELSEVIER Renewable and Sustainable Energy Reviews,* vol. 12, no. 5, pp. 1221-1250, 2009.

[21] I. Hadjipaschalis, A. Poullikkas and V. Efthimiou, "Overview of current and future energy storage technologies for electric power applications," *ELSEVIER Renewable and Sustainable Energy Reviews,* vol. 13, no. 6-7, pp. 1513-1522, 2009.

[22] Q. Liao, B. Sun, Y. Liu, J. Sun and G. Zhou, "A techno-economic analysis on NaS battery energy storage system supporting peak shaving," *Wiley International Journal of Energy Research,* vol. 40, no. 2, 2015.

[23] N. Kawakami, Y. Iijima, M. Fukuhara, M. Bando, Y. Sakanaka, K. Ogawa and T. Matsuda, "Development and field experiences of stabilization system using 34MW NAS batteries for a 51MW wind farm," in *2010 IEEE International Symposium on Industrial Electronics*, Bari, Italy, 4-7 July 2010.

[24] B. Zakeri and S. Syri, "Electrical energy storage systems: A comparative life cycle cost analysis," *ELSEVIER Renewable and Sustainable Energy Reviews,* vol. 42, pp. 569-596, 2015.

[25] S. Tewari and N. Mohan, "Value of NAS Energy Storage Toward Integrating Wind: Results From the Wind to Battery Project," *IEEE Transactions on Power Systems,* vol. 28, no. 1, pp. 532-541, 2013.

[26] L. Thaller, "Electrically rechargeable redox flow cells," in *9th Intersoc. Energy Conversion Eng. Conf.*, San Francisco, USA, 26-30 Aug. 1974.

[27] P. Leung, A. Shan, L. Sanz, C. Flox, J. Morante, Q. Xu, M. Mohamed, C. Ponce de León and F. Walsh, "Recent developments in organic redox flow batteries: A critical review," *ELSEVIER Journal of Power Sources,* vol. 360, pp. 243-283, 2017.

[28] F. Nadeem, S. Hussain, P. Tiwari, A. Goswani and T. Ustun, "Comparative Review of Energy Storage Systems, Their Roles, and Impacts on Future Power Systems," *IEEE Access,* vol. 7, pp. 4555-4585, 2019.

[29] C. Ponce de León, A. Frías-Ferrer, J. González-Garciá, D. Szánto and F. Walsh, "Redox flow cells for energy conversion," *ELSEVIER Journal of Power Sources,* vol. 160, no. 1, pp. 716-732, 2006.

[30] P. Leung, X. Li, C. Ponce de León, L. Berlouis, C. John Low and F. Walsh, "Progress in redox flow batteries, remaining challenges and their applications in energy storage," *RSC Advances,* vol. 2, no. 27, pp. 10125-10156, 2012.

[31] B. Dunn, H. Kamath and J.-M. Tarascon, "Electrical Energy Storage for the Grid: A Battery of Choices," *Science,* vol. 334, no. 6058, pp. 928-935, 2011.

[32] E. Chemali, M. Preindl, P. Malysz and A. Emadi, "Electrochemical and Electrostatic Energy Storage and Management Systems for Electric Drive Vehicles: State-of-the-Art Review and Future Trends," *IEEE Journal of Emerging and Selected Topics in Power Electronics,* vol. 4, no. 3, pp. 1117-1134, 2016.

[33] B. Diouf and R. Pode, "Potential of lithium-ion batteries in renewable energy," *ELSEVIER Renewable Energy,* vol. 76, pp. 375-380, 2015.

[34] M. Aneke and M. Wang, "Energy storage technologies and real life applications – A state of the art review," *ELSEVIER Applied Energy,* vol. 179, pp. 350-377, 2016.

[35] G. Zubi, R. Dufo-López, M. Carvalho and G. Pasaoglu, "The lithium-ion battery: State of the art and future perspectives," *ELSEVIER Renewable and Sustainable Energy Reviews,* vol. 89, pp. 292-308, 2018.

[36] A.-I. Stan, M. Świerczyński, D.-I. Stroe, R. Teodorescu and S. Andreasen, "Lithium ion battery chemistries from renewable energy storage to automotive and back-up power applications — An overview," in *2014 International Conference on Optimization of Electrical and Electronic Equipment (OPTIM)*, Bran, Romania, 22-24 May 2014.

[37] I. Tsiropoulos, D. Tarvydas and N. Lebedeva, "Li-ion batteries for mobility and stationary storage applications," European Commission JRC Science for Policy Report, 2018.

[38] L. Goldie-Scot, "A Behind the Scenes Take on Lithium-ion Battery Prices," BloombergNEF, 5 March 2019. [Online]. Available: https://about.bnef.com/blog/behind-scenes-take-lithium-ion-battery-prices/. [Accessed 10 June 2020].

[39] M. Amiryar and K. Pullen, "A Review of Flywheel Energy Storage System Technologies and Their Applications," *MDPI Applied Sciences,* vol. 7, no. 2, pp. 286-306, 2017.

[40] R. Peña-Alzola, R. Sebastián, J. Quesada and A. Colmenar, "Review of flywheel based energy storage systems," in *2011 IEEE International Conference on Power Engineering, Energy and Electrical Drives*, Malaga, Spain, 11-13 May 2011.

[41] A. Nourai, B. MArtin and D. Fitchett, "Testing the limits [electricity storage technologies]," *IEEE Power and Energy Magazine,* vol. 3, no. 2, pp. 40-46, 2005.

[42] R. Sebastián and R. Peña Alzola, "Flywheel energy storage systems: Review and simulation for an isolated wind power system," *ELSEVIER Renewable and Sustainable Energy Reviews,* vol. 16, no. 9, pp. 6803-6813, 2012.

[43] V. Fernão Pires, E. Romero-Cadaval, D. Vinnikov and J. MArtins, "Power converter interfaces for electrochemical energy storage systems – A review," *ELSEVIER Energy Conversion and Management,* vol. 86, pp. 453-475, 2014.

[44] J.-W. Choi and S.-K. Sul, "Fast current controller in three-phase AC/DC boost converter using d-q axis crosscoupling," *IEEE Transactions on Power Electronics,* vol. 13, no. 1, pp. 179 - 185, Jan. 1998.

[45] M.-T. Tsai and W. Tsai, "Analysis and design of three-phase AC-to-DC converters with high power factor and near-optimum feedforward," *IEEE Transactions on Industrial Electronics,* vol. 46, no. 3, pp. 535 - 543, Jun 1999.

[46] H. Komurcugil and O. Kukrer, "A novel current-control method for three-phase PWM AC/DC voltage-source converters," *IEEE Transactions on Industrial Electronics,* vol. 46, no. 3, pp. 544 - 553, Jun 1999.

[47] R. Zhang, V. Prasad, D. Boroyevich and F. Lee, "Three-dimensional space vector modulation for four-leg voltage-source converters," *IEEE Transactions on Power Electronics,* vol. 17, no. 3, pp. 314 - 326, May 2002.

[48] R. Zhang, F. Lee and D. Boroyevich, "Four-legged three-phase PFC rectifier with fault tolerant capability," in *2000 IEEE 31st Annual Power Electronics Specialists Conference. Conference Proceedings*, Galway, Ireland, 23-23 June 2000.

[49] F. Peng, "Z-source inverter," *IEEE Transactions on Industry Applications,* vol. 39, no. 2, pp. 504 - 510, Mar/Apr 2003.

[50] J. Anderson and F. Peng, "Four quasi-Z-Source inverters," in *2008 IEEE Power Electronics Specialists Conference*, Rhodes, Greece, 15-19 June 2008.

[51] J. Anderson and F. Peng, "A Class of Quasi-Z-Source Inverters," in *2008 IEEE Industry Applications Society Annual Meeting*, Edmonton, AB, Canada, 5-9 Oct. 2008.

[52] J. Rabkowski, "The bidirectional Z-source inverter as an energy storage/grid interface," in *EUROCON 2007 - The International Conference on "Computer as a Tool"*, Warsaw, Poland, 9-12 Sept. 2007.

[53] J. Ejea, E. Sanchis-Kilders, J. Carrasco, J. Espi and A. Ferreres, "Implementation of bi-directional AC-DC matrix converter," *IEEE Electronics Letters,* vol. 38, no. 16, pp. 933 - 934, Aug 2002.

[54] J. Zhu, Z. Xu, B. Jiang and C. Zhang, "Close-loop control of an AC-DC matrix converter for automotives," in *2011 IEEE Electrical Power and Energy Conference*, Winnipeg, MB, Canada, 3-5 Oct. 2011.

[55] K. You and F. Rahman, "Modulation and Control Schemes for A New Power Converter Based on Z-source and Matrix Converter for ISA 42 V PowerNet System," in *2005 IEEE International Conference on Power Electronics and Drives Systems*, Kuala Lumpur, Malaysia, 28 Nov.-1 Dec. 2005.

[56] S. Ponnalluri, G. Linhofer, J. Steinke and P. Steinmer, "Comparison of single and two stage topologies for interface of BESS or fuel cell system using the ABB standard power electronics building blocks," in *2005 IEEE European Conference on Power Electronics and Applications*, Dresden, Germany, 11-14 Sept. 2005.

[57] R. Schupbach and J. Balda, "Comparing DC-DC converters for power management in hybrid electric vehicles," in *IEEE International Electric Machines and Drives Conference, 2003. IEMDC'03.*, Madison, WI, USA, 1-4 June 2003.

[58] K. Zhiguo, Z. Chunbo, Y. Shiyan and C. Shukang, "Study of Bidirectional DC-DC Converter for Power Management in Electric Bus with Supercapacitors," in *2006 IEEE Vehicle Power and Propulsion Conference*, Windsor, UK, 6-8 Sept. 2006.

[59] F. Caricchi, F. Crescimbini, F. Capponi and L. Solero, "Study of bi-directional buck-boost converter topologies for application in electrical vehicle motor drives," in *APEC '98*

Thirteenth Annual Applied Power Electronics Conference and Exposition, Anaheim, CA, USA, 15-19 Feb. 1998.

[60] X. Zhang, Z. Wang, M. Cheng, S. Ding and W. Wang, "The random PWM based bi-directional buck-boost cascade converter for electric vehicles," in *2011 International Conference on Electrical Machines and Systems*, Beijing, China, 20-23 Aug. 2011.

[61] S.-J. Jang, T.-W. Lee, W.-C. Lee and C.-Y. Won, "Bi-directional dc-dc converter for fuel cell generation system," in *2004 IEEE 35th Annual Power Electronics Specialists Conference*, Aachen, Germany, 20-25 June 2004.

[62] F. Peng, H. Li, G.-J. Su and J. Lawler, "A new ZVS bidirectional DC-DC converter for fuel cell and battery application," *IEEE Transactions on Power Electronics,* vol. 19, no. 1, pp. 54 - 65, Jan. 2004.

[63] C. Klumpner, G. Asher and G. Chen, "Selecting the power electronic interface for a supercapattery based energy storage system," in *2009 IEEE Bucharest PowerTech*, Bucharest, Romania, 28 June-2 July 2009.

[64] M. Nowak, J. Hildebrandt and P. Luniewski, "Converters with AC transformer intermediate link suitable as interfaces for supercapacitor energy storage," in *2004 IEEE 35th Annual Power Electronics Specialists Conference*, Aachen, Germany, 20-25 June 2004.

[65] Z. Wang and H. Li, "Optimized operating mode of current-fed dual half bridges dc-dc converters for energy storage applications," in *2009 IEEE Energy Conversion Congress and Exposition*, San Jose, CA, USA, 20-24 Sept. 2009.

[66] J. Kim, H.-S. Song and K. Nam, "Asymmetric Duty Control of a Dual-Half-Bridge DC/DC Converter for Single-Phase Distributed Generators," *IEEE Transactions on Power Electronics,* vol. 26, no. 3, pp. 973 - 982, March 2011.

[67] H. Li, F. Peng and J. Lawler, "A natural ZVS medium-power bidirectional DC-DC converter with minimum number of devices," *IEEE Transactions on Industry Applications,* vol. 39, no. 2, pp. 525 - 535, Mar/Apr 2003.

[68] B. Bolund, H. Bernhoff and M. Leijon, "Flywheel energy and power storage systems," *ELSEVIER Renewable and Sustainable Energy Reviews,* vol. 11, no. 2, pp. 235-258, February 2007.

[69] S. Vazquez, S. Lukic, E. Galvan, L. Franquelo and J. Carrasco, "Energy Storage Systems for Transport and Grid Applications," *IEEE Transactions on Industrial Electronics,* vol. 57, no. 12, pp. 3881 - 3895, Dec. 2010.

[70] A. Nabae, I. Takahashi and H. Akagi, "A New Neutral-Point-Clamped PWM Inverter," *IEEE Transactions on Industry Applications,* Vols. IA-17, no. 5, pp. 518 - 523, Sept. 1981.

[71] B.-R. Lin and H.-H. Lu, "Multilevel AC/DC/AC converter for AC drives," *IEE Proceedings - Electric Power Applications,* vol. 146, no. 4, pp. 397 - 406, Jul 1999.

[72] M. Marchesoni and M. Mazzucchelli, "Multilevel converters for high power AC drives: a review," in *ISIE '93 - Budapest: IEEE International Symposium on Industrial Electronics Conference Proceedings*, Budapest, Hungary, 1-3 June 1993.

[73] I. Colak, E. Kabalci and R. Bayindir, "Review of multilevel voltage source inverter topologies and control schemes," *ELSEVIER Energy Conversion and Management,* vol. 52, no. 2, pp. 1114-1128, February 2011.

[74] R. Baker and L. Bannister, "Electric power converter". USA Patent US Patent 3867643, 1975.

[75] P. Hammond, "Medium voltage PWM drive and method". USA Patent US Patent 5625545, 1997.

[76] F. Peng and J. Lai, "Multilevel cascade voltage source inverter with seperate DC". USA Patent US Patent 5642275, 1997.

[77] L. Maharjan, S. Inoue and H. Akagi, "A Transformerless Energy Storage System Based on a Cascade Multilevel PWM Converter With Star Configuration," *IEEE Transactions on Industry Applications,* vol. 44, no. 5, pp. 1621-1630, Sept.-Oct. 2008.

[78] L. Maharjan, S. Inoue, H. Akagi and J. Asakura, "State-of-Charge (SOC)-Balancing Control of a Battery Energy Storage System Based on a Cascade PWM Converter," *IEEE Transactions on Power Electronics,* vol. 24, no. 6, pp. 1628 - 1636, June 2009.

[79] N. Mukherjee, D. Strickland, A. Cross and W. Hung, "Reliability estimation of second life battery system power electronic topologies for grid frequency response applications," in *6th IET International Conference on Power Electronics, Machines and Drives (PEMD 2012)*, Bristol, UK, 27-29 March 2012.

[80] L. Maharjan, T. Yamagishi and H. Akagi, "Active-Power Control of Individual Converter Cells for a Battery Energy Storage System Based on a Multilevel Cascade PWM Converter," *IEEE Transactions on Power Electronics,* vol. 27, no. 3, pp. 1099 - 1107, March 2012.

[81] M. Bragard, N. Soltau, S. Thomas and R. De Donker, "The Balance of Renewable Sources and User Demands in Grids: Power Electronics for Modular Battery Energy Storage Systems," *IEEE Transactions on Power Electronics,* vol. 25, no. 12, pp. 3049 - 3056, Dec. 2010.

[82] L. Maharjan, T. Yamagishi, H. Akagi and J. Asakura, "Fault-tolerant control for a battery energy storage system based on a cascade PWM converter," in *2009 IEEE 6th International Power Electronics and Motion Control Conference*, Wuhan, China, 17-20 May 2009.

[83] I. Trintis, S. Munk-Nielsen and R. Teodorescu, "Single stage grid converters for battery energy storage," in *5th IET International Conference on Power Electronics, Machines and Drives (PEMD 2010)*, Brighton, UK, 19-21 April 2010.

[84] A. Etxeberria, I. Vechiu, H. Camblong and J.-M. Vinassa, "Comparison of three topologies and controls of a hybrid energy storage system for microgrids," *ELSEVIER Energy Conversion and Management,* vol. 54, no. 1, pp. 113-121, February 2012.

[85] H. Patel and R. Hoft, "Generalized Techniques of Harmonic Elimination and Voltage Control in Thyristor Inverters: Part II --- Voltage Control Techniques," *IEEE Transactions on Industry Applications,* Vols. IA-10, no. 5, pp. 666 - 673, Sept. 1974.

[86] Y. Cheng, C. Qian, M. Crow, S. Pekarek and S. Arcitty, "A Comparison of Diode-Clamped and Cascaded Multilevel Converters for a STATCOM With Energy Storage," *IEEE Transactions on Industrial Electronics,* vol. 53, no. 5, pp. 1512 - 1521, Oct. 2006.

[87] S. Burusteta, J. Pou, S. Ceballos, I. Marino and J. Alzola, "Capacitor voltage balance limits in a multilevel-converter-based energy storage system," in *Proceedings of the 2011 14th IEEE European Conference on Power Electronics and Applications*, Birmingham, UK, 30 Aug.-1 Sept. 2011.

[88] T. Meynard and H. Foch, "Multi-level conversion: high voltage choppers and voltage-source inverters," in *PESC '92 Record. 23rd Annual IEEE Power Electronics Specialists Conference*, Toledo, Spain, 29 June-3 July 1992.

[89] R. Marquardt, "Current rectication circuit for voltage source inverters with separate energy stores replaces phase blocks with energy storing capacitors". DE Patent Patent DE 10103031, 2002.

[90] R. Marquardt and A. Lesnicar, "A new modular voltage source inverter topology," in *Rec. Eur. Conf. Power Electr*, 2003.

[91] H. M. and H. Akagi, "Control and Experiment of Pulsewidth-Modulated Modular Multilevel Converters," *IEEE Transactions on Power Electronics,* vol. 24, no. 7, pp. 1737 - 1746, July 2009.

[92] L. Baruschka and A. Mertens, "Comparison of Cascaded H-Bridge and Modular Multilevel Converters for BESS application," in *2011 IEEE Energy Conversion Congress and Exposition*, Phoenix, AZ, USA, 17-22 Sept. 2011.

[93] I. Trintis, S. Munk-Nielsen and R. Teodorescu, "A new modular multilevel converter with integrated energy storage," in *IECON 2011 - 37th Annual Conference of the IEEE Industrial Electronics Society*, Melbourne, VIC, Australia, 7-10 Nov. 2011.

[94] U.S. Department of Energy, "DOE Global Energy Storage Database," [Online]. Available: https://www.sandia.gov/ess/global-energy-storage-database/. [Accessed 10 June 2020].

[95] Federazione ANIE, "Report Anie Rinnovabili sui sistemi di accumulo abbinati a FER," [Online]. Available: https://anie.it/report-anie-rinnovabili-sui-sistemi-di-accumulo-abbinati-a-fer/?contesto-articolo=/servizi/ambiente-energia/notizie/#.Xt-9wkUzaUl. [Accessed 10 June 2020].

[96] Terna S.p.A., "Progetti Pilota di Accumulo," [Online]. Available: https://www.terna.it/it/sistema-elettrico/innovazione-sistema/progetti-pilota-accumulo. [Accessed 10 June 2020].

[97] A. Colavitto, A. Vicenzutti, D. Bosich and G. Sulligoi, "Open Challenges in Future Electric Ship Design: High-Frequency Disturbance Propagation in Integrated Power and Energy Systems on Ships," *IEEE Electrification Magazine,* vol. 7, no. 4, pp. 98 - 110, Dec. 2019.

[98] F. Hoadley, S. Kennedy and G. Skibinski, "Comparison of AC to DC rectifier topologies operating on various power distribution networks," in *2008 55th IEEE Petroleum and Chemical Industry Technical Conference*, Cincinnati, OH, USA, 22-24 Sept. 2008.

[99] *519-2014 - IEEE Recommended Practice and Requirements for Harmonic Control in Electric Power Systems,* IEEE, 11 June 2014.

[100] A. Dolara, G. Magistrati, R. Zich, L. Frosio and G. Marchegiani, "Harmonic analysis of output filters for grid connected converters in Battery Energy Storage Systems," in *2014*

16th International Conference on Harmonics and Quality of Power (ICHQP), Bucharest, Romania, 25-28 May 2014.

[101] "Jadrolinija," [Online]. Available: https://www.jadrolinija.hr/en/. [Accessed 17 07 2020].

Attachments

- Document “*Identification of research area, referent lines and referent ships*”;
- Document “*Preliminary Considerations on Machinery Configurations*”;
- Example datasheets of energy storage systems;
- Example datasheet of low voltage shore connection systems.